ISSN 0915-6364

NATIONAL INSTITUTE FOR FUSION SCIENCE

E1, E2, M1, and M2 Transitions in the Neon Isoelectronic Sequence

U.I. Safronova, C. Namba, I. Murakami,
W.R. Johnson and M.S. Safronova

(Received - Oct. 6, 2000)

NIFS-DATA-61 Jan. 2001

RESEARCH REPORT
NIFS-DATE Series

TOKI, JAPAN

E1, E2, M1, and M2 transitions in the neon isoelectronic sequence

U.I. Safronova[1,2], C. Namba[1], I. Murakami[1], W.R. Johnson[2] and M.S. Safronova[2]
[1]*National Institute for Fusion Science, Toki, Gifu, 509-5292, Japan*
[2]*Department of Physics, University of Notre Dame, Notre Dame, IN 46556, USA*

(October 4, 2000)

Abstract. A relativistic many-body method is developed to calculate energy and transition rates for multipole transitions in many-electron ions.

This method is based on relativistic many-body perturbation theory (MBPT), agrees with MCDF calculations in lowest-order, includes all second-order correlation corrections, includes corrections from negative energy states, and is *gauge independent*. Reduced matrix elements, oscillator strengths, and transition rates are calculated for electric dipole (E1) and quadrupole (E2) transitions and magnetic dipole (M1) and quadrupole (M2) transitions in Ne-like ions with nuclear charges ranging from $Z = 11$ to 100. The calculations start from a $1s^22s^22p^6$ Dirac-Fock potential. First-order perturbation theory is used to obtain intermediate-coupling coefficients, and second-order MBPT is used to determine the matrix elements. The contributions from negative-energy states are included in the second-order E1, M1, E2 and M2 matrix elements. The resulting transition energies and transition rates are compared with experimental values and with results from other recent calculations

Key words:atomic database - Excitation energies, oscillator strengths, transition rates

I. INTRODUCTION

Excitation energies, oscillator strengths and transition probabilities for $2s^22p^53l$ and $2s2p^63l$ states along the neon isoelectronic sequence have been studied theoretically and experimentally during the past 30-40 years. Z-expansion [1–3], Model Potential [4–7], CI [8–12], MCHF [13–15], R-matrix [16], MCDF [17], and relativistic many-body perturbation theory (MBPT) [18–20] have been used to calculate these quantities for Ne-like ions.

Nonrelativistic perturbation theory was previously used to calculate energy levels of $2s^22p^53l$ and $2s2p^63l$ states for neonlike ions in Refs. [1–3]. The contribution of Breit operators, calculated with exact nonrelativistic functions and represented as a power series in $1/Z$, were performed in Ref. [1,3]. In those papers, accurate data for ions with $Z = 20$-60 were obtained by introducing screening constants and including radiative and higher-order relativistic effects. The technique used in that work is referred to as the MZ method. This method and two versions of model potential methods [4–7] were compared in Ref. [21] for the 2-3 electric-dipole transition energies in Ne-like ions with nuclear charge Z=36-92. Relativistic MBPT method was applied to determine energies of four $2s^22p^53s$ levels and three $2s^22p^53d$ levels in the large range of Z=10-92 by Avgoustouglou *et al.* [19,20]. Additional to the second-order Coulomb and Breit energies, the all-order hole-core Coulomb correlation correction was taken into account in Refs. [19,20]. Importance of correlation correction was shown by Quinet *et al.* in Ref. [17], where the uncorrected MCDF energies are given. The difference between the experimental and uncorrected MCDF energies were treated by least-squares fitting. Resulting adjusted energies for $2s^22p^53l$ states were presented in Ref. [17] for ions Z=28-92 accordingly. The similar idea was used by Hibbert *et al.* [11] to fit energies obtained by the code CIV3. Accurate adjusted energies for $2s^22p^53l$ and $2s2p^63l$ states were presented in Ref. [11] for ions with Z=10-36.

Accurate measurements along the Ne isoelectronic are performed using a variety of light sources. Most accurate wavelength measurements come from plasma light sources, both magnetic-fusion and laser-produced plasmas. Early wavelength measurements on high-Z ions are by Aglitskii *et al.* [2], Boiko *et al.* [22], Gordon *et al.* [23,24], Jupén *et al.* [25], Gauthier *et al.* [26], Beiersdorfer *et al.* [27], and Buchet *et al.* [28]. Some of the work was summarized by Aglitskii *et al.* [21] in their report of measurements on Kr^{26+}-Nd^{50+} observed in a low-inductance vacuum spark-produced plasmas [21]. Beiersdorfer *et al.* [29] reported results in Ne-like Xe, La, Nd, and Eu obtained on the Princeton Tokamak. Some years later Beiersdorfer *et al.* in Refs. [30,31] presented spectra of Ne-like Yb and Th obtained in an electron-beam trap. Beam-foil spectroscopy of the 2-3 transitions in highly stripped gold and bismuth was reported by Chandler *et al.* [32] and Dietrich *et al.* [33]. Recently, accurate wavelengths measurements of the lasing and nonlasing lines in laser-produced germanium plasma were performed by Yuan *et al.* in Ref. [34]. Wavelengths for x-ray transitions in neonlike I^{43+}, Cs^{45+},and Ba^{46+} were measured with a flat crystal spectrometer on the Tokyo EBIT by Nakamura *et al.* in Ref. [35].

In the present paper, relativistic many-body perturbation theory (MBPT) is used to determine energies of $2s^22p^53l(J)$ and $2s2p^63l(J)$ states of Ne-like ions with nuclear charges $Z = 11 - 100$. Instead of using the $2s^22p^53l(J)$ and $2s2p^63l(J)$ designation of states, it is possible to define these states as hole-particle states: $2p^{-1}3l(J)$ and $2s^{-1}3l(J)$ [19,20] or even more simple

designations as $2p3l(J)$ and $2s3l(J)$ [3,5]. These short designations are used in present paper. Energies are calculated for the 16 even-parity excited states, and the 20 odd-parity excited states. The calculations are carried out to second-order in perturbation theory. Correction for the frequency-dependent Breit interaction is included in first order only. Lamb shift corrections to energies are also estimated and included.

Relativistic MBPT is used to determine reduced matrix elements, oscillator strengths, and transition rates into the ground state for all allowed and forbidden electric and magnetic dipole and quadrupole transitions (E1, M1, E2, M2) in Ne-like ions. Retarded E1 and E2 matrix elements are evaluated in both length and velocity forms. The MBPT calculations starting from a local potential are gauge independent order-by-order, providing "derivative terms" are included in the second- and higher-order matrix elements and careful attention is paid to negative-energy states. The present MBPT calculations start from a nonlocal $1s^22s^22p^6$ Dirac-Fock potential and consequently give gauge-dependent transition matrix elements. Second-order correlation corrections compensate almost exactly for the gauge dependence of the first-order matrix elements, leading to corrected matrix elements that differ by less than 1% in length and velocity forms throughout the periodic system.

II. THEORETICAL TECHNIQUE

Details of the MBPT method were presented in Ref. [18] for calculation of energies of hole-particle states, in Ref. [36] for calculation of energies of particle-particle states and in Ref. [37] for calculation of radiative transition rates in two-particle states. We will present here only the model space for Ne-like ions and the first- and second-order diagram contributions for hole-particle systems without repeating the detailed discussions given in [18], [36], and [37].

A. Model space

For atoms with one hole in closed shells and one electron above closed shells, the model space is formed from hole-particle states of the type $a_v^+a_a|0\rangle$, where $|0\rangle$ is the closed-shell $1s^2_{1/2}2s^2_{1/2}2p^2_{1/2}2p^4_{3/2}$ ground state. The single-particle indices v range over states in the valence shell and the single-hole indices a range over the closed core. For our study of low-lying states $2l^{-1}3l'$ states of Ne-like ions, values of a are $2s_{1/2}$, $2p_{1/2}$, and $2p_{3/2}$, while values of v are $3s_{1/2}$, $3p_{1/2}$, $3p_{3/2}$, $3d_{3/2}$, and $3d_{5/2}$. To obtain an orthonormal model states, we consider the coupled states $\Phi_{JM}(av)$ defined by

$$\Phi_{JM}(av) = \sqrt{(2J+1)} \sum_{m_a m_v} (-1)^{j_v - m_v} \begin{pmatrix} j_v & J & j_a \\ -m_v & M & m_a \end{pmatrix} \times a^\dagger_{vm_v} a_{am_a}|0\rangle \,. \tag{2.1}$$

Combining the $n = 2$ hole orbitals and the $n = 3$ particle orbitals in neon, we obtain 20 odd-parity states consisting of 3 $J = 0$ states, 7 $J = 1$ states, 6 $J = 2$ states, 3 $J = 3$ states, and one $J = 4$ states. Additionally, there are 16 even-parity states consisting of 3 $J = 0$ states, 6 $J = 1$ states, 5 $J = 2$ states, and 2 $J = 3$ states. The distribution of the 36 states in the model space is summarized in Table I.

B. Energy matrix

The first-order energy-matrix element for a hole-particle system $va(J)$ is

$$E^{(1)}[a'v'(J), av(J)] = \delta_{vv'}\delta_{aa'}(\epsilon_v - \epsilon_a) + \frac{1}{(2J+1)}(-1)^{j_v+j_a+J+1} Z_J(av'va') \tag{2.2}$$

where ϵ_i is the eigenvalue of the DHF equation for state i and where

$$Z_J(abcd) = X_J(abcd) + \sum_k (2J+1) X_k(abdc) \begin{Bmatrix} j_a & j_c & J \\ j_b & j_d & k \end{Bmatrix} \tag{2.3}$$

with

$$X_k(abcd) = \langle a||C_k||c\rangle\langle b||C_k||d\rangle R_k(abcd) \,. \tag{2.4}$$

The quantities C_k are normalized spherical harmonics and $R_k(abcd)$ are Slater integrals. The corresponding second-order energy matrix is

$$E^{(2)}[a'v'(J), av(J)] = \delta_{vv'}\delta_{aa'}(E_v^{(2)} + E_a^{(2)}) + \sum_{i=1,4} E^{R_i}[a'v'(J), av(J)] \,. \tag{2.5}$$

The second order one-particle $E_v^{(2)}$ and one-hole $E_a^{(2)}$ contributions are defined by three terms; double-sums, single-sums, and a one-potential term. This later term contributes only to the Breit-Coulomb correction. The second-order contribution for hole state a ($E_a^{(2)}$) is

$$\begin{aligned} E_a^{(2)} = &- \sum_{cmn}\sum_k \frac{(-1)^{j_m+j_n-j_a-j_c}}{(2j_a+1)(2k+1)} \frac{X_k(acmn)Z_k(mnac)}{\epsilon_{ac}-\epsilon_{mn}} \\ &+ \sum_{bcn}\sum_k \frac{(-1)^{j_a+j_n-j_b-j_c}}{(2j_a+1)(2k+1)} \frac{Z_k(bcan)X_k(anbc)}{\epsilon_{bc}-\epsilon_{an}} \\ &- 2\sum_{nb} \delta_{j_b j_n} \sqrt{\frac{2j_b+1}{2j_a+1}} \frac{\Delta(bn)Z_0(naba)}{\epsilon_b - \epsilon_n} \,, \end{aligned} \tag{2.6}$$

where

$$\Delta(bn) = \sum_c \delta_{j_b j_n} \sqrt{\frac{2j_c+1}{2j_b+1}} Z_0(bcnc)\,. \qquad (2.7)$$

Labels b and c designate core states and m and n designate virtual states. The second-order energy for the valence electron v ($E_v^{(2)}$) is found by replacing a by v in the above expression and changing the sign of each term. The second order hole-particle interaction energies $E^{R_i}([a'v'(J), av(J)]$ are:

$$E^{R_1}[a'v'(J), av(J)] = \sum_{mn}\sum_{kk'}(-1)^{J+j_a-j_v} \left\{ \begin{array}{cccc} k & k' & J \\ j_a & j_v & j_m \end{array} \right\} \left\{ \begin{array}{cccc} k & k' & J \\ j_{v'} & j_{a'} & j_n \end{array} \right\} \times \frac{X_k(va'mn) Z_{k'}(nmv'a)}{\varepsilon_{va'} - \varepsilon_{nm}} \qquad (2.8)$$

$$E^{R_2}[a'v'(J), av(J)] = \sum_{bc}\sum_{kk'}(-1)^{J+j_a-j_v} \left\{ \begin{array}{cccc} k & k' & J \\ j_v & j_a & j_b \end{array} \right\} \left\{ \begin{array}{cccc} k & k' & J \\ j_{a'} & j_{v'} & j_c \end{array} \right\} \times \frac{X_k(bcav') Z_{k'}(a'vcb)}{\varepsilon_{bc} - \varepsilon_{v'a}} \qquad (2.9)$$

$$E^{R_3}[a'v'(J), av(J)] = \frac{1}{(2J+1)^2} \sum_{nb} (-1)^{j_{a'}+j_b-j_{v'}-j_n} \times \left[\frac{Z_J(a'bv'n) Z_J(vnab)}{\varepsilon_{ba'} - \varepsilon_{v'n}} + \frac{Z_J(vban) Z_J(a'nv'b)}{\varepsilon_{vb} - \varepsilon_{na}} \right] + \sum_{nb}\sum_{k} \frac{1}{2k+1} (-1)^{j_{v'}+j_{a'}+j_b+j_n+k+J} \left\{ \begin{array}{cccc} j_v & j_a & J \\ j_{a'} & j_{v'} & k \end{array} \right\} \times \left[\frac{Z_k(vbv'n) Z_k(a'nab)}{\varepsilon_{bv} - \varepsilon_{v'n}} + \frac{Z_k(a'ban) Z_k(vnv'b)}{\varepsilon_{a'b} - \varepsilon_{na}} \right] \qquad (2.10)$$

$$E^{R_4}(a'v'J, avJ) = \frac{1}{(2J+1)} (-1)^{j_{v'}-j_{a'}+J} \left[\sum_{n\neq v} \delta(j_v j_n) \frac{\Delta(vn) Z_J(na'av')}{\varepsilon_v - \varepsilon_n} + \sum_n \delta(j_{a'} j_n) \frac{\Delta(a'n) Z_J(vnav')}{\varepsilon_{a'} - \varepsilon_n} + \sum_c \delta(j_{v'} j_c) \frac{Z_J(va'ac) \Delta(cv')}{\varepsilon_{v'} - \varepsilon_c} + \sum_{c\neq a} \delta(j_a j_c) \frac{Z_J(va'cv') \Delta(ca)}{\varepsilon_a - \varepsilon_c} + \sum_n \delta(j_a j_n) \frac{Z_J(va'nv') \Delta(na)}{\varepsilon_{va'} - \varepsilon_{nv'}} + \sum_{n(na\neq va')} \delta(j_{v'} j_n) \frac{Z_J(va'an) \Delta(nv')}{\varepsilon_{va'} - \varepsilon_{na}} + \sum_{c(cv\neq v'a)} \delta(j_{a'} j_c) \frac{\Delta(a'c) Z_J(vcav')}{\varepsilon_{v'a} - \varepsilon_{cv}} + \sum_c \delta(j_v j_c) \frac{\Delta(vc) Z_J(ca'av')}{\varepsilon_{v'a} - \varepsilon_{ca'}} \right] \qquad (2.11)$$

All of the above expressions were defined for the Coulomb interaction. When we include the Breit interaction in the calculation, the Coulomb matrix element $X_k(abcd)$ is modified according to the rule:

$$X_k(abcd) \Rightarrow X_k(abcd) + M_k(abcd) + N_k(abcd). \qquad (2.12)$$

The magnetic radial integrals M and N are defined by Eqs.(A4,A5) on Ref. [38].

C. Example: energy matrix for Mo^{32+}

In Tables II-III, we give details of the second-order energies for the special case of Ne-like molybdenum, $Z = 42$. The headings used in these tables are the same as those used in Ref. [36]. In Table II, we show the second-order contributions to the valence $E_v^{(2)}$ and hole $E_a^{(2)}$ energies, defined in Eq.(2.6). Contributions from each of the 3 distinct terms, double sum V_1, single sum V_2, and one-potential term V_3 are given in this table. The second-order Coulomb contributions and second-order Breit-Coulomb corrections are presented for $n = 2$ hole states and $n = 3$ particle states. The single sum contribution to hole states dominates the Coulomb corrections shown in Table II. The one-potential term V_3 contributes only to the Coulomb-Breit correction; where it is the dominant contribution. Sum of these diagram contribution gives the second order one-hole $E_a^{(2)} = V_1^{HF} + V_2^{HF}$ and one-particle $E_v^{(2)} = V_1^{HF} + V_2^{HF}$ contribution for the Coulomb energy and the second order one-hole $B_a^{(2)} = V_1^{BHF} + V_2^{BHF} + V_3^{BHF}$ and one-particle $B_v^{(2)} = V_1^{BHF} + V_2^{BHF} + V_3^{BHF}$ contribution for the Breit-Coulomb corrections. The orbitals used in the present calculation were obtained as linear combinations of B-splines. These B-spline basis orbitals were determined using the method described in Ref. [39]. We used 40 B-splines of order 8 for each single-particle angular momentum state and we included all orbitals with orbital angular momentum $l \leq 7$ in our single-particle basis.

In Table III we give diagonal and non-diagonal matrix elements of the second-order interaction energy for the hole-particle system defined in Eqs. (2.8-2.11). There are 36 diagonal and 142 non-diagonal matrix elements for $(2l3l')\,(J)$ hole-particle states in jj coupling. We calculated contributions for the 178 matrix elements using both sets of basis DHF orbitals. The Table III includes data

for one 1×1 matrix: $(2p_{3/2}3d_{5/2})\,(4)$,
for one 2×2 matrices: $(2p_{3/2}3p_{3/2}) + (2s_{1/2}3d_{5/2})\,(3)$

for three 3×3 matrices:
$(2p_{3/2}3p_{3/2}) + (2p_{3/2}3p_{3/2}) + (2s_{1/2}3s_{1/2})$ (0),
$(2p_{1/2}3s_{1/2}) + (2p_{3/2}3d_{3/2}) + (2s_{1/2}3p_{1/2})$ (0), and
$(2p_{3/2}3d_{3/2}) + (2p_{3/2}3d_{5/2}) + (2p_{1/2}3d_{5/2})$ (3);
for one 5×5 matrices:
$(2p_{3/2}3p_{1/2})+(2p_{3/2}3p_{3/2})+(2p_{1/2}3p_{3/2})+(2s_{1/2}3d_{3/2})$
$+ (2s_{1/2}3d_{5/2})$ (2);
for two 6×6 matrices:
$(2p_{3/2}3p_{1/2})+(2p_{3/2}3p_{3/2})+(2p_{1/2}3p_{1/2})+(2p_{1/2}3p_{3/2})$
$+ (2s_{1/2}3s_{1/2}) + (2s_{1/2}3d_{3/2})$ (1) and
$(2p_{3/2}3s_{1/2})+(2p_{3/2}3d_{5/2})+(2p_{3/2}3d_{3/2})+(2p_{1/2}3d_{3/2})$
$+ (2p_{1/2}3d_{5/2}) + (2s_{1/2}3p_{3/2})$ (2); and
for one 7×7 matrices:
$(2p_{3/2}3s_{1/2})+(2p_{1/2}3s_{1/2})+(2p_{3/2}3d_{3/2})+(2p_{3/2}3d_{5/2})$
$+ (2p_{1/2}3d_{3/2}) + (2s_{1/2}3p_{1/2}) + (2s_{1/2}3p_{3/2})$ (1)

The second-order Coulomb contributions and the second-order Breit-Coulomb corrections from each of the 4 distinct terms, double sum R_1, single sum R_2, RPA term R_3 and one-potential term R_4 are given in this table. As can be seen from Table III, the single sum R_2 and RPA term R_3 are larger than the double sum R_1, but they have opposite sign in many cases and almost compensate each other. The largest contribution for the second-order Breit-Coulomb corrections are from the one-potential term R_4. This term did not contribute in the Coulomb case. It should be noted, that the diagram contributions of non-diagonal matrix elements are 2-5 times smaller than the diagram contributions of diagonal ones.

Resulting sum of these diagram contributions are given in two last columns of Table IV:
$E^{(2)}[a'v'(J), av(J)] =$
$\delta_{vv'}\delta_{aa'}(E_v^{(2)} + E_a^{(2)}) + R_1^{HF} + R_2^{HF} + R_3^{HF}$ and
$B^{(2)}[a'v'(J), av(J)] =$
$\delta_{vv'}\delta_{aa'}(B_v^{(2)} + B_a^{(2)}) + R_1^{BHF} + R_2^{BHF} + R_3^{BHF} + R_4^{BHF}$.
In this table, we present also results for the first-order Coulomb contributions and the first-order Breit-Coulomb corrections. It should be noted that corrections for the frequency-dependent Breit interaction are calculated in the first order only. As can be seen from Table IV, that the ratio of non-diagonal and diagonal matrix elements is smaller for the first-order diagram contributions than for the second-order diagram contributions. The second difference in the first- and second-order diagram contributions is the symmetry properties: the symmetric first-order non-diagonal matrix elements and the non-symmetric second-order non-diagonal matrix elements. As can be seen from Table IV, the values of $E^{(2)}[a'v'(J), av(J)]$ and $B^{(2)}[av(J), a'v'(J)]$ matrix elements differ in some cases in 2-3 times and even they have opposite sign.

In the previous section, we gave analytical formulas for the first- and second-order contributions $E^{(1)}[a'v'(J), av(J)]$, $E^{(2)}[a'v'(J), av(J)]$, and $B^{(2)}[a'v'(J), av(J)]$ to the energy matrix. To determine the first-order energies of the states under consideration, we diagonalize the symmetric first-order effective Hamiltonian, including both the Coulomb and Breit interactions. The first-order expansion coefficient $C^N[av(J)]$ is the N-th eigenvector of the first-order effective Hamiltonian, and $E^{(1)}[N]$ is the corresponding eigenvalue. The resulting eigenvectors are used to determine the second-order Coulomb correction $E^{(2)}[N]$, the second-order Breit correction $B^{(2)}[N]$ and the QED correction $E_{\rm Lamb}[N]$. Usually, either LS or jj designations are used to label the resulting eigenvectors rather than simply enumerating with an index N.

In Table V, we list the following contributions to the energies of 36 excited states in Mo^{32+}: $E^{(0+1)} = E^{(0)} + E^{(1)} + B^{(1)}$, the second-order Coulomb energy $E^{(2)}$, the second-order Breit correction $B^{(2)}$, the QED correction $E_{\rm Lamb}$, and the total theoretical energy $E^{(\rm tot)}$. The QED correction is approximated as the sum of the one-electron self energy and the first-order vacuum-polarization energy. The self-energy contribution is estimated for s, $p_{1/2}$ and $p_{3/2}$ orbitals by interpolating among the values obtained by Mohr [40] using Coulomb wavefunctions. For this purpose, an effective nuclear charge $Z_{\rm eff}$ is obtained by finding the value of $Z_{\rm eff}$ required to give a Coulomb orbital with the same average $\langle r \rangle$ as the DHF orbital.

When starting calculations from relativistic Dirac-Fock wavefunctions, it is natural to use jj designations for uncoupled transition and energy matrix elements; however, neither jj nor LS coupling describes the *physical* states properly, except for the single-configuration state $2p_{3/2}3d_{5/2}(4) \equiv 2p3d\ ^3F_4$. Both designations are given in Table V.

D. Z-dependences of eigenvectors and eigenvalues in Ne-like ions

In Figs. 1-20, we illustrate the Z-dependence of the eigenvectors and eigenvalues of the $2lj\ 3l'j'$ (J) hole-particle states. Strong mixing between states inside of odd-parity complex with J=1 discussed in many papers (see, for example, [19,20]). Additionally, we found strong mixing inside the odd-parity complex with J=2, and even-parity complex with J=1. In Figs. 1-5, the mixing between $[2p_{1/2}3s_{1/2}(1)]+[2p_{3/2}3d_{3/2}(1)]+[2p_{3/2}3d_{5/2}(1)]$ states for Z=51-55 and between $[2p_{1/2}3d_{3/2}(1)]$ $+[2s_{1/2}3p_{1/2}(1)]$ states for Z=69-70 is illustrated. Strong mixing between $[2p_{3/2}3d_{5/2}(2)]+[2p_{3/2}3d_{3/2}(2)]$ states for Z=36-37 is presented in Figs. 6, 7. The mixing coefficients for $2p3p\ ^3D_2$ and $2s3d\ ^3D_2$ levels are shown in Figs. 8, 9.

The energy diagrams are illustrated in Figs. 14-20. We show LS designations for small Z and jj for large Z in these figures. Usually, either LS or jj designations are used to label the resulting eigenvectors rather than simply enumerating with an index N. As can be seen from Fig. 14 a such numeration leads to change of level labels. The labels of the first and second levels in Fig. 14 are exchanged: $2p3s\ ^3P_0$, $2p3d\ ^3P_0$ for $Z \leq 51$ and $2p3d\ ^3P_0$,

$2p3s\,^3P_0$ for $Z > 51$ in LS designations and $2p_{1/2}3s_{1/2}(0)$, $2p_{3/2}3d_{3/2}(0)$ reverts into $2p_{3/2}3d_{3/2}(0)$, $2p_{1/2}3s_{1/2}(0)$. Using the same designations for the whole energy interval could be lead to the crossing energy levels inside of one complex that is forbidden by Wigner and Neumann theorem (see, for example in Ref. [41]. There are more complicated changes of level labels. As can be seen from Fig. 15, the $2p_{1/2}3d_{3/2}(1)$ level is situated between $2s_{1/2}3p_{1/2}(1)$ and $2s_{1/2}3p_{2/2}(1)$ levels for $Z > 70$. The low-lying $2p_{1/2}3s_{1/2}(1)$ level is mowed for high Z between $2s_{1/2}3p_{1/2}(1)$ and $2p_{3/2}3d_{5/2}(1)$ levels.

E. Radiative transitions to the ground state

The first-order reduced multipole matrix element $Z_K^{(1)}$ for a transition between the ground state $|0\rangle$ and the uncoupled hole-particle state $\Phi_{JM}(av)$ of Eq. (2.1) is

$$Z_K^{(1)}[0 - av(J)] = \frac{1}{\sqrt{2J+1}} Z_J(av)\delta_{JK} \,. \qquad (2.13)$$

The multipole matrix $Z_K(av)$ element, which includes retardation, can be expressed in terms of the operator $t_K^{(1)}$ given in length and velocity forms by equations Eqs.(38) and (39), respectively, of Ref. [42] by

$$Z_K(av) = \frac{(2K+1)!!}{k^K} \langle a \| \, t_K^{(1)} \, \| v \rangle \,.$$

The second-order reduced matrix element $Z_K^{(2)}[0 - av(J)]$ consists of three contributions: $Z_K^{(\mathrm{RPA})}$, $Z_K^{(\mathrm{HF})}$, and $Z_K^{(\mathrm{derv})}$:

$$\begin{aligned} & Z_K^{(\mathrm{RPA})}[0 - av(J)] \\ &= \frac{1}{\sqrt{2J+1}} \delta_{JK} (-1)^{j_b + j_n + K} \frac{1}{2K+1} \\ &\times \sum_{b,n} \left[\frac{Z_K(bn) Z_K(anvb)}{\varepsilon_{bv} - \varepsilon_{na}} + \frac{Z_K(abvn) Z_K(nb)}{\varepsilon_{ba} - \varepsilon_{nv}} \right] \end{aligned} \qquad (2.14)$$

$$\begin{aligned} & Z_K^{(\mathrm{HF})}[0 - av(J)] \\ &= \frac{1}{\sqrt{2J+1}} \delta_{JK} \sum_n \left[\frac{Z_K(an)\Delta(nv)}{\varepsilon_v - \varepsilon_n} + \frac{\Delta(na) Z_K(nv)}{\varepsilon_a - \varepsilon_n} \right] \end{aligned} \qquad (2.15)$$

The derivative term

$$Z_K^{(\mathrm{derv})}(av) = \frac{(2K+1)!!}{k^{K-1}} \langle a \| \, dt_K^{(1)}/dk \, \| v \rangle$$

is just the derivative of the the first order matrix element with respect to the transition energy. It is introduced to account for the first-order change in transition energy. An auxiliary quantity $P_K^{(\mathrm{derv})}$ is defined by

$$P_K^{(\mathrm{derv})}[0 - (av)J] = \frac{1}{\sqrt{2J+1}} Z_J^{(\mathrm{derv})}(av)\delta_{JK} \,. \qquad (2.16)$$

The derivative term $Z_K^{(\mathrm{derv})}(av)$ is given in length and velocity forms by Eqs. (10) and (11) of Ref. [37] for the special case $K = 1$.

The coupled dipole transition matrix element between the ground state and the N-th excited state in Ne-like ions is given by

$$\begin{aligned} & Q^{(1+2)}(0 - N) \\ &= -\frac{1}{E^{(1)}[N]} \sum_{av} C_1^N[av(J)] \\ &\quad \times \Big\{ [\epsilon_a - \epsilon_v] \Big[Z^{(1+2)}[0 - av(J)] + B^{(2)}[0 - av(J)] \Big] \\ &\quad + \Big[-E^{(1)}[N] - \epsilon_a + \epsilon_v \Big] P_1^{(\mathrm{derv})}[0 - av(J)] \Big\} \end{aligned} \qquad (2.17)$$

Here $Z^{(1+2)} = Z_1^{(1)} + Z_1^{(\mathrm{RPA})}$. (Note that $Z_1^{(\mathrm{HF})}$ vanishes since we start from a HF basis.) In Eq. (2.17), we let $B^{(2)} = B_1^{(\mathrm{RPA})} + B_1^{(\mathrm{HF})}$ represent second-order corrections arising from the Breit interaction. Using the above formulas and the results for uncoupled reduced matrix elements, we transform from uncoupled reduced matrix elements to intermediate coupled matrix elements between physical states.

The uncoupled reduced matrix elements are calculated in both length and velocity gauges.

F. Electric dipole matrix element

The electric-dipole matrix element $Z_1(av)$, which includes retardation, is given in lengths and velocity forms as:

length form

$$\begin{aligned} Z_1(av) &= \langle \kappa_a \| C_1 \| \, \kappa_v \rangle \\ &\times \frac{3}{k} \int_0^\infty dr \, \{ j_1(kr) \, [G_a(r) G_v(r) + F_a(r) F_v(r)] \\ &+ j_2(kr) \frac{\kappa_a - \kappa_v}{2} \, [G_a(r) F_v(r) + F_a(r) G_v(r)] \\ &+ j_2(kr) \, [G_a(r) F_v(r) - F_a(r) G_v(r)] \} \,, \end{aligned} \qquad (2.18)$$

velocity form

$$\begin{aligned} & Z_1(av) = \langle \kappa_a \| C_1 \| \, \kappa_v \rangle \\ & \times \frac{1}{k} \int_0^\infty dr \, \{ [j_2(kr) + j_0(kr)] \, [G_a(r) F_v(r) - F_a(r) G_v(r)] \\ & - \frac{\kappa_a - \kappa_v}{2} \, [-j_2(kr) + 2 j_0(kr)] \, [G_a(r) F_v(r) + F_a(r) G_v(r)] \Big\} \end{aligned} \qquad (2.19)$$

The electric-dipole derivative matrix element $Z_1^{\mathrm{derv}}(av)$, which includes retardation, is given in length and velocity forms as:

length form

$$Z_1^{(\mathrm{derv})}(av) = \langle \kappa_a \| C_1 \| \, \kappa_v \rangle \, \frac{3}{k} \qquad (2.20)$$

$$\times \int_0^\infty dr[j_1(kr) - (kr)j_2(kr)]\,[G_a(r)G_v(r) + F_a(r)F_v(r)]$$
$$+ \langle \kappa_a \,\|C_2\|\, \kappa_v\rangle \frac{3}{k}\int_0^\infty dr[(kr)j_1(kr) - 3j_2(kr)]$$
$$\times\left[\frac{\kappa_a - \kappa_v}{2}\,[G_a(r)F_v(r) + F_a(r)G_v(r)]\right.$$
$$\left. + [G_a(r)F_v(r) - F_a(r)G_v(r)]\right]$$

velocity form

$$Z_1^{(\rm derv)}(av) = \langle \kappa_a \,\|C_1\|\, \kappa_v\rangle$$
$$\times\frac{3}{k}\int_0^\infty dr[-j_2(kr)]\,[G_a(r)G_v(r) - F_a(r)F_v(r)]$$
$$+ \langle \kappa_a \,\|C_1\|\, \kappa_v\rangle \frac{3}{k}\int_0^\infty dr[-(kr)j_1(kr) + j_2(kr)]$$
$$\times\left[-\frac{\kappa_a - \kappa_v}{2}\,[G_a(r)F_v(r) + F_a(r)G_v(r)]\right] \qquad (2.21)$$

Here κ_a is the angular momentum quantum number [$\kappa_a = \mp(j_a + \frac{1}{2})$ for $j_a = (l_a \pm \frac{1}{2})$], and $k = \omega\alpha$, where $\omega = \varepsilon_v - \varepsilon_a$ is the photon energy and α is the fine-structure constant. The functions $G_a(r)$ and $F_a(r)$ are large- and small-component radial Dirac-Fock wavefunctions, respectively. The quantity $C_{1q}(\hat{r})$ is a normalized spherical harmonic and $\langle \kappa_a \,\|C_k\|\, \kappa_v\rangle$ is equal to

$$\langle \kappa_a \,\|C_k\|\, \kappa_v\rangle = (-1)^{k-j_v-1/2}\sqrt{[j_a][j_v][l_a][l_v]} \qquad (2.22)$$
$$\times \begin{pmatrix} l_a & l_v & k \\ 0 & 0 & 0 \end{pmatrix} \begin{Bmatrix} j_a & j_v & k \\ l_v & l_a & 1/2 \end{Bmatrix}$$
$$= (-1)^{j_a+1/2}\sqrt{[j_a][j_v]} \begin{pmatrix} j_a & j_v & k \\ -\frac{1}{2} & \frac{1}{2} & 0 \end{pmatrix} \pi(l_a + l_v + k).$$

The differences between length- and velocity-forms, are illustrated for the uncoupled $0 - 2p_{3/2}3d_{3/2}(1)$ matrix element in Fig. 21. It should be noted, that the first-order matrix element $Z^{(1)}$ is proportional $1/Z$, the second-order Coulomb matrix element $Z^{(2)}$ is proportional $1/Z^2$, and the second-order Breit matrix element $B^{(2)}$ is almost independent of Z (see [37]). Taking into account this dependence, $Z^{(1)} \times Z$, $Z^{(2)} \times Z^2$ and $B^{(2)} \times 10^4$ are shown in the figure. These Z-dependencies apply to the first-order matrix elements $Z^{(1)}$, the second-order matrix elements $Z^{(2)}$ and $B^{(2)}$ for high-Z ions. As can be seen from Fig. 21, all these matrix elements are positive, except the second-order matrix elements $Z^{(2)}$ in length form that becomes negative for Z >21. The differences between results in length- and velocity-forms shown in Fig. 21 are compensated by "derivative terms" $P^{(\rm derv)}$, as shown later. It should be noted, that $P^{(\rm derv)}$ in the length form almost equals $Z^{(1)}$ in length form, whereas $P^{(\rm derv)}$ in velocity form is smaller than $Z^{(1)}$ in velocity form by three to four orders of magnitude.

In Table VI, we list values of *uncoupled* first- and second-order dipole matrix elements $Z^{(1)}$, $Z^{(2)}$, $B^{(2)}$, together with derivative terms $P^{(\rm derv)}$ for Ne-like molybdenum, Z=42. We list values for the 7 dipole transitions between odd-parity states with J=1 and the ground state. The derivative terms shown in Table VI arise because transition amplitudes depend on energy, and the transition energy changes order-by-order in MBPT calculations. Both length (L) and velocity (V) forms are given for the matrix elements. We can see that the first-order matrix elements $Z_L^{(1)}$ and $Z_V^{(1)}$ differ by 10-20%; the L–V differences between second-order matrix elements are much larger for some transitions as be seen by comparing $Z_L^{(2)}$ and $Z_V^{(2)}$. It can be also seen from Table VI, that $P^{(\rm derv)}$ in length form almost equals $Z^{(1)}$ in length form but that $P^{(\rm derv)}$ in velocity form is smaller than $Z^{(1)}$ in velocity form by three to four orders of magnitude.

Values of *coupled* reduced matrix elements in length and velocity forms are given in Table VII for the transitions considered in Table VI. Although we use an intermediate-coupling scheme, it is nevertheless convenient to label the physical states using the jj scheme. We see that L and V forms of the coupled matrix elements in Table VII differ only in the fourth or fifth digits. These L–V differences arise because we start our MBPT calculations using a non-local Dirac-Fock (DF) potential. If we were to replace the DF potential by a local potential, the differences would disappear completely. The last two columns in Table VII shows L and V values of *coupled* reduced matrix elements calculated without the second-order contribution. As can be seen from this table, removing the second-order contribution increases the $L - V$ differences.

It should be emphasized that we include the negative energy state (NES) contributions to sums over intermediate states (see, for detail, Ref. [37]). Ignoring the NES contributions leads to small changes in the L-form matrix elements but substantial changes in some of the V-form matrix elements, with a consequent loss of gauge independence.

G. Magnetic-dipole matrix element

The magnetic dipole matrix element $Z_1(av)$, which includes retardation, is given by

$$Z_1(av) = \langle -\kappa_a \,\|C_1\|\, \kappa_v\rangle \frac{6}{\alpha k}\int_0^\infty dr \frac{(\kappa_a + \kappa_v)}{2} j_1(kr)$$
$$\times [G_a(r)F_v(r) + F_a(r)G_v(r)]\,, \qquad (2.23)$$

$$Z_1^{(\rm derv)}(av) = \langle -\kappa_a \,\|C_1\|\, \kappa_v\rangle$$
$$\times \frac{6}{\alpha k}\int_0^\infty dr \frac{(\kappa_a + \kappa_v)}{2}\,[j_1(kr) - (kr)j_2(kr)]$$
$$\times [G_a(r)F_v(r) + F_a(r)G_v(r)]\,. \qquad (2.24)$$

The magnetic dipole matrix element $Z_1(av)$, without retardation, is given by

$$Z_1(av) = \langle -\kappa_a \,\|C_1\|\, \kappa_v\rangle \frac{1}{\alpha}(\kappa_a + \kappa_v)$$
$$\times \int_0^\infty dr(r)\,[G_a(r)F_v(r) + F_a(r)G_v(r)]\,, \qquad (2.25)$$

$$Z_1^{(\mathrm{derv})}(av) = Z_1(av)\,. \qquad (2.26)$$

The nonrelativistic limit is different for transitions inside of one configurations, $n_a = n_v$, and transitions between different configurations, $n_a \neq n_v$. For the case $n_a = n_v$, we obtain

$$Z_1^{\mathrm{NR}}(av) = -\left\langle -\kappa_a \left\| C_1 \right\| \kappa_v \right\rangle (\kappa_a + \kappa_v - 1) \times \frac{(\kappa_a + \kappa_v)}{2} \int_0^\infty dr P_a(r) P_v(r)\,, \qquad (2.27)$$

where $P_a(r)$ is a nonrelativistic limit the large-component radial wavefunction $G_a(r)$. The case $n_a \neq n_v$ was considered in many papers for $1s^2\ {}^1S_0$- $1s2s\ {}^3S_1$ transitions (see for example Ref. [42]). The nonrelativistic limit in this case is proportional to Z^2, and for transitions with $l_a = l_v = 0$ the matrix element is given by [43]

$$Z_1^{\mathrm{NR}}(av) = -(\alpha Z)^2 \sqrt{\frac{2}{3}} \left[\frac{3}{Z} \int_0^\infty \frac{1}{r} dr P_a(r) P_v(r) + \frac{\omega^2}{2Z^2} \int_0^\infty r^2 dr P_a(r) P_v(r) \right]. \qquad (2.28)$$

Using hydrogenic wavefunctions, we find

$$M_{1s2s}^{\mathrm{NR}} = -(\alpha Z)^2 \frac{16}{27\sqrt{3}}, \qquad M_{2s3s}^{\mathrm{NR}} = -(\alpha Z)^2 \frac{2^4 23}{5^5}. \qquad (2.29)$$

The difference between M1 uncoupled matrix elements, calculated in different approximations, is illustrated for the $0 - 2pj3pj'(1)$ matrix element in Figs. 22-25. The first-order matrix elements $Z_{\mathrm{NR}}^{(1)}$, $Z_{\mathrm{R}}^{(1)}$, and $Z_{\mathrm{RF}}^{(1)}$ are calculated using Eqs. (2.27), (2.25) and (2.23) accordingly. The second-order Coulomb $Z_{\mathrm{CL}}^{(2)}$ and Breit $Z_{\mathrm{BR}}^{(2)}$ matrix elements are defined by Eqs. (2.14), (2.15), and (2.23). As can be seen from Figs. 22-25, the curves of $Z_{\mathrm{NR}}^{(1)}$ are almost coincided with the curves of $Z_{\mathrm{R}}^{(1)}$ and $Z_{\mathrm{RF}}^{(1)}$ for the $0 - 2p_{1/2}3p_{3/2}(1)$ and $0 - 2p_{3/2}3p_{1/2}(1)$ transitions but differ for the $0 - 2p_{1/2}3p_{1/2}(1)$ and $0 - 2p_{3/2}3p_{3/2}(1)$ transitions (compare Figs. 22, 24 and Figs. 23, 25). The values of $Z_{\mathrm{NR}}^{(1)}$ are in two times smaller than the values of $Z_{\mathrm{R}}^{(1)}$ for the $0 - 2p_{1/2}3p_{1/2}(1)$ and $0 - 2p_{3/2}3p_{3/2}(1)$ transitions. The frequency-dependent relativistic matrix elements $Z_{\mathrm{RF}}^{(1)}$ differ from the relativistic matrix elements $Z_{\mathrm{R}}^{(1)}$ by 5-10% for all kind of transitions. The M1 uncoupled second-order matrix elements $Z_{\mathrm{CL}}^{(2)}$ are comparable with the first-order matrix elements $Z_{\mathrm{RF}}^{(1)}$ only for small Z. As can be seen from Eq. (2.28), the first-order matrix elements $Z_{\mathrm{RF}}^{(1)}$ are proportional Z^2. The second-order Coulomb matrix elements $Z_{\mathrm{CL}}^{(2)}$ are proportional Z and increase very slowly with Z, the second-order Breit matrix elements $Z_{\mathrm{BR}}^{(2)}$ are proportional Z^3 and become comparable with $Z_{\mathrm{CL}}^{(2)}$ for very high Z.

Ab initio relativistic calculations require a careful treatment of negative-energy states (virtual electron-positron pairs). In the second-order expressions (2.14) and (2.15) such contribution explicitly arises from the terms in the sum over states i and n for which $\varepsilon_i < -mc^2$. The effect of the NES contributions to M1-amplitudes has been studied recently in Ref. [43]. The NES contributions drastically change the second-order Breit matrix elements $Z_{BR}^{(2)}$. It could be noted that the $Z_{BR}^{(2)}$ contributes only by 2-5% in M1 uncoupled matrix elements and, as a result, the including of negative-energy states changes the value of M1 matrix element by 2-5%.

In Figs. 26-31, we illustrate the Z-dependence of the of line strengths for the six magnetic-dipole transitions into the ground state. In these figures we presented the values of line strengths $S_{\mathrm{NR}}^{(1)}$, $S_{\mathrm{R}}^{(1)}$, $S_{\mathrm{RF}}^{(1)}$, and $S_{\mathrm{RF}}^{(1+2)}$ calculated in the same approximations as we discussed for M1 uncoupled matrix elements: $Z_{\mathrm{NR}}^{(1)}$, $Z_{\mathrm{R}}^{(1)}$, $Z_{\mathrm{RF}}^{(1)}$, and $Z_{\mathrm{RF}}^{(1+2)} + Z_{\mathrm{BR}}^{(2)}$. In the last one the derivative term, $P_1^{(\mathrm{derv})}$ (see Eq.(2.16)) is included.

Strong mixing inside of even-parity complex with J=1 between $2p_{3/2}3p_{1/2}$ and $2p_{3/2}3p_{3/2}$ states (see, Figs. 10, 11) for small Z and between $2p_{1/2}3p_{3/2}$ and $2s_{1/2}3s_{1/2}$ states (see, Figs. 12, 13) for high Z leads to the sharp features in the curves shown in the Figs. 27- 30. As can be seen from Figs. 27-29, the deep minimum is shifted by using different approximations. In these case it could be difficult to compare results for M1 transitions obtained by different approximation: nonrelativistic or relativistic approximations. We will discuss this question later. These singularities are consequence of coupling between states governed by the first order mixing coefficients $C_1^N[av(J)]$ in Eq. (2.17). However, some of the singularities are caused by the second order uncoupled matrix elements. As can be seen from Figs. 30, 31 some small singularities still remain for $2s_{1/2}3s_{1/2}$ (1) and $2s_{1/2}3d_{3/2}$ (1) states in the Z=11-20 range. These $2s_{1/2}3s_{1/2}$ (1) and $2s_{1/2}3d_{3/2}$ (1) states are autoionizing for the $2p_j$-hole threshold in the Z=11-20 ranges. In this case, the singularity is caused by the positive part of spectra in the sum over n in Eq. (2.14) for $Z_1^{(\mathrm{RPA})}$. Our conclusion concerning the importance of autoionizing states in low-Z Ne-ions for calculations of the line strengths can be extended to other atomic characteristics.

H. Electric quadrupole matrix element

The electric-quadrupole matrix element $Z_2(av)$, which includes retardation, is given in velocity and length forms as:

length gauge

$$Z_2(av) = \left\langle \kappa_a \left\| C_2 \right\| \kappa_v \right\rangle \frac{15}{k^2} \int_0^\infty dr \left\{ j_2(kr) \left[G_a(r) G_v(r) + F_a(r) F_v(r) \right] \right.$$

$$+j_3(kr)\frac{\kappa_a-\kappa_v}{3}\left[G_a(r)F_v(r)+F_a(r)G_v(r)\right]$$
$$+j_3(kr)\left[G_a(r)F_v(r)-F_a(r)G_v(r)\right]\Big\}, \quad (2.30)$$

velocity form

$$Z_2(av)=\langle\kappa_a\|C_2\|\kappa_v\rangle\frac{3}{k^2} \quad (2.31)$$
$$\times\int_0^\infty dr\left[2j_1(kr)+2j_3(kr)\right]\left[G_a(r)F_v(r)-F_a(r)G_v(r)\right]$$
$$+\langle\kappa_a\|C_2\|\kappa_v\rangle\frac{3}{k^2}\frac{\kappa_a-\kappa_v}{3}$$
$$\times\int_0^\infty dr\left[2j_3(kr)-3j_1(kr)\right]\left[G_a(r)F_v(r)+F_a(r)G_v(r)\right].$$

The reduced matrix element for the derivative term is given by the following expressions:

length gauge

$$Z_2^{(\mathrm{derv})}(av)=\langle\kappa_a\|C_2\|\kappa_v\rangle$$
$$\times\frac{15}{k^2}\int_0^\infty dr[2j_2(kr)-(kr)j_3(kr)]$$
$$\times\left[G_a(r)G_v(r)+F_a(r)F_v(r)\right]$$
$$+\langle\kappa_a\|C_2\|\kappa_v\rangle\frac{15}{k^2}\int_0^\infty dr[(kr)j_2(kr)-4j_3(kr)]$$
$$\times\Big[\frac{\kappa_a-\kappa_v}{3}\left[G_a(r)F_v(r)+F_a(r)G_v(r)\right]$$
$$+\left[G_a(r)F_v(r)-F_a(r)G_v(r)\right]\Big] \quad (2.32)$$

velocity form

$$Z_2^{(\mathrm{derv})}(av)=\langle\kappa_a\|C_2\|\kappa_v\rangle\frac{3}{k^2}$$
$$\times\int_0^\infty dr[2j_1(kr)-8j_3(kr)]\left[G_a(r)G_v(r)-F_a(r)F_v(r)\right]$$
$$+\langle\kappa_a\|C_2\|\kappa_v\rangle\frac{3}{k^2}\int_0^\infty dr\left[G_a(r)F_v(r)+F_a(r)G_v(r)\right]$$
$$\times\left[-\frac{\kappa_a-\kappa_v}{3}\right][-5(kr)j_2(kr)+8j_3(kr)+3j_1(kr)] \quad (2.33)$$

The nonrelativistic limit for the length and velocity forms of electric-quadrupole matrix element $Z_2(av)$ is equal to

length gauge

$$Z_2^{nr}(av)=Z(av)=\langle\kappa_a\|C_2\|\kappa_v\rangle\int_0^\infty dr(r)^2P_a(r)P_v(r). \quad (2.34)$$

velocity form

$$Z_2^{nr}(av)=-\langle\kappa_a\|C_2\|\kappa_v\rangle(\varepsilon_v-\varepsilon_a)$$
$$\times\frac{\alpha}{k}\int_0^\infty dr(r)^2P_a(r)P_v(r). \quad (2.35)$$

The nonrelativistic limit for the derivative term of electric-quadrupole matrix element $Z_2^{(\mathrm{dera})}(av)$ is equal to

length gauge

$$Z_2^{(\mathrm{derv})}(av)=\langle\kappa_a\|C_2\|\kappa_v\rangle\,2\int_0^\infty dr(r)^2P_a(r)P_v(r), \quad (2.36)$$

velocity form

$$Z_2^{(\mathrm{derv})}(av)=-\langle\kappa_a\|C_2\|\kappa_v\rangle(\varepsilon_v-\varepsilon_a)$$
$$\times\frac{\alpha}{k}\int_0^\infty dr(r)^2P_a(r)P_v(r). \quad (2.37)$$

The differences between length- and velocity-forms, are illustrated for the uncoupled $0-2p_{3/2}3p_{1/2}(1)$ matrix element in Fig. 32. It should be noted, that the first-order matrix element $Z^{(1)}$ is proportional $1/Z^2$, the second-order Coulomb matrix element $Z^{(2)}$ is proportional $1/Z^3$, and the second-order Breit matrix element $B^{(2)}$ is proportional $1/Z$. Taking into account this dependence, $Z^{(1)}\times Z^2$, $Z^{(2)}\times Z^3$ and $B^{(2)}\times Z\times 10^4$ are shown in the figure. These Z-dependencies apply to the first-order matrix elements $Z^{(2)}$, the second-order matrix elements $B^{(2)}$ and $Z^{(2)}$ for high-Z ions. The contribution of the second-order matrix elements $Z^{(2)}$ is larger in velocity form (Fig. 32). The differences between results in length- and velocity-forms shown in Fig. 32 are compensated by "derivative terms" $P^{(\mathrm{derv})}$, as shown later. It should be noted, that $P^{(\mathrm{derv})}$ in the velocity form almost equals $Z^{(1)}$ in velocity form, whereas $P^{(\mathrm{derv})}$ in length form is larger than $Z^{(1)}$ in length form by factor two.

In Table VIII, we list values of *uncoupled* first- and second-order electric-quadrupole matrix elements $Z^{(1)}$, $Z^{(2)}$, $B^{(2)}$, together with derivative terms $P^{(\mathrm{derv})}$ for Ne-like molybdenum, Z=42. We list values for the 5 electric-quadrupole transitions between even-parity states with J=2 and the ground state. The derivative terms shown in Table VIII arise because transition amplitudes depend on energy, and the transition energy changes order-by-order in MBPT calculations. Both length (L) and velocity (V) forms are given for the matrix elements. We can see that the first-order matrix elements $Z_L^{(1)}$ and $Z_V^{(1)}$ differ by 5-10%; the L–V differences between second-order matrix elements are much larger for some transitions as can be seen by comparing $Z_L^{(2)}$ and $Z_V^{(2)}$. It can be also seen from Table VIII, that $P^{(\mathrm{derv})}$ in velocity form almost equals $Z^{(1)}$ in velocity form but that $P^{(\mathrm{derv})}$ in length form is larger by factor two than $Z^{(1)}$ in length form.

Values of *coupled* reduced matrix elements in length and velocity forms are given in Table IX for the transitions considered in Table VIII. Although we use an intermediate-coupling scheme, it is nevertheless convenient to label the physical states using the jj scheme. We see that L and V forms of the coupled matrix elements in Table IX differ only in the fourth or fifth digits. These L–V differences arise because we start our MBPT calculations using a non-local Dirac-Fock (DF) potential. If we were to replace the DF potential by a local potential, the differences would disappear completely. The

last two columns in Table IX shows L and V values of *coupled* reduced matrix elements calculated without the second-order contribution. As can be seen from this table, removing the second-order contribution increases the $L-V$ differences.

It should be emphasized that we include negative energy state (NES) contributions to sums over intermediate states. The NES contributions drastically change the second-order Breit matrix elements $B^{(2)}$. It could be noted that the $B^{(2)}$ contributes only by 0.05-0.1% in E2 uncoupled matrix elements (see Table VIII) and, as a result, the including of negative-energy states changes the value of E2 matrix element by 0.05-0.1% (see Table IX).

I. Magnetic-quadrupole matrix element

The magnetic-quadrupole matrix element $Z_2(av)$, which includes retardation, is given as:

$$Z_2(av) = \langle -\kappa_a \| C_2 \| \kappa_v \rangle \frac{30}{\alpha k^2} \frac{(\kappa_a + \kappa_v)}{3} \times \int_0^\infty dr j_2(kr) \left[G_a(r) F_v(r) + F_a(r) G_v(r) \right] \quad (2.38)$$

The magnetic-quadrupole derivative matrix element $Z_2(av)$, which includes retardation, is equal to

$$Z_2^{(\mathrm{derv})}(av) = \langle -\kappa_a \| C_2 \| \kappa_v \rangle \frac{30}{\alpha(k)^2} \times \int_0^\infty dr \frac{(\kappa_a + \kappa_v)}{3} \left[2j_2(kr) - (kr) j_3(kr) \right] \times \left[G_a(r) F_v(r) + F_a(r) G_v(r) \right] . \quad (2.39)$$

The nonrelativistic limit for the magnetic-quadrupole matrix element $Z_2(av)$ is

$$\frac{1}{2} Z_2^{(\mathrm{derv})\mathrm{nr}}(av) = Z_2^{nr}(av) = - \langle -\kappa_a \| C_1 \| \kappa_v \rangle \times \frac{\kappa_a + \kappa_v}{3} (\kappa_a + \kappa_v - 2) \int_0^\infty dr(r) P_a(r) P_v(r) , \quad (2.40)$$

where $P_a(r)$ is a nonrelativistic limit of the large-component radial wavefunction $G_a(r)$.

In Table X, we list values of *uncoupled* first- and second-order magnetic-quadrupole matrix elements $Z^{(1)}$, $Z^{(2)}$, $B^{(2)}$, together with derivative terms $P^{(\mathrm{derv})}$ for Ne-like molybdenum, Z=42. We list values for the 6 magnetic-quadrupole transitions between odd-parity states with J=2 and the ground state. The derivative terms shown in Table X arise because transition amplitudes depend on energy, and the transition energy changes order-by-order in MBPT calculations. The first-order matrix elements, $Z_{\mathrm{R}}^{(1)}$, and $Z_{\mathrm{RF}}^{(1)}$ are calculated using Eqs. (2.40) and (2.38) accordingly. As can be seen from Table X, the difference between $Z_{\mathrm{R}}^{(1)}$, and $Z_{\mathrm{RF}}^{(1)}$ is about 1%. The importance of the negative energy state (NES) is illustrated for the second-order Breit matrix elements $B^{(2)}$. In Table X, we compare the values of $B^{(2)}$, calculated without the NES contributions and $B_{NES}^{(2)}$, calculated with including the NES contributions. The difference between $B^{(2)}$, and $B_{NES}^{(2)}$ is about 10%. It should be noted that the first-order magnetic-quadrupole matrix elements $0-2p_{3/2}3p_{3/2}(2)$ is equal to zero. It can be also seen from Table X, that the values of $P^{(\mathrm{derv})}$ is larger by factor two than the values of $Z^{(1)}$.

In Table XI, we present the Z-dependence of line strengths S for magnetic quadrupole (M2) lines in Ne-like ions. In this table the values of line strengths S for Z=20, 30, 40, 50,60, 70, 80, 90, and 100 are given. The S-values are obtained in intermediate-coupling scheme, nevertheless, both LS and jj designations are shown in this table. Among the 6 transitions presented in Table XI, there is the one transition with zero uncoupled matrix element, $0-2p_{3/2}3p_{3/2}(2)$. The only second-order contribution is responsible for the non-zero S-value of this transition. As can be seen from Table XI, the S value of this transitions becomes the smallest S value comparison with values of other five transitions for high Z.

III. COMPARISON OF RESULTS WITH OTHER THEORY AND EXPERIMENT

We calculate energies of the 16 even-parity $2s_{1/2}^{-1}3s_{1/2}(J)$, $2pj^{-1}3pj'(J)$, and $2s_{1/2}^{-1}3dj(J)$ excited states and the 20 odd-parity $2s_{1/2}^{-1}3pj(J)$, $2pj^{-1}3s_{1/2}(J)$, and $2pj^{-1}3dj'(J)$ excited states for Ne-like ions with nuclear charges ranging from Z=11-100. Reduced matrix elements, oscillator strengths, and transition rates are determined for E1, M1, E2, and M2 allowed and forbidden transitions into the ground state for each ions. Comparisons are also given with other theoretical results and with experimental data. Our results are presented in three parts: transition energies, E1 oscillator strengths, and E1, M1, E2, and M2 transition probabilities.

A. Excitation energies

The n=2–3 transitions in Ne-like ions have been thoroughly investigated, theoretically and experimentally. In Tables XII-XVI, our MBPT results of energies are compared with other theoretical calculations and experimental measurements. Detailed comparison between our MBPT results and the MBPT results recently presented by Avgoustouglou *et al.* [19,20] are given in Table XII. There are two different approaches in these two MBPT calculations. In present paper, it is used the closed-shell Dirac-Fock potential, however, in Refs. [19,20] all virtual orbitals were generated in the field of the hole state. The using of $V^{(N-1)}$, $1s^22s^22p^5$ potential is very convenient if there is only one hole state that was really used in

[19,20]. In that paper, only $2p^{-1}3l(J)$ states were investigated. The influence of the $2s^{-1}3l(J)$ states could be taken into account by summing all order diagrams. The using of $V^{(N)}$, $1s^22s^22p^6$ potential allows to treat $2s^{-1}3l(J)$ and $2p^{-1}3l(J)$ simultaneously. This is advantage of the MBPT method presented in our paper. Our disadvantage is the limitation of our calculations by the second-order perturbation theory. It was shown in Refs. [19,20], that the third-order hole-core Coulomb correlation energy $E^{(3+)}$ is about 0.1 a.u. for NeI. This correction is rapidly decreases with Z; the value of $E^{(3+)}$ is about 0.015 a.u. for Ca^{10+}. Comparison of results for the four $2p^{-1}3s(J)$ and three $2p^{-1}3d(1)$ states presented in Table XII confirms this prediction. As can be seen from this table, our MBPT energies differ from results in [19,20] by 0.03-0.05 a.u. for NaII, Z=11 and 0.003-0.03 a.u. for Ca^{10+}, Z=20. It should be noted that the largest difference 0.03 a.u. is happened for the $2p3d\ ^3D_1$ level for ions with nuclear charges ranging from Z=11-26. This difference could be explained by strong mixing all $2p_{3/2}3d_{3/2}(1)$, $2p_{3/2}3d_{5/2}(1)$, and $2p_{1/2}3d_{3/2}(1)$ states including in odd-parity complex with J=1 (see, Fig. 3).

In Table XIII, our MBPT results of energies are compared with theoretical energies presented by Safronova *et al.* [3], adjusted data of energies performed by Hibbert *et al.* [11], and NIST recommended data from Refs. [44–46] for odd-parity states with J=1 in Ne-like ions with Z=19-28. Correlation, relativistic, and radiative effects were taken into in Ref. [3] by using the second-order perturbation theory with hydrogenic basis set. The code CIV3 with incorporating variationally optimized orbitals and a modified Breit-Pauli Hamiltonian was used in Ref. [11] to calculate $2s^22p^6$, $2s^22p^53l$, and $2s2p^63l$ energies of Ne-like ions with Z=10-36. Using experimental data for all ions up to Cu^{19+}, it was incorporated corrections to individual levels by adjusting the diagonal elements of the Hamiltonian matrix in Ref. [11]. As can be seen from Table XIII, adjusted data from [11] are in excellent agreement with NIST data [44–46] for all levels, except the $2s2p^63p\ ^{1,3}P_1$ levels. Disagreement between adjusted data and NIST data for these two $2s2p^63p\ ^{1,3}P_1$ levels increases with Z: from 3000-8000 cm^{-1} for Z=19 up to 140000 cm^{-1} for Z=28. It is also seen from Table XIII, the increasing of disagreement between adjusted and NIST data for $2s^22p^53d\ ^3D_1$, $^1P_1$ levels: from 300-700 cm^{-1} for Z=19 up to 4700-7100 cm^{-1} for Z=28. As can be seen from Table XIII, our data are in a good agreement with experimental data: the disagreement in $2p3d\ ^{1,3}P_1$, $2p3s\ ^3P_1$, and $2s3p\ ^3P_1$ energies is about 300-3000 cm^{-1}, except three levels ($2p3s\ ^1P_1$, $2p3d\ ^3D_1$ and $2s3p\ ^1P_1$), where disagreement is about 2000-4000 cm^{-1}. Disagreement between MBPT data and NIST data for the two $2s2p^63p\ ^{1,3}P_1$ levels is about 1000-3000 cm^{-1}.

Accurate x-ray measurements on Y^{29+}–Nd^{50+} observed in a low-inductance vacuum spark-produced plasmas were reported by Aglitskii *et al.* [21]. In Tables XIV, XV, our MBPT results of energies are compared with experimental measurements from that paper. Theoretical results for ions considered in Refs. [19,20] are also included in Tables XIV. As can be seen from this table, our results agree better with experimental measurements than results from [19,20]. The energies of $2s2p^6\ ^{1,3}P_1$ levels are given in Table XV for high-Z ions. Our results are compared with measurements from [21] for Y^{29+}–Se^{48+} ions and few results for Ag^{37+}, Xe^{44+}, Yb^{60+}, Au^{69+}, and Bi^{73+} reported by Beiersdorfer *et al.* in Refs. [27,29,30], Chandler *et al.* [32], and Dietrich *et al.* [33]. As can be seen from Table XV, the experimental results for Ag^{37+} and Xe^{44+} disagree by 0.3-0.7 a.u.. Our MBPT results are between these two experimental measurements.

Accurate x-ray measurements of $2p$-$3p$, $2s$-$3d$ electric-quadruple and $2s$-$3p$ magnetic-quadruple wavelengths were reported by Beiersdorfer *et al.* in Refs. [27,29–31], Chandler *et al.* [32], and Dietrich *et al.* [33] for Ne-like Ag, Xe, La, Nd, Eu, Yb, Au, Bi, and Th. Our MBPT data are compared with those measurements in Table XVI. We include results for all 36 $2l^{-1}3l'(J)$ levels in this table. As can be seen from Table XVI, our theoretical data are in excellent agreement with experimental measurements. We hope that our predicted data for other lines given in this table could be useful for future experiments.

B. Oscillator strengths and for dipole transitions to the ground state

As mentioned previously, line strengths, oscillator strengths and transition rates for dipole transitions between the odd parity states with J=1 and the ground state are calculated in Ne-like ions with nuclear charges ranging from Z=11-100. Results are obtained in both length and velocity forms but only length-form results are tabulated since length-velocity differences are less than 1% for most cases.

In Figs. 33-35, we present the Z-dependence of oscillator strengths for transitions from $J = 1$ excited states to the ground state. The sharp features in the curves shown in these figures can be explained in many cases by strong mixing of states inside of the odd-parity complex with J=1. In Figs. 33, 34 the double cusp in the interval Z=51-55 is due to mixing between $[2p_{1/2}3s_{1/2}(1)]+[2p_{3/2}3d_{3/2}(1)]+[2p_{3/2}3d_{5/2}(1)]$ states. The mixing of the $[2p_{1/2}3d_{3/2}(1)]+[2s_{1/2}3p_{1/2}(1)]$ states in the Z=69-70 range gives a singularity in the curve with the $2s3p\ ^3P_1$ label (Fig. 35).

These singularities are a consequence of coupling between states governed by the first order mixing coefficients $C_1^N[av(J)]$ in Eq. (2.17). However, some of the singularities are caused by the second order uncoupled matrix elements. As can be seen from expression for $Z_K^{(\mathrm{RPA})}$, Eq. (2.14), the dominator of one term is $\epsilon_{bv}-\epsilon_{na}$. When $v = 3p_{3/2}$, $a = 2s_{1/2}$ and $n = 4d_{3/2}$, $b = 2p_{3/2}$, the sign of denominator is changed in the interval Z=18-19 and the denominator becomes very small for Z=19. In

these cases, the contribution of the term with this small denominator becomes much larger than other contributions, leading to new singularities in the Z-dependence of the oscillator strengths. It is possible to remove some of these singularities by increasing our model space to include $2p_jnd_{j'}$ states with n=4,5 and simultaneously removing these states from sum over n in expression for $Z_K^{(\mathrm{RPA})}$ in Eq. (2.14).

In Table XVII, our MBPT results of oscillator strengths are compared with theoretical results presented by Quinet *et al.* in Ref. [17]. The multiconfigurational Dirac-Fock (MCDF) method, combined with semi-empirical correction to the *Ab initio* values of the energy levels, was used in Ref. [17]. The difference between MBPT and MCDF results increases when Z decreases from 1% for very high-Z ions up to 10% for ions with Z=28.

C. The E1, E2, M1, and M2 transition probabilities

The E1, E2, M1, and M2 transition probabilities $A^{(q)}[0-2lj3l'j'(J)]$ (s^{-1}) given in Figs. 36-39 and Tables XVIII-XXI were obtained in terms of line strengths $S^{(q)}[0-2lj3l'j'(J)]$ and energy $E[2lj3l'j'(J)]$ (a.u.) relative to the ground state using the relation

$$A^{(q)}[0-2lj3l'j'(J)] = \frac{a^{(q)}}{(2J+1)}E^k[2lj3l'j'(J)]S^{(q)}[0-2lj3l'j'(J)] \quad (3.1)$$

where

$$\begin{aligned} E1 = q, \quad k = 3, \quad a^{(q)} &= 2.1420 \times 10^{10} \\ M1 = q, \quad k = 3, \quad a^{(q)} &= 2.8516 \times 10^{5} \\ E2 = q, \quad k = 5, \quad a^{(q)} &= 5.7032 \times 10^{4} \\ M2 = q, \quad k = 5, \quad a^{(q)} &= 7.5926 \times 10^{-1} \end{aligned} \quad (3.2)$$

Transition rates for the seven electric dipole lines are given in Fig. 36 and Table XVIII. As can be seen in Fig. 36, the curves describing $2p3s\ ^3P_1$ and $2s3p\ ^1P_1$ transition rates are smoothly increased with Z, without any sharp feature. It was already mentioned about strong mixing between $[2p_{1/2}3s_{1/2}(1)]+[2p_{3/2}3d_{3/2}(1)]+[2p_{3/2}3d_{5/2}(1)]$ states in the interval Z=51-55. This mixing causes the exchange of labels $2p3d\ ^3P_1$ and $2p3d\ ^3D_1$ and the sharp minimum in the $2p3s\ ^1P_1$ transition rates for Z=52. There are also the minima in the curves describing the $2p3d\ ^3P_1$ (Z=45), $2p3d\ ^3D_1$ (Z=58), and $2s3p\ ^3P_1$ (Z=66) transition rates. Comparison with results performed by Ivanova *et al.* in Ref. [5] confirms our conclusion about these sharp features in the Z-dependences of 2-3 E1 transition rates (see Table XVIII). In Table XVIII, we compare also our MBPT calculations with E1 transition rates calculated by using SUPERSTRUCTURE code [8,9,12] and CIV code [11]. As can be seen from Table XVIII, the disagreement in all results is about 10-20%, except cases with singularities in the curves of transition rates. In this cases, (see, for example, the $2p3d\ ^3P_1$ transition rates for Z=42) our MBPT data are in better agreement with data from Ref. [5], than with data from Ref. [12].

Disagreement between different theoretical results is much larger for magnetic-dipole, M1 transitions rates than for electric-dipole, E1 transitions rates that can be seen from comparison results given in Tables XVIII and XIX. In Table XIX, we compare our MBPT calculations with theoretical results obtained by SUPERSTRUCTURE code [8,9,12] and relativistic perturbation model potential code (RPTMP) [5]. In previous section, we compare results for M1 uncoupled matrix elements (see Figs. 22-25) and M1 line strengths (see Figs. 26-31) calculated by using nonrelativistic, relativistic and frequency-dependent relativistic first-order matrix elements (Eqs. (2.27), (2.25), and (2.23)). The difference in approximation leads to the difference in results by a factor two even for uncoupled matrix elements and drastically changes Z-dependence of coupled matrix elements. The largest difference is between results obtained for nonrelativistic or relativistic first-order matrix elements. It should be noted that in SUPERSTRUCTUTRE code, the wavefunctions were determined by diagonalization of nonrelativistic Hamiltonian using orbitals calculated in a scaled Thomas-Fermi-Dirac-Amaldi (TFDA) potential. These nonrelativistic functions were used to calculate M1 matrix elements. As can be seen from Table XIX, our MBPT results and SUPERSTRUCTUTRE results from [8,9,12], differ by 20-30% for $2p3p\ ^3P_1$ transition rates and by factor 2-3 for $2p3p\ ^3S_1, ^3D_1\ ^1P_1$ transition rates. The difference between two results in three magnitude for $2p3p\ ^3D_1$ transition rates with Z=29 can be explained by the minimum in the curve of $2p3p\ ^3D_1$ transition rates shown in Fig. 37. Much better agreement was found between our results and results obtained by using RPTMP method in Ref. [5], where used relativistic approach. As can be seen from Table XIX, the difference between MBPT results and results from Ref. [5] is about 20% for many cases.

The E2 transition rates are less sensitive to different approximations than the M1 transition rates that can be seen from comparison Tables XIX and XX. In Table XX, our MBPT calculations are compared with theoretical results obtained by SUPERSTRUCTURE code [8,9,12] and by RPTMP code [5]. As can seen from this table, the disagreement between results is about 10-20% for most of cases. It should be noted that there is the very small difference between the $2p3p\ ^3D_2, ^3P_2, ^1D_2$ transition rates. This can be seen from Table XX and Fig. 38. In this figure, transition rates for the six electric quadrupole lines are illustrated. These curves describing E2 transition rates are smoothly increased with Z, without any sharp feature except some singularity for the $2s3d\ ^{1,3}D_2$ transition rates for small Z. These singularities are caused by the second order uncoupled matrix elements that was already discussed in the previous section.

The similar smooth Z-dependence is shown in Fig. 39. In this figure, the transition rates for the six magnetic quadrupole lines are presented. As can be seen from Fig. 39, the curve describing the $2p3d\ ^3P_2$ transition rate crosses the five other curves M2 transitions rates to be the smallest one between M2 rates for Z >54. This decreasing of the $2p3d\ ^3P_2$ transition rates can be explained that for high Z the jj coupling scheme is more suitable than LS coupling scheme. The value of uncoupled $0 - 2p_{3/2}3p_{3/2}(2)$ matrix element is not equal to zero only because of the second-order contribution. The mixing inside of odd-parity complex with J=2 becomes smaller with increasing Z, as can be seen from Figs. 6, 7, and the coupled $0 - 2p3d\ ^3P_2$ matrix element is almost equal to uncoupled $0 - 2p_{3/2}3p_{3/2}(2)$ matrix element. This is very interesting example to observe when intermediate-coupling scheme converts to pure jj coupling scheme. In Table XXI, our MBPT calculations are compared with theoretical results obtained by MCDF code [13] and by RPTMP code [5]. As can be seen from this table, the disagreement between results for high-Z ions is about 10-20%. The largest disagreement between MBPT and MCDF [13] results, we found in the $2p3d\ ^3F_2$ transition rate for small-Z ions. This disagreement, can be explained by strong mixing for this level between $2p_{3/2}3d_{3/2}(2)$ and $2p_{3/2}3d_{5/2}(2)$ states.

IV. CONCLUSION

We have presented a systematic second-order relativistic MBPT study of excitation energy, reduced matrix elements, oscillator strengths, and transition rates for Δn=1 electric and magnetic dipole and quadrupole transitions in Ne-like ions with nuclear charges ranging from Z =11-100. The retarded $E1, E2, M1, M2$ matrix elements included correlation corrections from Coulomb and Breit interactions. Contributions from virtual electron-positron pairs were also included in the second-order matrix elements. Both length and velocity forms of the $E1, E2$ matrix elements were evaluated, and small differences, caused by the non-locality of the starting HF potential, were found between the two forms. Second-order MBPT transition energies were used to evaluate oscillator strengths and transition rates. Good agreement our MBPT data with other accurate theoretical results obtained for low-Z ions, gives us possibility to conclude that the MBPT method can provide accurate data for all-Z ions.

ACKNOWLEDGMENTS

U.I.Safronova would like to thank the members of the Data and Planning Center, the National Institute for Fusion Science for their hospitality, friendly support and many interesting discussions.

REFERENCES

[1] L. A. Bureeva and U. I. Safronova, Phys. Scripta, **20**, 81 (1979).
[2] E. V. Aglitskii, E. Ya. Golts, Yu. A. Levykin, A. M. Livshits, S. L. Mandelshtam and U. I. Safronova, Opt. Spectrosc. **46**, 590 (1979).
[3] U.I. Safronova, M. S. Safronova and R. Bruch, Phys. Scripta, **49**, 446 (1994).
[4] E. P. Ivanova and A. V. Glushkov, Journ. Quant. Spectr. Rad. Transf., **36**, 127 (1986).
[5] E. P. Ivanova and A. V. Gulov, Atomic Data and Nucl. Data Tables **49**, 1 (1991).
[6] U. I. Safronova and J.-F. Wyart, Phys. Scripta, **46**, 134 (1992).
[7] E. P. Ivanova and I. P. Grant, J. Phys. B, **31**, 2671 (1998).
[8] A. K. Bhatia, U. Feldman and J. F. Seely, Atomic Data and Nucl. Data Tables **32**, 435 (1985).
[9] A. K. Bhatia and G. A. Doschek, Atomic Data and Nucl. Data Tables **52**, 1 (1992).
[10] Y. Kagawa, Y. Honda and S. Kiyokawa, Phys. Rev. A, **44**, 7092 (1991).
[11] A. Hibbert, M. Le Dourneuf, and M. Mohan, Atomic Data and Nucl. Data Tables **53**, 23 (1993).
[12] M. Cornille, J. Dubau and S. Jacquemot, Atomic Data and Nucl. Data Tables **58**, 1 (1994).
[13] W. Fielder, Jr., D. L. Lin and D. Ton-That, Phys. Rev. A, **19**, 741 (1979).
[14] A. K. Das, Astr. J.,**468**, 445 (1996).
[15] C. Hongshan, D. Chenzhong and Z. Xiaoxin, Journ. Quant. Spectr. Rad. Transf., **61**, 143 (1999).
[16] A. Hibbert and M. P. Scott, J. Phys. B, **27**, 1315 (1994).
[17] P. Quinet, T. Gorilia and E. Biémont, Phys. Scripta, **44**, 164 (1991).
[18] E. Avgoustoglou, W. R. Johnson, D. R. Plante, J. Sapirstein, S. Sheinerman and S. A. Blundell, Phys. Rev. A **46**, 5478 (1992).
[19] E. Avgoustoglou, W. R. Johnson and J. Sapirstein, Phys. Rev. A **51**, 1196 (1995).
[20] E. Avgoustoglou and Z. W. Liu, Phys. Rev. A **54**, 1351 (1996).
[21] E. V. Aglitskii, E. P. Ivanova, S. A. Panin, U. I. Safronova, S.I. Ulitin, L. A., Vainshtein and J.-F. Wyart, Phys. Scripta, **40**, 601 (1989).
[22] V. A. Boiko, A. Ya. Faenov and S. A. Pikuz, Journ. Quant. Spectr. Rad. Transf., **19**, 11 (1979).
[23] H. Gordon, M. G. Hobby, N. J. Peacock and R. D. Cowan, J. Phys. B, **12**, 881 (1979).
[24] H. Gordon, H. G. Hobby and N. J. Peacock, J. Phys. B, **13**, 1985 (1980).
[25] C. Jupén and U. Litzén, Phys. Scripta, **30**, 112 (1984).
[26] J.-C. Gauthier, J.-P. Geindre, P. Monier, E. Luc-Koenig and J.-F. Wyart, J. Phys. B, **19**, L391 (1986).
[27] P. Beiersdorfer, M. Bitter, S. von Goeler, S. Cohen, K.

W. Hill, J. Timberlake, R. S. Walling, M. H. Chen, P. L. Hagelstein and J. H. Scofield, Phys. Rev. A **34**, 1297 (1986).

[28] J. P. Buchet, M. C. Buchet-Poulizac, A. Denis, J. Desesquelles, M. Druetta, S. Martin, D. Leclerc, E. Luc-Koenig, and J.-F. Wyart, Nucl. Instrum. Methods Phys. Res. B, **31**, 177 (1988).

[29] P. Beiersdorfer, S. von Goeler, M. Bitter, E. Hinnov, R. Bell, S. Bernabei, J. Felt, K. W. Hill, R. Hulse, J. Stevens, S. Suckewer, J. Timberlake, A. Wouters, M.H. Chen, J. H. Scofield, D. D. Dietrich, M. Gerassimenko, E. Silver, R. S. Walling and P. L. Hagelstein, Phys. Rev. A **37**, 4153 (1988).

[30] P. Beiersdorfer, M. H. Chen, R. E. Marrs and M. A. Levine, Phys. Rev. A **41**, 3453 (1990).

[31] P. Beiersdorfer, Nucl. Instrum. Methods Phys. Res. B, **56**, 1144 (1991).

[32] G. A. Chandler, M. H. Chen, D. D. Dietrich, P. O. Egan, K. P. Ziock, P. H. Mokler, S. Reusch and D. H. H. Hoffmann, Phys. Rev. A **39**, 565 (1989).

[33] D. D. Dietrich, A. Simionovici, M. H. Chen, G. Chandler, C. J. Hailey, P. O. Egan, P. H. Mokler, S. Reusch and D. H. H. Hoffmann, Phys. Rev. A **41**, 1450 (1990).

[34] G. Yuan, Y. Kato, R. Kodama, K. Murai and T. Kagava, Phys. Scripta, **53**, 197 (1996).

[35] N. Nakamura, D. Kato and S. Ohtani, Phys. Rev. A **61**, 052510 (2000).

[36] M. S. Safronova, W. R. Johnson and U. I. Safronova, Phys. Rev. A **53**, 4036 (1996).

[37] U. I. Safronova, W. R. Johnson, M. S. Safronova and A. Derevianko, Phys. Scr. **59**, 286 (1999).

[38] M. H. Chen, K. T. Cheng and W. R. Johnson, Phys. Rev. A **47**, 3692 (1993).

[39] W. R. Johnson, S. A. Blundell and J. Sapirstein, Phys. Rev. A**37**, 2764 (1988).

[40] P. J. Mohr, Ann. Phys. (N.Y.) **88**, 26 (1974); Ann. Phys. (N.Y.) **88**, 52 (1974); Phys. Rev. Lett. **34**, 1050 (1975).

[41] L. D. Landau and E. M. Lifshitz, p. 281 *Quantum Mechanics-Non-Relativistic Theory*, Pergamon Press, London (1963)

[42] W. R. Johnson, D. R. Plante and J. Sapirstein, Advances in Atomic, Molecular, and Optical Physics **35**, 255 (1995).

[43] U. I. Safronova, W. R. Johnson and A. Derevianko, 1999, *Phys. Scripta*, **60**, 46.

[44] J. Shugar and Ch. Corliss, J. Phys. Chem. Ref. Data **14**, Suppl. 2 (1985)

[45] W. C. Martin, J. R. Fuhr and W. L. Wiese, J. Phys. Chem. Ref. Data **17**, Suppl. 3 (1988)

[46] J. R. Fuhr, W.C. Martin and W. L. Wiese, J. Phys. Chem. Ref. Data **17**, Suppl. 4 (1988)

TABLE I. Possible hole-particle states in the $2lj3l'j'$ complex; jj and LS coupling schemes

Even-parity states		Odd-parity states	
jj coupling	LS coupling	jj coupling	LS coupling
$2p_{3/2}3p_{3/2}$ (0)	$2p3p\ ^3P_0$	$2p_{1/2}3s_{1/2}$ (0)	$2p3s\ ^3P_0$
$2p_{1/2}3p_{1/2}$ (0)	$2p3p\ ^1S_0$	$2p_{3/2}3d_{3/2}$ (0)	$2p3d\ ^3P_0$
$2s_{1/2}3s_{1/2}$ (0)	$2s3s\ ^1S_0$	$2s_{1/2}3p_{1/2}$ (0)	$2s3p\ ^3P_0$
$2p_{3/2}3p_{1/2}$ (1)	$2p3p\ ^3S_1$	$2p_{3/2}3s_{1/2}$ (1)	$2p3s\ ^3P_1$
$2p_{3/2}3p_{3/2}$ (1)	$2p3p\ ^3D_1$	$2p_{1/2}3s_{1/2}$ (1)	$2p3s\ ^1P_1$
$2p_{1/2}3p_{1/2}$ (1)	$2p3p\ ^1P_1$	$2p_{3/2}3d_{3/2}$ (1)	$2p3d\ ^3P_1$
$2p_{1/2}3p_{3/2}$ (1)	$2p3p\ ^3P_1$	$2p_{3/2}3d_{5/2}$ (1)	$2p3d\ ^3D_1$
$2s_{1/2}3s_{1/2}$ (1)	$2s3s\ ^3S_1$	$2p_{1/2}3d_{3/2}$ (1)	$2p3d\ ^1P_1$
$2s_{1/2}3d_{3/2}$ (1)	$2s3d\ ^3D_1$	$2s_{1/2}3p_{1/2}$ (1)	$2s3p\ ^3P_1$
		$2s_{1/2}3p_{3/2}$ (1)	$2s3p\ ^1P_1$
$2p_{3/2}3p_{1/2}$ (2)	$2p3p\ ^3D_2$	$2p_{3/2}3s_{1/2}$ (2)	$2p3s\ ^3P_2$
$2p_{3/2}3p_{3/2}$ (2)	$2p3p\ ^3P_2$	$2p_{3/2}3d_{5/2}$ (2)	$2p3d\ ^3P_2$
$2p_{1/2}3p_{3/2}$ (2)	$2p3p\ ^1D_2$	$2p_{3/2}3d_{3/2}$ (2)	$2p3d\ ^3F_2$
$2s_{1/2}3d_{3/2}$ (2)	$2s3d\ ^3D_2$	$2p_{1/2}3d_{3/2}$ (2)	$2p3d\ ^1D_2$
$2s_{1/2}3d_{5/2}$ (2)	$2s3d\ ^1D_2$	$2p_{1/2}3d_{5/2}$ (2)	$2p3d\ ^3D_2$
		$2s_{1/2}3p_{3/2}$ (2)	$2s3p\ ^3P_2$
$2p_{3/2}3p_{3/2}$ (3)	$2p3p\ ^3D_3$	$2p_{3/2}3d_{3/2}$ (3)	$2p3d\ ^3F_3$
$2s_{1/2}3d_{5/2}$ (3)	$2s3d\ ^3D_3$	$2p_{3/2}3d_{5/2}$ (3)	$2p3d\ ^3D_3$
		$2p_{1/2}3d_{5/2}$ (3)	$2p3d\ ^1F_3$
		$2p_{3/2}3d_{5/2}$ (4)	$2p3d\ ^3F_4$

TABLE II. Contributions to the one-electron $E_v^{(2)}$ and one-hole energy $E_a^{(2)}$ for ions with a $1s^22s^22p^6$ core from the three diagrams $V_1 - V_3$ evaluated for the case of molybdenum, $Z = 42$.

	(a) - Coulomb Interaction:			(b) - Breit Correction:		
	$V_1^{\rm HF}$	$V_2^{\rm HF}$	$V_3^{\rm HF}$	$V_1^{\rm BHF}$	$V_2^{\rm BHF}$	$V_3^{\rm BHF}$
$2s_{1/2}$	0.05831	-0.16649		0.00458	-0.00307	0.02143
$2p_{1/2}$	0.10097	-0.16856		0.00684	-0.00330	0.02529
$2p_{3/2}$	0.09865	-0.15647		0.00547	-0.00210	0.02514
$3s_{1/2}$	-0.03908	0.00937		-0.00084	0.00027	-0.00359
$3p_{1/2}$	-0.04682	0.00968		-0.00128	0.00033	-0.00448
$3p_{3/2}$	-0.04462	0.00931		-0.00118	0.00026	-0.00454
$3d_{3/2}$	-0.04866	0.00766		-0.00118	0.00059	-0.00446
$3d_{5/2}$	-0.04726	0.00784		-0.00086	0.00036	-0.00419

TABLE III. Diagonal and nondiagonal contributions to the second-order interaction term in the effective Hamiltonian matrix from diagrams $R_1 - R_4$ calculated using HF orbitals. These contributions are given for a hole-particle ion with a $1s^2 2s^2 2p^6 3$ core, in the case of molybdenum, $Z = 42$.

	(a) Coulomb Interaction:				(b) - Breit Correction:			
	$R_1^{\rm HF}$	$R_2^{\rm HF}$	$R_3^{\rm HF}$	$R_4^{\rm HF}$	$R_1^{\rm BHF}$	$R_2^{\rm BHF}$	$R_3^{\rm BHF}$	$R_4^{\rm BHF}$
Even parity states, J=0								
$2p_{3/2}3p_{3/2}, 2p_{3/2}3p_{3/2}$	-0.00817	-0.03287	0.01935		-0.00038	-0.00056	0.00023	0.00137
$2p_{1/2}3p_{1/2}, 2p_{1/2}3p_{1/2}$	-0.00188	-0.01274	0.01048		-0.00028	-0.00031	0.00043	0.00254
$2s_{1/2}3s_{1/2}, 2s_{1/2}3s_{1/2}$	-0.00136	-0.00915	0.00040		-0.00009	-0.00024	0.00013	0.00141
$2p_{3/2}3p_{3/2}, 2p_{1/2}3p_{1/2}$	0.00914	0.02958	-0.01171		0.00020	0.00011	0.00048	0.00083
$2p_{1/2}3p_{1/2}, 2p_{3/2}3p_{3/2}$	0.00943	0.03056	-0.01300		0.00015	0.00011	0.00035	0.00090
$2p_{3/2}3p_{3/2}, 2s_{1/2}3s_{1/2}$	-0.00538	-0.01945	0.02552		-0.00009	-0.00016	0.00001	-0.00020
$2s_{1/2}3s_{1/2}, 2p_{3/2}3p_{3/2}$	-0.00608	-0.02121	0.02782		0.00001	-0.00018	0.00011	-0.00027
$2p_{1/2}3p_{1/2}, 2s_{1/2}3s_{1/2}$	0.00396	0.01422	-0.01765		0.00006	0.00006	0.00005	0.00040
$2s_{1/2}3s_{1/2}, 2p_{1/2}3p_{1/2}$	0.00426	0.01501	-0.01829		-0.00001	0.00006	0.00013	0.00045
Even parity states, J=1								
$2p_{3/2}3p_{1/2}, 2p_{3/2}3p_{1/2}$	0.00783	0.01131	-0.01027		0.00001	-0.00009	0.00079	0.00325
$2p_{3/2}3p_{3/2}, 2p_{3/2}3p_{3/2}$	0.00804	0.01274	-0.01708		0.00031	0.00036	-0.00023	0.00220
$2p_{1/2}3p_{1/2}, 2p_{1/2}3p_{1/2}$	0.00705	0.01274	-0.01055		0.00034	0.00032	-0.00045	0.00355
$2p_{1/2}3p_{3/2}, 2p_{1/2}3p_{3/2}$	0.00730	0.01271	-0.01263		0.00006	-0.00020	0.00108	0.00245
$2s_{1/2}3s_{1/2}, 2s_{1/2}3s_{1/2}$	0.00420	0.00916	-0.01067		0.00015	0.00024	-0.00018	0.00160
$2s_{1/2}3d_{3/2}, 2s_{1/2}3d_{3/2}$	0.00632	0.00508	-0.02749		0.00011	0.00009	0.00049	0.00233
$2p_{3/2}3p_{1/2}, 2p_{3/2}3p_{3/2}$	-0.00284	-0.00234	0.00955		-0.00011	-0.00010	0.00030	-0.00008
$2p_{3/2}3p_{3/2}, 2p_{3/2}3p_{1/2}$	-0.00282	-0.00236	0.00979		-0.00009	-0.00010	0.00030	-0.00009
$2p_{3/2}3p_{1/2}, 2p_{1/2}3p_{1/2}$	-0.00015	0.00001	0.00108		0.00002	0.00002	-0.00021	0.00000
$2p_{1/2}3p_{1/2}, 2p_{3/2}3p_{1/2}$	-0.00014	0.00001	0.00116		0.00000	0.00002	0.00010	0.00000
$2p_{3/2}3p_{1/2}, 2p_{1/2}3p_{3/2}$	0.00281	0.00309	-0.01228		0.00019	0.00016	-0.00016	0.00006
$2p_{1/2}3p_{3/2}, 2p_{3/2}3p_{1/2}$	0.00275	0.00326	-0.01381		0.00019	0.00017	-0.00008	0.00009
$2p_{3/2}3p_{1/2}, 2s_{1/2}3s_{1/2}$	-0.00268	-0.00217	-0.00435		-0.00002	-0.00001	-0.00014	-0.00008
$2s_{1/2}3s_{1/2}, 2p_{3/2}3p_{1/2}$	-0.00254	-0.00239	-0.00160		-0.00007	-0.00001	-0.00016	-0.00019
$2p_{3/2}3p_{1/2}, 2s_{1/2}3d_{3/2}$	0.00053	-0.00152	0.00416		-0.00002	0.00003	0.00005	0.00016
$2s_{1/2}3d_{3/2}, 2p_{3/2}3p_{1/2}$	0.00048	-0.00178	0.00278		-0.00002	0.00003	0.00015	0.00025
$2p_{3/2}3p_{3/2}, 2p_{1/2}3p_{1/2}$	0.00178	0.00171	-0.00559		-0.00005	-0.00023	0.00038	0.00004
$2p_{1/2}3p_{1/2}, 2p_{3/2}3p_{3/2}$	0.00176	0.00176	-0.00609		-0.00004	-0.00023	0.00067	0.00005
$2p_{3/2}3p_{3/2}, 2p_{1/2}3p_{3/2}$	-0.00276	-0.00252	0.00954		-0.00012	-0.00008	0.00041	-0.00002
$2p_{1/2}3p_{3/2}, 2p_{3/2}3p_{3/2}$	-0.00271	-0.00263	0.01062		-0.00011	-0.00008	-0.00007	-0.00004
$2p_{3/2}3p_{3/2}, 2s_{1/2}3s_{1/2}$	0.00299	0.00276	0.00413		0.00006	0.00006	0.00004	0.00011
$2s_{1/2}3s_{1/2}, 2p_{3/2}3p_{3/2}$	0.00285	0.00302	0.00121		0.00009	0.00007	0.00008	0.00019
$2p_{3/2}3p_{3/2}, 2s_{1/2}3d_{3/2}$	0.00042	-0.00146	0.00387		0.00004	0.00005	-0.00022	0.00006
$2s_{1/2}3d_{3/2}, 2p_{3/2}3p_{3/2}$	0.00038	-0.00171	0.00288		0.00006	0.00005	-0.00033	0.00010
$2p_{1/2}3p_{1/2}, 2p_{1/2}3p_{3/2}$	-0.00014	0.00001	0.00106		-0.00001	-0.00001	0.00000	0.00000
$2p_{1/2}3p_{3/2}, 2p_{1/2}3p_{1/2}$	-0.00014	0.00001	0.00108		0.00001	-0.00001	0.00000	0.00000
$2p_{1/2}3p_{1/2}, 2s_{1/2}3s_{1/2}$	0.00089	0.00081	0.00137		-0.00002	-0.00006	0.00023	0.00000
$2s_{1/2}3s_{1/2}, 2p_{1/2}3p_{1/2}$	0.00086	0.00086	0.00084		-0.00001	-0.00007	0.00020	0.00001
$2p_{1/2}3p_{1/2}, 2s_{1/2}3d_{3/2}$	0.00139	-0.00441	0.01185		-0.00001	-0.00004	0.00025	0.00035
$2s_{1/2}3d_{3/2}, 2p_{1/2}3p_{1/2}$	0.00130	-0.00498	0.00963		-0.00002	-0.00005	0.00023	0.00051
$2p_{1/2}3p_{3/2}, 2s_{1/2}3s_{1/2}$	-0.00251	-0.00261	-0.00322		-0.00005	-0.00002	-0.00009	-0.00001
$2s_{1/2}3s_{1/2}, 2p_{1/2}3p_{3/2}$	-0.00245	-0.00273	-0.00190		-0.00005	-0.00002	-0.00002	-0.00004
$2p_{1/2}3p_{3/2}, 2s_{1/2}3d_{3/2}$	0.00043	-0.00168	0.00438		0.00000	-0.00003	0.00015	0.00003
$2s_{1/2}3d_{3/2}, 2p_{1/2}3p_{3/2}$	0.00040	-0.00189	0.00376		-0.00002	-0.00003	0.00015	0.00006
$2s_{1/2}3s_{1/2}, 2s_{1/2}3d_{3/2}$	0.00000	0.00000	0.00000		0.00001	0.00000	-0.00010	0.00000
$2s_{1/2}3d_{3/2}, 2s_{1/2}3s_{1/2}$	0.00000	0.00000	0.00000		0.00001	0.00000	-0.00013	0.00000
Even parity states, J=2								
$2p_{3/2}3p_{1/2}, 2p_{3/2}3p_{1/2}$	0.00584	0.00936	-0.00388		0.00014	0.00010	-0.00011	0.00321
$2p_{3/2}3p_{3/2}, 2p_{3/2}3p_{3/2}$	0.00416	0.00739	0.00139		-0.00009	-0.00016	0.00071	0.00213
$2p_{1/2}3p_{3/2}, 2p_{1/2}3p_{3/2}$	0.00536	0.01033	-0.00572		0.00017	0.00021	-0.00025	0.00242
$2s_{1/2}3d_{3/2}, 2s_{1/2}3d_{3/2}$	0.00387	0.00102	-0.01373		0.00012	0.00002	-0.00045	0.00222
$2s_{1/2}3d_{5/2}, 2s_{1/2}3d_{5/2}$	0.00259	-0.00101	-0.00855		-0.00003	-0.00001	0.00041	0.00144
$2p_{3/2}3p_{1/2}, 2p_{3/2}3p_{3/2}$	-0.00055	-0.00102	0.00072		-0.00003	-0.00006	0.00014	0.00000
$2p_{3/2}3p_{3/2}, 2p_{3/2}3p_{1/2}$	-0.00056	-0.00103	0.00073		-0.00003	-0.00006	0.00014	0.00000

	R_1^{HF}	R_2^{HF}	R_3^{HF}	R_4^{HF}	R_1^{BHF}	R_2^{BHF}	R_3^{BHF}	R_4^{BHF}
Even parity states, J=2								
$2p_{3/2}3p_{1/2}, 2p_{1/2}3p_{3/2}$	-0.00190	-0.00309	0.00749		-0.00019	-0.00016	0.00020	-0.00004
$2p_{1/2}3p_{3/2}, 2p_{3/2}3p_{1/2}$	-0.00192	-0.00325	0.00831		-0.00019	-0.00017	0.00025	-0.00006
$2p_{3/2}3p_{1/2}, 2s_{1/2}3d_{3/2}$	0.00152	-0.00263	0.01013		0.00008	0.00001	-0.00015	0.00037
$2s_{1/2}3d_{3/2}, 2p_{3/2}3p_{1/2}$	0.00135	-0.00309	0.00658		0.00010	0.00001	-0.00028	0.00063
$2p_{3/2}3p_{1/2}, 2s_{1/2}3d_{5/2}$	-0.00012	0.00233	-0.00279		0.00003	0.00002	-0.00008	-0.00013
$2s_{1/2}3d_{5/2}, 2p_{3/2}3p_{1/2}$	-0.00015	0.00272	-0.00217		0.00006	0.00002	-0.00016	-0.00018
$2p_{3/2}3p_{3/2}, 2p_{1/2}3p_{3/2}$	-0.00056	-0.00112	0.00089		-0.00004	-0.00001	-0.00017	-0.00001
$2p_{1/2}3p_{3/2}, 2p_{3/2}3p_{3/2}$	-0.00059	-0.00117	0.00091		-0.00004	-0.00002	0.00015	-0.00001
$2p_{3/2}3p_{3/2}, 2s_{1/2}3d_{3/2}$	0.00058	0.00020	0.00224		0.00006	0.00003	-0.00013	0.00007
$2s_{1/2}3d_{3/2}, 2p_{3/2}3p_{3/2}$	0.00050	0.00022	0.00111		0.00008	0.00003	-0.00022	0.00012
$2p_{3/2}3p_{3/2}, 2s_{1/2}3d_{5/2}$	0.00068	0.00022	0.00269		0.00002	0.00003	-0.00008	0.00009
$2s_{1/2}3d_{5/2}, 2p_{3/2}3p_{3/2}$	0.00058	0.00025	0.00120		0.00005	0.00004	-0.00012	0.00016
$2p_{1/2}3p_{3/2}, 2s_{1/2}3d_{3/2}$	-0.00022	0.00322	-0.00557		0.00002	0.00006	-0.00012	0.00000
$2s_{1/2}3d_{3/2}, 2p_{1/2}3p_{3/2}$	-0.00021	0.00361	-0.00509		0.00006	0.00006	-0.00013	-0.00001
$2p_{1/2}3p_{3/2}, 2s_{1/2}3d_{5/2}$	0.00129	-0.00224	0.00909		-0.00001	-0.00002	0.00013	0.00016
$2s_{1/2}3d_{5/2}, 2p_{1/2}3p_{3/2}$	0.00119	-0.00253	0.00731		0.00002	-0.00003	0.00016	0.00025
$2s_{1/2}3d_{3/2}, 2s_{1/2}3d_{5/2}$	-0.00297	-0.00496	0.01548		-0.00009	-0.00006	-0.00006	-0.00006
$2s_{1/2}3d_{5/2}, 2s_{1/2}3d_{3/2}$	-0.00297	-0.00498	0.01560		-0.00011	-0.00006	-0.00006	-0.00006
Even parity states, J=3								
$2p_{3/2}3p_{3/2}, 2p_{3/2}3p_{3/2}$	0.00753	0.01276	-0.01377		0.00031	0.00036	-0.00043	0.00220
$2s_{1/2}3d_{5/2}, 2s_{1/2}3d_{5/2}$	0.00619	0.00507	-0.02588		0.00017	0.00003	-0.00022	0.00141
$2p_{3/2}3p_{3/2}, 2s_{1/2}3d_{5/2}$	0.00155	-0.00535	0.01397		0.00002	-0.00005	-0.00001	0.00027
$2s_{1/2}3d_{5/2}, 2p_{3/2}3p_{3/2}$	0.00140	-0.00626	0.01024		-0.00001	-0.00006	-0.00002	0.00045
Odd parity states, J=0								
$2p_{1/2}3s_{1/2}, 2p_{1/2}3s_{1/2}$	0.00620	0.01038	-0.00903		0.00003	-0.00009	0.00066	0.00199
$2p_{3/2}3d_{3/2}, 2p_{3/2}3d_{3/2}$	0.00969	0.00080	-0.01625		-0.00007	0.00000	0.00191	0.00255
$2s_{1/2}3p_{1/2}, 2s_{1/2}3p_{1/2}$	0.00487	0.00733	-0.00884		0.00000	-0.00004	0.00051	0.00295
$2p_{1/2}3s_{1/2}, 2p_{3/2}3d_{3/2}$	0.00054	-0.00574	0.00900		-0.00009	-0.00010	0.00029	-0.00012
$2p_{3/2}3d_{3/2}, 2p_{1/2}3s_{1/2}$	0.00051	-0.00589	0.00925		-0.00013	-0.00011	0.00022	-0.00013
$2p_{1/2}3s_{1/2}, 2s_{1/2}3p_{1/2}$	-0.00245	-0.00387	-0.00366		-0.00015	-0.00017	-0.00001	0.00004
$2s_{1/2}3p_{1/2}, 2p_{1/2}3s_{1/2}$	-0.00236	-0.00434	-0.00061		-0.00020	-0.00018	0.00007	-0.00006
$2p_{3/2}3d_{3/2}, 2s_{1/2}3p_{1/2}$	-0.00143	0.00949	-0.02636		0.00012	0.00002	-0.00031	-0.00067
$2s_{1/2}3p_{1/2}, 2p_{3/2}3d_{3/2}$	-0.00134	0.01032	-0.02738		0.00008	0.00002	-0.00047	-0.00077
Odd parity states, J=1								
$2p_{3/2}3s_{1/2}, 2p_{3/2}3s_{1/2}$	0.00369	0.00367	0.00054		-0.00002	-0.00002	0.00022	0.00171
$2p_{1/2}3s_{1/2}, 2p_{1/2}3s_{1/2}$	0.00485	0.00714	-0.00411		0.00005	0.00008	-0.00009	0.00195
$2p_{3/2}3d_{3/2}, 2p_{3/2}3d_{3/2}$	0.00688	-0.00057	-0.00555		0.00011	0.00001	0.00028	0.00246
$2p_{3/2}3d_{5/2}, 2p_{3/2}3d_{5/2}$	0.00648	-0.00027	-0.00721		-0.00008	-0.00001	0.00010	0.00196
$2p_{1/2}3d_{3/2}, 2p_{1/2}3d_{3/2}$	0.00498	-0.00127	-0.00027		0.00001	-0.00003	-0.00011	0.00279
$2s_{1/2}3p_{1/2}, 2s_{1/2}3p_{1/2}$	0.00433	0.00687	-0.00600		0.00009	0.00004	-0.00013	0.00286
$2s_{1/2}3p_{3/2}, 2s_{1/2}3p_{3/2}$	0.00344	0.00613	-0.00399		0.00005	0.00005	-0.00003	0.00189
$2p_{3/2}3s_{1/2}, 2p_{1/2}3s_{1/2}$	-0.00194	-0.00434	0.00668		-0.00006	-0.00003	-0.00011	-0.00005
$2p_{1/2}3s_{1/2}, 2p_{3/2}3s_{1/2}$	-0.00198	-0.00452	0.00725		-0.00009	-0.00003	-0.00007	-0.00006
$2p_{3/2}3s_{1/2}, 2p_{3/2}3d_{3/2}$	0.00133	0.00006	0.00086		0.00001	-0.00005	0.00015	0.00003
$2p_{3/2}3d_{3/2}, 2p_{3/2}3s_{1/2}$	0.00132	0.00007	0.00067		-0.00004	-0.00005	0.00015	0.00004
$2p_{3/2}3s_{1/2}, 2p_{3/2}3d_{5/2}$	0.00292	0.00899	-0.01109		0.00012	0.00008	-0.00017	0.00012
$2p_{3/2}3d_{5/2}, 2p_{3/2}3s_{1/2}$	0.00298	0.00962	-0.01257		0.00009	0.00009	-0.00022	0.00015
$2p_{3/2}3s_{1/2}, 2p_{1/2}3d_{3/2}$	-0.00244	-0.00402	0.00404		-0.00009	0.00001	0.00004	-0.00009
$2p_{1/2}3d_{3/2}, 2p_{3/2}3s_{1/2}$	-0.00249	-0.00446	0.00535		-0.00002	0.00001	0.00027	-0.00014
$2p_{3/2}3s_{1/2}, 2s_{1/2}3p_{1/2}$	-0.00131	-0.00006	-0.01064		-0.00002	0.00002	-0.00014	-0.00011
$2s_{1/2}3p_{1/2}, 2p_{3/2}3s_{1/2}$	-0.00112	-0.00007	-0.00861		-0.00001	0.00002	-0.00004	-0.00025
$2p_{3/2}3s_{1/2}, 2s_{1/2}3p_{3/2}$	0.00083	0.00390	-0.01144		0.00013	0.00023	-0.00035	-0.00004
$2s_{1/2}3p_{3/2}, 2p_{3/2}3s_{1/2}$	0.00097	0.00465	-0.01371		0.00020	0.00027	-0.00027	-0.00006
$2p_{1/2}3s_{1/2}, 2p_{3/2}3d_{3/2}$	0.00042	0.00518	-0.00729		0.00007	0.00009	-0.00026	0.00014
$2p_{3/2}3d_{3/2}, 2p_{1/2}3s_{1/2}$	0.00043	0.00532	-0.00756		0.00011	0.00009	-0.00022	0.00015
$2p_{1/2}3s_{1/2}, 2p_{3/2}3d_{5/2}$	0.00238	0.00272	-0.00205		0.00001	0.00002	-0.00008	0.00012
$2p_{3/2}3d_{5/2}, 2p_{1/2}3s_{1/2}$	0.00238	0.00280	-0.00233		-0.00002	0.00002	-0.00011	0.00013

	$R_1^{\rm HF}$	$R_2^{\rm HF}$	$R_3^{\rm HF}$	$R_4^{\rm HF}$	$R_1^{\rm BHF}$	$R_2^{\rm BHF}$	$R_3^{\rm BHF}$	$R_4^{\rm BHF}$
Odd parity states, J=1								
$2p_{1/2}3s_{1/2}, 2p_{1/2}3d_{3/2}$	-0.00144	-0.00578	0.00714		-0.00006	-0.00006	0.00022	-0.00018
$2p_{1/2}3d_{3/2}, 2p_{1/2}3s_{1/2}$	-0.00149	-0.00618	0.00792		-0.00008	-0.00006	0.00027	-0.00022
$2p_{1/2}3s_{1/2}, 2s_{1/2}3p_{1/2}$	0.00161	0.00387	-0.00411		0.00014	0.00017	-0.00016	-0.00008
$2s_{1/2}3p_{1/2}, 2p_{1/2}3s_{1/2}$	0.00160	0.00434	-0.00643		0.00020	0.00018	-0.00009	-0.00004
$2p_{1/2}3s_{1/2}, 2s_{1/2}3p_{3/2}$	-0.00113	0.00006	-0.01070		-0.00003	-0.00002	-0.00016	-0.00002
$2s_{1/2}3p_{3/2}, 2p_{1/2}3s_{1/2}$	-0.00099	0.00007	-0.00936		-0.00003	-0.00002	0.00001	-0.00010
$2p_{3/2}3d_{3/2}, 2p_{3/2}3d_{5/2}$	-0.00199	-0.00092	0.00688		0.00001	0.00001	-0.00050	0.00005
$2p_{3/2}3d_{5/2}, 2p_{3/2}3d_{3/2}$	-0.00199	-0.00092	0.00698		-0.00009	0.00001	-0.00050	0.00004
$2p_{3/2}3d_{3/2}, 2p_{1/2}3d_{3/2}$	-0.00225	-0.00126	0.00958		-0.00012	-0.00001	0.00043	-0.00004
$2p_{1/2}3d_{3/2}, 2p_{3/2}3d_{3/2}$	-0.00221	-0.00130	0.01018		-0.00009	-0.00001	0.00062	-0.00004
$2p_{3/2}3d_{3/2}, 2s_{1/2}3p_{1/2}$	-0.00159	0.00424	-0.01618		0.00004	0.00008	-0.00009	-0.00035
$2s_{1/2}3p_{1/2}, 2p_{3/2}3d_{3/2}$	-0.00155	0.00461	-0.01672		0.00000	0.00008	-0.00021	-0.00040
$2p_{3/2}3d_{3/2}, 2s_{1/2}3p_{3/2}$	-0.00052	-0.00627	0.01096		-0.00010	-0.00012	0.00035	0.00011
$2s_{1/2}3p_{3/2}, 2p_{3/2}3d_{3/2}$	-0.00058	-0.00691	0.01176		-0.00003	-0.00013	0.00038	0.00014
$2p_{3/2}3d_{5/2}, 2p_{1/2}3d_{3/2}$	0.00017	-0.00018	0.00220		0.00014	0.00001	0.00070	-0.00033
$2p_{1/2}3d_{3/2}, 2p_{3/2}3d_{5/2}$	0.00016	-0.00018	0.00035		0.00005	0.00001	0.00019	-0.00029
$2p_{3/2}3d_{5/2}, 2s_{1/2}3p_{1/2}$	-0.00155	-0.00849	0.01013		-0.00007	0.00000	0.00031	0.00047
$2s_{1/2}3p_{1/2}, 2p_{3/2}3d_{5/2}$	-0.00161	-0.00921	0.01067		-0.00007	0.00000	0.00005	0.00052
$2p_{3/2}3d_{5/2}, 2s_{1/2}3p_{3/2}$	-0.00345	-0.00313	-0.01001		-0.00005	-0.00006	0.00030	-0.00013
$2s_{1/2}3p_{3/2}, 2p_{3/2}3d_{5/2}$	-0.00347	-0.00344	-0.01023		-0.00001	-0.00006	-0.00012	-0.00015
$2p_{1/2}3d_{3/2}, 2s_{1/2}3p_{1/2}$	0.00202	0.00000	0.00990		0.00003	0.00000	-0.00026	0.00007
$2s_{1/2}3p_{1/2}, 2p_{1/2}3d_{3/2}$	0.00203	0.00000	0.00995		0.00006	0.00000	-0.00010	0.00008
$2p_{1/2}3d_{3/2}, 2s_{1/2}3p_{3/2}$	0.00209	0.00724	-0.00558		0.00011	0.00005	-0.00037	-0.00004
$2s_{1/2}3p_{3/2}, 2p_{1/2}3d_{3/2}$	0.00213	0.00762	-0.00594		0.00002	0.00005	-0.00016	-0.00005
$2s_{1/2}3p_{1/2}, 2s_{1/2}3p_{3/2}$	-0.00082	-0.00088	0.00459		0.00000	-0.00001	-0.00012	-0.00008
$2s_{1/2}3p_{3/2}, 2s_{1/2}3p_{1/2}$	-0.00082	-0.00089	0.00474		-0.00003	-0.00001	-0.00012	-0.00008
Odd parity states, J=2								
$2p_{3/2}3s_{1/2}, 2p_{3/2}3s_{1/2}$	0.00654	0.00971	-0.00923		0.00009	0.00012	-0.00003	0.00178
$2p_{3/2}3d_{5/2}, 2p_{3/2}3d_{5/2}$	0.00670	0.00096	-0.00803		0.00012	0.00002	0.00023	0.00150
$2p_{3/2}3d_{3/2}, 2p_{3/2}3d_{3/2}$	0.00521	-0.00006	-0.00017		0.00001	-0.00002	0.00048	0.00242
$2p_{1/2}3d_{3/2}, 2p_{1/2}3d_{3/2}$	0.00766	0.00398	-0.01172		0.00026	0.00010	-0.00031	0.00260
$2p_{1/2}3d_{5/2}, 2p_{1/2}3d_{5/2}$	0.00598	-0.00016	-0.00444		0.00012	0.00000	0.00020	0.00161
$2s_{1/2}3p_{3/2}, 2s_{1/2}3p_{3/2}$	0.00467	0.00774	-0.01157		0.00008	0.00007	0.00003	0.00196
$2p_{3/2}3s_{1/2}, 2p_{3/2}3d_{5/2}$	0.00041	-0.00360	0.00543		-0.00006	-0.00007	0.00021	-0.00002
$2p_{3/2}3d_{5/2}, 2p_{3/2}3s_{1/2}$	0.00036	-0.00385	0.00576		-0.00009	-0.00008	0.00023	-0.00001
$2p_{3/2}3s_{1/2}, 2p_{3/2}3d_{3/2}$	-0.00017	0.00158	-0.00240		0.00002	-0.00002	0.00006	0.00002
$2p_{3/2}3d_{3/2}, 2p_{3/2}3s_{1/2}$	-0.00016	0.00168	-0.00254		0.00003	-0.00002	0.00006	0.00002
$2p_{3/2}3s_{1/2}, 2p_{1/2}3d_{3/2}$	0.00007	-0.00079	0.00117		0.00003	0.00003	-0.00011	-0.00002
$2p_{1/2}3d_{3/2}, 2p_{3/2}3s_{1/2}$	0.00006	-0.00087	0.00126		0.00001	0.00003	-0.00012	-0.00002
$2p_{3/2}3s_{1/2}, 2p_{1/2}3d_{5/2}$	-0.00037	0.00383	-0.00565		0.00002	0.00003	-0.00005	0.00005
$2p_{1/2}3d_{5/2}, 2p_{3/2}3s_{1/2}$	-0.00030	0.00425	-0.00612		0.00008	0.00003	0.00003	0.00005
$2p_{3/2}3s_{1/2}, 2s_{1/2}3p_{3/2}$	-0.00261	-0.00390	-0.00327		-0.00016	-0.00023	0.00020	-0.00009
$2s_{1/2}3p_{3/2}, 2p_{3/2}3s_{1/2}$	-0.00245	-0.00465	0.00251		-0.00021	-0.00027	0.00028	-0.00026
$2p_{3/2}3d_{5/2}, 2p_{3/2}3d_{3/2}$	-0.00017	0.00116	-0.00104		-0.00001	-0.00001	-0.00003	0.00000
$2p_{3/2}3d_{3/2}, 2p_{3/2}3d_{5/2}$	-0.00018	0.00116	-0.00105		0.00002	-0.00001	-0.00003	0.00000
$2p_{3/2}3d_{5/2}, 2p_{1/2}3d_{3/2}$	0.00101	0.00036	-0.00250		0.00003	-0.00001	0.00002	-0.00002
$2p_{1/2}3d_{3/2}, 2p_{3/2}3d_{5/2}$	0.00098	0.00038	-0.00305		0.00000	-0.00001	0.00010	-0.00002
$2p_{3/2}3d_{5/2}, 2p_{1/2}3d_{5/2}$	-0.00207	-0.00030	0.00660		-0.00010	0.00000	0.00012	0.00010
$2p_{1/2}3d_{5/2}, 2p_{3/2}3d_{5/2}$	-0.00202	-0.00031	0.00784		-0.00010	0.00000	0.00008	0.00009
$2p_{3/2}3d_{5/2}, 2s_{1/2}3p_{3/2}$	-0.00077	0.00641	-0.01743		0.00008	0.00011	-0.00022	-0.00023
$2s_{1/2}3p_{3/2}, 2p_{3/2}3d_{5/2}$	-0.00072	0.00705	-0.01841		0.00004	0.00013	-0.00026	-0.00027
$2p_{3/2}3d_{3/2}, 2p_{1/2}3d_{3/2}$	0.00162	0.00184	-0.00573		0.00005	0.00002	-0.00008	0.00001
$2p_{1/2}3d_{3/2}, 2p_{3/2}3d_{3/2}$	0.00159	0.00191	-0.00646		0.00004	0.00002	0.00018	0.00002
$2p_{3/2}3d_{3/2}, 2p_{1/2}3d_{5/2}$	0.00186	0.00185	-0.00812		0.00007	0.00003	-0.00007	-0.00002
$2p_{1/2}3d_{5/2}, 2p_{3/2}3d_{3/2}$	0.00184	0.00192	-0.00903		0.00006	0.00004	-0.00005	-0.00001
$2p_{3/2}3d_{3/2}, 2s_{1/2}3p_{3/2}$	0.00035	-0.00280	0.00758		-0.00004	-0.00005	0.00012	0.00007
$2s_{1/2}3p_{3/2}, 2p_{3/2}3d_{3/2}$	0.00032	-0.00309	0.00802		-0.00001	-0.00006	0.00017	0.00009

	R_1^{HF}	R_2^{HF}	R_3^{HF}	R_4^{HF}	R_1^{BHF}	R_2^{BHF}	R_3^{BHF}	R_4^{BHF}
Odd parity states, J=2								
$2p_{1/2}3d_{3/2}, 2p_{1/2}3d_{5/2}$	0.00004	0.00020	0.00048		0.00004	0.00001	-0.00017	0.00000
$2p_{1/2}3d_{5/2}, 2p_{1/2}3d_{3/2}$	0.00004	0.00020	0.00047		0.00002	0.00001	-0.00017	0.00000
$2p_{1/2}3d_{3/2}, 2s_{1/2}3p_{3/2}$	-0.00013	0.00145	-0.00382		-0.00001	-0.00004	0.00014	-0.00002
$2s_{1/2}3p_{3/2}, 2p_{1/2}3d_{3/2}$	-0.00013	0.00153	-0.00393		-0.00003	-0.00004	0.00017	-0.00002
$2p_{1/2}3d_{5/2}, 2s_{1/2}3p_{3/2}$	0.00064	-0.00710	0.01881		-0.00004	0.00003	-0.00009	0.00015
$2s_{1/2}3p_{3/2}, 2p_{1/2}3d_{5/2}$	0.00061	-0.00746	0.01929		0.00001	0.00003	-0.00012	0.00018
Odd parity states, J=3								
$2p_{3/2}3d_{3/2}, 2p_{3/2}3d_{3/2}$	0.00652	0.00139	-0.00777		0.00029	0.00001	-0.00075	0.00247
$2p_{3/2}3d_{5/2}, 2p_{3/2}3d_{5/2}$	0.00326	-0.00240	0.00574		-0.00003	-0.00004	0.00027	0.00157
$2p_{1/2}3d_{5/2}, 2p_{1/2}3d_{5/2}$	0.00545	0.00082	-0.00444		0.00008	0.00002	0.00003	0.00171
$2p_{3/2}3d_{3/2}, 2p_{3/2}3d_{5/2}$	-0.00063	-0.00085	0.00016		0.00000	-0.00001	-0.00012	0.00002
$2p_{3/2}3d_{5/2}, 2p_{3/2}3d_{3/2}$	-0.00063	-0.00085	0.00017		-0.00001	-0.00001	-0.00012	0.00002
$2p_{3/2}3d_{3/2}, 2p_{1/2}3d_{5/2}$	-0.00275	-0.00369	0.00868		-0.00014	-0.00007	0.00011	0.00006
$2p_{1/2}3d_{5/2}, 2p_{3/2}3d_{3/2}$	-0.00277	-0.00384	0.00977		-0.00013	-0.00007	0.00008	0.00005
$2p_{3/2}3d_{5/2}, 2p_{1/2}3d_{5/2}$	0.00063	0.00071	-0.00470		-0.00003	0.00001	0.00000	0.00001
$2p_{1/2}3d_{5/2}, 2p_{3/2}3d_{5/2}$	0.00057	0.00074	-0.00509		-0.00003	0.00001	0.00014	0.00001
Odd parity states, J=4								
$2p_{3/2}3d_{5/2}, 2p_{3/2}3d_{5/2}$	0.00912	0.00507	-0.01647		0.00030	0.00006	-0.00054	0.00148

TABLE IV. Contributions to energy matrix $E[2l_1j_1\ 3l_2j_2(J), 2l_3j_3\ 3l_4j_4(J)] = E^{(0)}+E^{(1)}+E^{(2)}+B^{(1)}_{hf}+B^{(2)}$ before diagonalization. These contributions are given for a hole-particle ion with a $1s^22s^22p^6$ core, in the case of molybdenum, $Z = 42$. Notation: $E^{(0)}[2l_1j_1\ 3l_2j_2(J), 2l_3j_3\ 3l_4j_4(J)] = \delta_{l_1,l_3}\delta_{j_1,j_3}\delta_{l_2,l_4}\delta_{j_2,j_4}\ [-E^{(0)}(2l_1j_1) + E^{(0)}(3l_2j_2)]$;
$E^{(0)}(2s_{1/2})$= -168.77729, $E^{(0)}(2p_{1/2})$=-160.66905, $E^{(0)}(2p_{3/2})$=-156.56044, $E^{(0)}(3s_{1/2})$= -65.83451, $E^{(0)}(3p_{1/2})$= -63.24491, $E^{(0)}(3p_{3/2})$= -62.24632, $E^{(0)}(3d_{3/2})$= -58.84571, $E^{(0)}(3d_{5/2})$= -58.63305.

$2l_1j_1\ 3l_2j_2, 2l_3j_3\ 3l_4j_4$	$E^{(1)}$	$B^{(1)}_{hf}$	$E^{(2)}$	$B^{(2)}$
		Even parity states, J=0		
$2p_{3/2}3p_{3/2}, 2p_{3/2}3p_{3/2}$	-2.14875	-0.11363	-0.11482	0.02371
$2p_{1/2}3p_{1/2}, 2p_{1/2}3p_{1/2}$	-2.69622	-0.17075	-0.10885	0.02578
$2s_{1/2}3s_{1/2}, 2s_{1/2}3s_{1/2}$	-2.60244	-0.10796	-0.14801	0.01998
$2p_{3/2}3p_{3/2}, 2p_{1/2}3p_{1/2}$	-0.72929	-0.00262	0.02702	0.00162
$2p_{1/2}3p_{1/2}, 2p_{3/2}3p_{3/2}$	-0.72929	-0.00262	0.02698	0.00152
$2p_{3/2}3p_{3/2}, 2s_{1/2}3s_{1/2}$	0.18869	0.00465	0.00069	-0.00044
$2s_{1/2}3s_{1/2}, 2p_{3/2}3p_{3/2}$	0.18869	0.00465	0.00054	-0.00033
$2p_{1/2}3p_{1/2}, 2s_{1/2}3s_{1/2}$	-0.14649	-0.00145	0.00053	0.00057
$2s_{1/2}3s_{1/2}, 2p_{1/2}3p_{1/2}$	-0.14649	-0.00145	0.00098	0.00062
		Even parity states, J=1		
$2p_{3/2}3p_{1/2}, 2p_{3/2}3p_{1/2}$	-3.37375	-0.10232	-0.08608	0.02705
$2p_{3/2}3p_{3/2}, 2p_{3/2}3p_{3/2}$	-3.35664	-0.12992	-0.08942	0.02569
$2p_{1/2}3p_{1/2}, 2p_{1/2}3p_{1/2}$	-3.39517	-0.18304	-0.09548	0.02716
$2p_{1/2}3p_{3/2}, 2p_{1/2}3p_{3/2}$	-3.34304	-0.19098	-0.09551	0.02675
$2s_{1/2}3s_{1/2}, 2s_{1/2}3s_{1/2}$	-3.13379	-0.11407	-0.13521	0.02059
$2s_{1/2}3d_{3/2}, 2s_{1/2}3d_{3/2}$	-3.60542	-0.11406	-0.16528	0.02089
$2p_{3/2}3p_{1/2}, 2p_{3/2}3p_{3/2}$	-0.15311	0.00186	0.00437	0.00001
$2p_{3/2}3p_{3/2}, 2p_{3/2}3p_{1/2}$	-0.15311	0.00186	0.00461	0.00002
$2p_{3/2}3p_{1/2}, 2p_{1/2}3p_{1/2}$	0.00000	0.00069	0.00094	-0.00017
$2p_{1/2}3p_{1/2}, 2p_{3/2}3p_{1/2}$	0.00000	0.00069	0.00103	0.00011
$2p_{3/2}3p_{1/2}, 2p_{1/2}3p_{3/2}$	-0.16879	-0.00207	-0.00638	0.00026
$2p_{1/2}3p_{3/2}, 2p_{3/2}3p_{1/2}$	-0.16879	-0.00207	-0.00780	0.00037
$2p_{3/2}3p_{1/2}, 2s_{1/2}3s_{1/2}$	-0.41220	-0.00035	-0.00920	-0.00025
$2s_{1/2}3s_{1/2}, 2p_{3/2}3p_{1/2}$	-0.41220	-0.00035	-0.00653	-0.00042
$2p_{3/2}3p_{1/2}, 2s_{1/2}3d_{3/2}$	-0.10279	0.00107	0.00317	0.00021
$2s_{1/2}3d_{3/2}, 2p_{3/2}3p_{1/2}$	-0.10279	0.00107	0.00148	0.00041
$2p_{3/2}3p_{3/2}, 2p_{1/2}3p_{1/2}$	-0.10675	0.00461	-0.00211	0.00014
$2p_{1/2}3p_{1/2}, 2p_{3/2}3p_{3/2}$	-0.10675	0.00461	-0.00257	0.00044
$2p_{3/2}3p_{3/2}, 2p_{1/2}3p_{3/2}$	-0.15039	0.00200	0.00426	0.00019
$2p_{1/2}3p_{3/2}, 2p_{3/2}3p_{3/2}$	-0.15039	0.00200	0.00528	-0.00031
$2p_{3/2}3p_{3/2}, 2s_{1/2}3s_{1/2}$	-0.46176	-0.00088	0.00987	0.00026
$2s_{1/2}3s_{1/2}, 2p_{3/2}3p_{3/2}$	-0.46176	-0.00088	0.00707	0.00043
$2p_{3/2}3p_{3/2}, 2s_{1/2}3d_{3/2}$	0.08617	-0.00309	0.00283	-0.00008
$2s_{1/2}3d_{3/2}, 2p_{3/2}3p_{3/2}$	0.08617	-0.00309	0.00155	-0.00011
$2p_{1/2}3p_{1/2}, 2p_{1/2}3p_{3/2}$	0.00000	0.00047	0.00093	-0.00003
$2p_{1/2}3p_{3/2}, 2p_{1/2}3p_{1/2}$	0.00000	0.00047	0.00095	-0.00001
$2p_{1/2}3p_{1/2}, 2s_{1/2}3s_{1/2}$	-0.14355	0.00146	0.00307	0.00014
$2s_{1/2}3s_{1/2}, 2p_{1/2}3p_{1/2}$	-0.14355	0.00146	0.00256	0.00014
$2p_{1/2}3p_{1/2}, 2s_{1/2}3d_{3/2}$	0.28325	0.00182	0.00884	0.00055
$2s_{1/2}3d_{3/2}, 2p_{1/2}3p_{1/2}$	0.28325	0.00182	0.00595	0.00067
$2p_{1/2}3p_{3/2}, 2s_{1/2}3s_{1/2}$	-0.40686	0.00052	-0.00833	-0.00017
$2s_{1/2}3s_{1/2}, 2p_{1/2}3p_{3/2}$	-0.40686	0.00052	-0.00708	-0.00014
$2p_{1/2}3p_{3/2}, 2s_{1/2}3d_{3/2}$	-0.09380	0.00079	0.00313	0.00015
$2s_{1/2}3d_{3/2}, 2p_{1/2}3p_{3/2}$	-0.09380	0.00079	0.00227	0.00016
$2s_{1/2}3s_{1/2}, 2s_{1/2}3d_{3/2}$	0.00000	-0.00132	0.00000	-0.00009
$2s_{1/2}3d_{3/2}, 2s_{1/2}3s_{1/2}$	0.00000	-0.00132	0.00000	-0.00012
		Even parity states, J=2		
$2p_{3/2}3p_{1/2}, 2p_{3/2}3p_{1/2}$	-3.31492	-0.11267	-0.08364	0.02643
$2p_{3/2}3p_{3/2}, 2p_{3/2}3p_{3/2}$	-3.16091	-0.12385	-0.08019	0.02564
$2p_{1/2}3p_{3/2}, 2p_{1/2}3p_{3/2}$	-3.28432	-0.20078	-0.09292	0.02591
$2s_{1/2}3d_{3/2}, 2s_{1/2}3d_{3/2}$	-3.44872	-0.12437	-0.15803	0.01979
$2s_{1/2}3d_{5/2}, 2s_{1/2}3d_{5/2}$	-3.35156	-0.12632	-0.15457	0.02007

	$E^{(1)}$	$B^{(1)}_{hf}$	$E^{(2)}$	$B^{(2)}$
		Even parity states, J=2		
$2p_{3/2}3p_{1/2}, 2p_{3/2}3p_{3/2}$	0.00954	0.00044	-0.00084	0.00005
$2p_{3/2}3p_{3/2}, 2p_{3/2}3p_{1/2}$	0.00954	0.00044	-0.00086	0.00005
$2p_{3/2}3p_{1/2}, 2p_{1/2}3p_{3/2}$	0.09228	0.00152	0.00250	-0.00019
$2p_{1/2}3p_{3/2}, 2p_{3/2}3p_{1/2}$	0.09228	0.00152	0.00314	-0.00018
$2p_{3/2}3p_{1/2}, 2s_{1/2}3d_{3/2}$	-0.30292	-0.00328	0.00902	0.00032
$2s_{1/2}3d_{3/2}, 2p_{3/2}3p_{1/2}$	-0.30292	-0.00328	0.00483	0.00045
$2p_{3/2}3p_{1/2}, 2s_{1/2}3d_{5/2}$	-0.00726	-0.00108	-0.00059	-0.00016
$2s_{1/2}3d_{5/2}, 2p_{3/2}3p_{1/2}$	-0.00726	-0.00108	0.00040	-0.00026
$2p_{3/2}3p_{3/2}, 2p_{1/2}3p_{3/2}$	0.00826	0.00047	-0.00079	-0.00023
$2p_{1/2}3p_{3/2}, 2p_{3/2}3p_{3/2}$	0.00826	0.00047	-0.00085	0.00008
$2p_{3/2}3p_{3/2}, 2s_{1/2}3d_{3/2}$	0.11682	-0.00234	0.00301	0.00002
$2s_{1/2}3d_{3/2}, 2p_{3/2}3p_{3/2}$	0.11682	-0.00234	0.00183	0.00002
$2p_{3/2}3p_{3/2}, 2s_{1/2}3d_{5/2}$	-0.14220	-0.00084	0.00360	0.00007
$2s_{1/2}3d_{5/2}, 2p_{3/2}3p_{3/2}$	-0.14220	-0.00084	0.00203	0.00013
$2p_{1/2}3p_{3/2}, 2s_{1/2}3d_{3/2}$	0.05274	-0.00137	-0.00257	-0.00005
$2s_{1/2}3d_{3/2}, 2p_{1/2}3p_{3/2}$	0.05274	-0.00137	-0.00170	-0.00002
$2p_{1/2}3p_{3/2}, 2s_{1/2}3d_{5/2}$	0.27890	0.00159	0.00814	0.00026
$2s_{1/2}3d_{5/2}, 2p_{1/2}3p_{3/2}$	0.27890	0.00159	0.00597	0.00040
$2s_{1/2}3d_{3/2}, 2s_{1/2}3d_{5/2}$	-0.19107	-0.00062	0.00755	-0.00026
$2s_{1/2}3d_{5/2}, 2s_{1/2}3d_{3/2}$	-0.19107	-0.00062	0.00765	-0.00028
		Even parity states, J=3		
$2p_{3/2}3p_{3/2}, 2p_{3/2}3p_{3/2}$	-3.35664	-0.13339	-0.08661	0.02549
$2s_{1/2}3d_{5/2}, 2s_{1/2}3d_{5/2}$	-3.58454	-0.13395	-0.05404	-0.00329
$2p_{3/2}3p_{3/2}, 2s_{1/2}3d_{5/2}$	-0.31607	-0.00074	0.01016	0.00022
$2s_{1/2}3d_{5/2}, 2p_{3/2}3p_{3/2}$	-0.31607	-0.00074	0.00538	0.00036
		Odd parity states, J=0		
$2p_{1/2}3s_{1/2}, 2p_{1/2}3s_{1/2}$	-3.21316	-0.19463	-0.08974	0.02726
$2p_{3/2}3d_{3/2}, 2p_{3/2}3d_{3/2}$	-3.87933	-0.11784	-0.10458	0.02784
$2s_{1/2}3p_{1/2}, 2s_{1/2}3p_{1/2}$	-3.27937	-0.08679	-0.14196	0.02093
$2p_{1/2}3s_{1/2}, 2p_{3/2}3d_{3/2}$	-0.05389	0.00241	0.00380	-0.00003
$2p_{3/2}3d_{3/2}, 2p_{1/2}3s_{1/2}$	-0.05389	0.00241	0.00387	-0.00015
$2p_{1/2}3s_{1/2}, 2s_{1/2}3p_{1/2}$	0.43065	0.00145	-0.00998	-0.00028
$2s_{1/2}3p_{1/2}, 2p_{1/2}3s_{1/2}$	0.43065	0.00145	-0.00731	-0.00038
$2p_{3/2}3d_{3/2}, 2s_{1/2}3p_{1/2}$	0.43608	-0.00470	-0.01830	-0.00084
$2s_{1/2}3p_{1/2}, 2p_{3/2}3d_{3/2}$	0.43608	-0.00470	-0.01840	-0.00115
		Odd parity states, J=1		
$2p_{3/2}3s_{1/2}, 2p_{3/2}3s_{1/2}$	-3.05252	-0.12796	-0.07963	0.02624
$2p_{1/2}3s_{1/2}, 2p_{1/2}3s_{1/2}$	-3.14048	-0.20000	-0.08942	0.02666
$2p_{3/2}3d_{3/2}, 2p_{3/2}3d_{3/2}$	-3.60254	-0.13362	-0.09806	0.02632
$2p_{3/2}3d_{5/2}, 2p_{3/2}3d_{5/2}$	-2.96217	-0.15006	-0.09824	0.02580
$2p_{1/2}3d_{3/2}, 2p_{1/2}3d_{3/2}$	-3.20753	-0.21380	-0.10516	0.02642
$2s_{1/2}3p_{1/2}, 2s_{1/2}3p_{1/2}$	-3.21893	-0.09604	-0.14012	0.02037
$2s_{1/2}3p_{3/2}, 2s_{1/2}3p_{3/2}$	-3.11372	-0.11288	-0.13792	0.01943
$2p_{3/2}3s_{1/2}, 2p_{1/2}3s_{1/2}$	-0.10227	-0.00009	0.00040	-0.00025
$2p_{1/2}3s_{1/2}, 2p_{3/2}3s_{1/2}$	-0.10227	-0.00009	0.00075	-0.00025
$2p_{3/2}3s_{1/2}, 2p_{3/2}3d_{3/2}$	0.08276	-0.00123	0.00226	0.00014
$2p_{3/2}3d_{3/2}, 2p_{3/2}3s_{1/2}$	0.08276	-0.00123	0.00206	0.00010
$2p_{3/2}3s_{1/2}, 2p_{3/2}3d_{5/2}$	-0.15652	-0.00439	0.00082	0.00014
$2p_{3/2}3d_{5/2}, 2p_{3/2}3s_{1/2}$	-0.15652	-0.00439	0.00004	0.00011
$2p_{3/2}3s_{1/2}, 2p_{1/2}3d_{3/2}$	0.14458	0.00363	-0.00242	-0.00014
$2p_{1/2}3d_{3/2}, 2p_{3/2}3s_{1/2}$	0.14458	0.00363	-0.00161	0.00012
$2p_{3/2}3s_{1/2}, 2s_{1/2}3p_{1/2}$	-0.33598	0.00163	-0.01202	-0.00025
$2s_{1/2}3p_{1/2}, 2p_{3/2}3s_{1/2}$	-0.33598	0.00163	-0.00980	-0.00028
$2p_{3/2}3s_{1/2}, 2s_{1/2}3p_{3/2}$	0.03350	-0.00127	-0.00672	-0.00004
$2s_{1/2}3p_{3/2}, 2p_{3/2}3s_{1/2}$	0.03350	-0.00127	-0.00809	0.00014
$2p_{1/2}3s_{1/2}, 2p_{3/2}3d_{3/2}$	-0.01117	-0.00247	-0.00170	0.00004
$2p_{3/2}3d_{3/2}, 2p_{1/2}3s_{1/2}$	-0.01117	-0.00247	-0.00180	0.00013

	$E^{(1)}$	$B^{(1)}_{hf}$	$E^{(2)}$	$B^{(2)}$
		Odd parity states, J=1		
$2p_{1/2}3s_{1/2}, 2p_{3/2}3d_{5/2}$	0.15382	-0.00180	0.00304	0.00007
$2p_{3/2}3d_{5/2}, 2p_{1/2}3s_{1/2}$	0.15382	-0.00180	0.00286	0.00002
$2p_{1/2}3s_{1/2}, 2p_{1/2}3d_{3/2}$	-0.08075	0.00306	-0.00009	-0.00008
$2p_{1/2}3d_{3/2}, 2p_{1/2}3s_{1/2}$	-0.08075	0.00306	0.00025	-0.00009
$2p_{1/2}3s_{1/2}, 2s_{1/2}3p_{1/2}$	-0.19648	-0.00065	0.00137	0.00007
$2s_{1/2}3p_{1/2}, 2p_{1/2}3s_{1/2}$	-0.19648	-0.00065	-0.00048	0.00025
$2p_{1/2}3s_{1/2}, 2s_{1/2}3p_{3/2}$	-0.32845	0.00119	-0.01177	-0.00023
$2s_{1/2}3p_{3/2}, 2p_{1/2}3s_{1/2}$	-0.32845	0.00119	-0.01028	-0.00016
$2p_{3/2}3d_{3/2}, 2p_{3/2}3d_{5/2}$	-0.37260	-0.00748	0.00397	-0.00043
$2p_{3/2}3d_{5/2}, 2p_{3/2}3d_{3/2}$	-0.37260	-0.00748	0.00407	-0.00054
$2p_{3/2}3d_{3/2}, 2p_{1/2}3d_{3/2}$	0.00696	0.00966	0.00608	0.00026
$2p_{1/2}3d_{3/2}, 2p_{3/2}3d_{3/2}$	0.00696	0.00966	0.00667	0.00048
$2p_{3/2}3d_{3/2}, 2s_{1/2}3p_{1/2}$	0.30965	0.00196	-0.01353	-0.00032
$2s_{1/2}3p_{1/2}, 2p_{3/2}3d_{3/2}$	0.30965	0.00196	-0.01366	-0.00053
$2p_{3/2}3d_{3/2}, 2s_{1/2}3p_{3/2}$	0.09768	0.00589	0.00417	0.00024
$2s_{1/2}3p_{3/2}, 2p_{3/2}3d_{3/2}$	0.09768	0.00589	0.00427	0.00036
$2p_{3/2}3d_{5/2}, 2p_{1/2}3d_{3/2}$	-0.52100	0.01230	0.00219	0.00053
$2p_{1/2}3d_{3/2}, 2p_{3/2}3d_{5/2}$	-0.52100	0.01230	0.00033	-0.00005
$2p_{3/2}3d_{5/2}, 2s_{1/2}3p_{1/2}$	0.04660	0.00630	0.00009	0.00071
$2s_{1/2}3p_{1/2}, 2p_{3/2}3d_{5/2}$	0.04660	0.00630	-0.00016	0.00051
$2p_{3/2}3d_{5/2}, 2s_{1/2}3p_{3/2}$	0.35193	0.00540	-0.01659	0.00006
$2s_{1/2}3p_{3/2}, 2p_{3/2}3d_{5/2}$	0.35193	0.00540	-0.01714	-0.00034
$2p_{1/2}3d_{3/2}, 2s_{1/2}3p_{1/2}$	0.25278	-0.00670	0.01192	-0.00016
$2s_{1/2}3p_{1/2}, 2p_{1/2}3d_{3/2}$	0.25278	-0.00670	0.01198	0.00003
$2p_{1/2}3d_{3/2}, 2s_{1/2}3p_{3/2}$	-0.07317	-0.00786	0.00375	-0.00025
$2s_{1/2}3p_{3/2}, 2p_{1/2}3d_{3/2}$	-0.07317	-0.00786	0.00381	-0.00014
$2s_{1/2}3p_{1/2}, 2s_{1/2}3p_{3/2}$	-0.08352	-0.00332	0.00289	-0.00020
$2s_{1/2}3p_{3/2}, 2s_{1/2}3p_{1/2}$	-0.08352	-0.00332	0.00303	-0.00024
		Odd parity states, J=2		
$2p_{3/2}3s_{1/2}, 2p_{3/2}3s_{1/2}$	-3.19667	-0.13028	-0.08051	0.02631
$2p_{3/2}3d_{5/2}, 2p_{3/2}3d_{5/2}$	-3.60279	-0.14470	-0.09761	0.02571
$2p_{3/2}3d_{3/2}, 2p_{3/2}3d_{3/2}$	-3.51426	-0.13156	-0.09384	0.02635
$2p_{1/2}3d_{3/2}, 2p_{1/2}3d_{3/2}$	-3.66151	-0.20856	-0.10866	0.02642
$2p_{1/2}3d_{5/2}, 2p_{1/2}3d_{5/2}$	-3.63849	-0.21417	-0.10563	0.02608
$2s_{1/2}3p_{3/2}, 2s_{1/2}3p_{3/2}$	-3.23028	-0.11175	-0.14266	0.01962
$2p_{3/2}3s_{1/2}, 2p_{3/2}3d_{5/2}$	-0.03761	0.00138	0.00224	0.00005
$2p_{3/2}3d_{5/2}, 2p_{3/2}3s_{1/2}$	-0.03761	0.00138	0.00227	0.00005
$2p_{3/2}3s_{1/2}, 2p_{3/2}3d_{3/2}$	-0.01628	-0.00054	-0.00100	0.00008
$2p_{3/2}3d_{3/2}, 2p_{3/2}3s_{1/2}$	-0.01628	-0.00054	-0.00102	0.00009
$2p_{3/2}3s_{1/2}, 2p_{1/2}3d_{3/2}$	-0.00762	-0.00148	0.00045	-0.00007
$2p_{1/2}3d_{3/2}, 2p_{3/2}3s_{1/2}$	-0.00762	-0.00148	0.00046	-0.00009
$2p_{3/2}3s_{1/2}, 2p_{1/2}3d_{5/2}$	-0.03766	0.00001	-0.00218	0.00005
$2p_{1/2}3d_{5/2}, 2p_{3/2}3s_{1/2}$	-0.03766	0.00001	-0.00217	0.00019
$2p_{3/2}3s_{1/2}, 2s_{1/2}3p_{3/2}$	0.43806	0.00329	-0.00977	-0.00027
$2s_{1/2}3p_{3/2}, 2p_{3/2}3s_{1/2}$	0.43806	0.00329	-0.00459	-0.00046
$2p_{3/2}3d_{5/2}, 2p_{3/2}3d_{3/2}$	-0.05902	-0.00029	-0.00005	-0.00006
$2p_{3/2}3d_{3/2}, 2p_{3/2}3d_{5/2}$	-0.05902	-0.00029	-0.00007	-0.00003
$2p_{3/2}3d_{5/2}, 2p_{1/2}3d_{3/2}$	-0.08668	0.00225	-0.00113	0.00002
$2p_{1/2}3d_{3/2}, 2p_{3/2}3d_{5/2}$	-0.08668	0.00225	-0.00170	0.00008
$2p_{3/2}3d_{5/2}, 2p_{1/2}3d_{5/2}$	-0.18842	0.00238	0.00423	0.00012
$2p_{1/2}3d_{5/2}, 2p_{3/2}3d_{5/2}$	-0.18842	0.00238	0.00551	0.00007
$2p_{3/2}3d_{5/2}, 2s_{1/2}3p_{3/2}$	0.26445	-0.00171	-0.01179	-0.00025
$2s_{1/2}3p_{3/2}, 2p_{3/2}3d_{5/2}$	0.26445	-0.00171	-0.01207	-0.00036
$2p_{3/2}3d_{3/2}, 2p_{1/2}3d_{3/2}$	0.08938	0.00203	-0.00227	-0.00001
$2p_{1/2}3d_{3/2}, 2p_{3/2}3d_{3/2}$	0.08938	0.00203	-0.00296	0.00025
$2p_{3/2}3d_{3/2}, 2p_{1/2}3d_{5/2}$	-0.10811	-0.00079	-0.00441	0.00001
$2p_{1/2}3d_{5/2}, 2p_{3/2}3d_{3/2}$	-0.10811	-0.00079	-0.00527	0.00003

	$E^{(1)}$	$B^{(1)}_{hf}$	$E^{(2)}$	$B^{(2)}$
		Odd parity states, J=2		
$2p_{3/2}3d_{3/2}, 2s_{1/2}3p_{3/2}$	0.11561	0.00133	0.00512	0.00011
$2s_{1/2}3p_{3/2}, 2p_{3/2}3d_{3/2}$	0.11561	0.00133	0.00525	0.00019
$2p_{1/2}3d_{3/2}, 2p_{1/2}3d_{5/2}$	0.00000	-0.00081	0.00072	-0.00013
$2p_{1/2}3d_{5/2}, 2p_{1/2}3d_{3/2}$	0.00000	-0.00081	0.00072	-0.00015
$2p_{1/2}3d_{3/2}, 2s_{1/2}3p_{3/2}$	0.05628	0.00093	-0.00251	0.00007
$2s_{1/2}3p_{3/2}, 2p_{1/2}3d_{3/2}$	0.05628	0.00093	-0.00253	0.00008
$2p_{1/2}3d_{5/2}, 2s_{1/2}3p_{3/2}$	0.27523	-0.00121	0.01234	0.00005
$2s_{1/2}3p_{3/2}, 2p_{1/2}3d_{5/2}$	0.27523	-0.00121	0.01244	0.00010
		Odd parity states, J=3		
$2p_{3/2}3d_{3/2}, 2p_{3/2}3d_{3/2}$	-3.60670	-0.14514	-0.09868	0.02547
$2p_{3/2}3d_{5/2}, 2p_{3/2}3d_{5/2}$	-3.42713	-0.14543	-0.09065	0.02561
$2p_{1/2}3d_{5/2}, 2p_{1/2}3d_{5/2}$	-3.56781	-0.21821	-0.10517	0.02599
$2p_{3/2}3d_{3/2}, 2p_{3/2}3d_{5/2}$	-0.01039	-0.00078	-0.00131	-0.00010
$2p_{3/2}3d_{5/2}, 2p_{3/2}3d_{3/2}$	-0.01039	-0.00078	-0.00131	-0.00012
$2p_{3/2}3d_{3/2}, 2p_{1/2}3d_{5/2}$	0.11432	0.00076	0.00224	-0.00005
$2p_{1/2}3d_{5/2}, 2p_{3/2}3d_{3/2}$	0.11432	0.00076	0.00315	-0.00008
$2p_{3/2}3d_{5/2}, 2p_{1/2}3d_{5/2}$	0.04753	0.00197	-0.00335	-0.00001
$2p_{1/2}3d_{5/2}, 2p_{3/2}3d_{5/2}$	0.04753	0.00197	-0.00378	0.00012
		Odd parity states, J=4		
$2p_{3/2}3d_{5/2}, 2p_{3/2}3d_{5/2}$	-3.69280	-0.15490	-0.09952	0.02513

TABLE V. Energies of Ne-like molybdenum, Z=42 relative to the ground state. $E^{(0+1)} \equiv E^{(0)} + E^{(1)} + B^{(1)}$

LS-coupling	jj-coupling	$E^{(0+1)}$	$E^{(2)}$	$B^{(2)}$	$E_{\rm LAMB}$	$E_{\rm tot}$
$2p3p\ ^3P_0$	$2p_{3/2}3p_{3/2}(0)$	91.8510	-0.1012	0.0246	-0.0047	91.7698
$2p3p\ ^1S_0$	$2p_{1/2}3p_{1/2}(0)$	94.7484	-0.1225	0.0249	0.0006	94.6514
$2s3s\ ^1S_0$	$2s_{1/2}3s_{1/2}(0)$	100.2417	-0.1480	0.0199	-0.0674	100.0462
$2p3p\ ^3S_1$	$2p_{3/2}3p_{1/2}(1)$	89.7840	-0.0860	0.0270	-0.0068	89.7182
$2p3p\ ^3D_1$	$2p_{3/2}3p_{3/2}(1)$	90.8239	-0.0899	0.0258	-0.0052	90.7545
$2p3p\ ^1P_1$	$2p_{1/2}3p_{1/2}(1)$	93.8402	-0.0956	0.0271	0.0010	93.7728
$2p3p\ ^3P_1$	$2p_{1/2}3p_{3/2}(1)$	94.8700	-0.0968	0.0267	0.0023	94.8022
$2s3s\ ^3S_1$	$2s_{1/2}3s_{1/2}(1)$	99.7699	-0.1338	0.0207	-0.0667	99.5900
$2s3d\ ^3D_1$	$2s_{1/2}3d_{3/2}(1)$	106.2204	-0.1649	0.0209	-0.0880	105.9883
$2p3p\ ^3D_2$	$2p_{3/2}3p_{1/2}(2)$	89.8803	-0.0835	0.0264	-0.0067	89.8165
$2p3p\ ^3P_2$	$2p_{3/2}3p_{3/2}(2)$	91.0273	-0.0802	0.0256	-0.0051	90.9677
$2p3p\ ^1D_2$	$2p_{1/2}3p_{3/2}(2)$	94.9325	-0.0932	0.0259	0.0027	94.8679
$2s3d\ ^3D_2$	$2s_{1/2}3d_{3/2}(2)$	106.2738	-0.1516	0.0196	-0.0879	106.0539
$2s3d\ ^1D_2$	$2s_{1/2}3d_{5/2}(2)$	106.7656	-0.1609	0.0202	-0.0875	106.5376
$2p3p\ ^3D_3$	$2p_{3/2}3p_{3/2}(3)$	90.8176	-0.0863	0.0255	-0.0051	90.7518
$2s3d\ ^3D_3$	$2s_{1/2}3d_{5/2}(3)$	106.4321	-0.0544	-0.0033	-0.0874	106.2871
$2p3s\ ^3P_0$	$2p_{1/2}3s_{1/2}(0)$	91.4073	-0.0888	0.0273	0.0213	91.3670
$2p3d\ ^3P_0$	$2p_{3/2}3d_{3/2}(0)$	93.6979	-0.1031	0.0279	-0.0071	93.6156
$2s3p\ ^3P_0$	$2s_{1/2}3p_{1/2}(0)$	102.2052	-0.1443	0.0208	-0.0875	101.9942
$2p3s\ ^3P_1$	$2p_{3/2}3s_{1/2}(1)$	87.5287	-0.0801	0.0262	0.0136	87.4884
$2p3s\ ^1P_1$	$2p_{1/2}3s_{1/2}(1)$	91.4753	-0.0904	0.0266	0.0213	91.4329
$2p3d\ ^3P_1$	$2p_{3/2}3d_{3/2}(1)$	93.8092	-0.0939	0.0260	-0.0070	93.7344
$2p3d\ ^3D_1$	$2p_{3/2}3d_{5/2}(1)$	94.8970	-0.1000	0.0263	-0.0062	94.8171
$2p3d\ ^1P_1$	$2p_{1/2}3d_{3/2}(1)$	98.4600	-0.1067	0.0263	0.0003	98.3799
$2s3p\ ^3P_1$	$2s_{1/2}3p_{1/2}(1)$	102.2493	-0.1383	0.0203	-0.0873	102.0441
$2s3p\ ^1P_1$	$2s_{1/2}3p_{3/2}(1)$	103.3370	-0.1392	0.0195	-0.0860	103.1313
$2p3s\ ^3P_2$	$2p_{3/2}3s_{1/2}(2)$	87.3861	-0.0802	0.0263	0.0136	87.3459
$2p3d\ ^3P_2$	$2p_{3/2}3d_{5/2}(2)$	94.0298	-0.0948	0.0262	-0.0068	93.9544
$2p3d\ ^3F_2$	$2p_{3/2}3d_{3/2}(2)$	94.1939	-0.0960	0.0259	-0.0064	94.1174
$2p3d\ ^1D_2$	$2p_{1/2}3d_{3/2}(2)$	97.9568	-0.1087	0.0264	0.0009	97.8754
$2p3d\ ^3D_2$	$2p_{1/2}3d_{5/2}(2)$	98.1817	-0.1072	0.0260	0.0013	98.1018
$2s3p\ ^3P_2$	$2s_{1/2}3p_{3/2}(2)$	103.2248	-0.1421	0.0196	-0.0858	103.0165
$2p3d\ ^3F_3$	$2p_{3/2}3d_{3/2}(3)$	93.9594	-0.0989	0.0255	-0.0069	93.8790
$2p3d\ ^3D_3$	$2p_{3/2}3d_{5/2}(3)$	94.3546	-0.0905	0.0256	-0.0062	94.2835
$2p3d\ ^1F_3$	$2p_{1/2}3d_{5/2}(3)$	98.2537	-0.1051	0.0260	0.0016	98.1761
$2p3d\ ^3F_4$	$2p_{3/2}3d_{5/2}(4)$	94.0797	-0.0995	0.0251	-0.0062	93.9990

TABLE VI. E1 uncoupled reduced matrix elements in length L and velocity V forms for odd-parity transitions into the ground state in Mo^{32+}.

$av(J)$	$Z_L^{(1)}$	$Z_V^{(1)}$	$Z_L^{(2)}$	$Z_V^{(2)}$	$B_L^{(2)}$	$B_V^{(2)}$	$P_L^{(\rm derv)}$	$P_V^{(\rm derv)}$
$2p_{3/2}3s_{1/2}(1)$	-0.039269	-0.037253	-0.001920	-0.001694	-0.000093	-0.000020	-0.038945	0.000031
$2p_{1/2}3s_{1/2}(1)$	-0.024205	-0.022987	-0.001469	-0.001262	-0.000111	-0.000048	-0.023881	0.000214
$2p_{3/2}3d_{3/2}(1)$	0.060681	0.057688	-0.000580	0.000595	0.000101	-0.000022	0.060625	0.000296
$2p_{3/2}3d_{5/2}(1)$	0.181119	0.172191	-0.001765	0.001839	0.000254	-0.000065	0.179768	-0.001475
$2p_{1/2}3d_{3/2}(1)$	-0.129576	-0.123282	0.001442	-0.001070	-0.000281	0.000036	-0.128916	0.000399
$2s_{1/2}3p_{1/2}(1)$	0.055251	0.052692	0.000859	0.001187	0.000003	-0.000069	0.054858	-0.000027
$2s_{1/2}3p_{3/2}(1)$	0.072600	0.069291	0.001306	0.001650	0.000066	-0.000036	0.071730	-0.000672

TABLE VII. E1 coupled reduced matrix elements in length L and velocity V forms for odd-parity transitions into the ground state in Mo^{32+}.

	MBPT		First order	
$av(J)$	L	V	L	V
$2p_{3/2}3s_{1/2}(1)$	0.048063	0.047973	0.046140	0.043791
$2p_{1/2}3s_{1/2}(1)$	-0.037756	-0.037685	-0.036248	-0.034441
$2p_{3/2}3d_{3/2}(1)$	-0.003992	-0.003992	-0.004052	-0.003851
$2p_{3/2}3d_{5/2}(1)$	0.170333	0.170226	0.172035	0.163554
$2p_{1/2}3d_{3/2}(1)$	-0.156141	-0.156054	-0.157792	-0.150125
$2s_{1/2}3p_{1/2}(1)$	-0.040111	-0.040065	-0.039214	-0.037421
$2s_{1/2}3p_{3/2}(1)$	0.066582	0.066509	0.065087	0.062157

TABLE VIII. E2 uncoupled reduced matrix elements in length L and velocity V forms for even-parity transitions into the ground state in Mo^{32+}.

$av(J)$	$Z_L^{(1)}$	$Z_V^{(1)}$	$Z_L^{(2)}$	$Z_V^{(2)}$	$B_L^{(2)}$	$B_V^{(2)}$	$P_L^{(\mathrm{derv})}$	$P_V^{(\mathrm{derv})}$
$2p_{3/2}3p_{1/2}(2)$	0.016820	0.016077	0.000319	0.000392	0.000023	0.000002	0.033582	0.016077
$2p_{3/2}3p_{3/2}(2)$	0.016157	0.015372	0.000334	0.000405	0.000030	0.000008	0.032213	0.015372
$2p_{1/2}3d_{3/2}(2)$	0.014794	0.014005	0.000345	0.000412	0.000044	0.000015	0.029449	0.014005
$2s_{1/2}3d_{3/2}(2)$	-0.028815	-0.027526	-0.000636	-0.000962	-0.000046	-0.000012	-0.057507	-0.027526
$2s_{1/2}3d_{5/2}(2)$	-0.035170	-0.033255	-0.000878	-0.001292	-0.000047	-0.000007	-0.070016	-0.033255

TABLE IX. E2 coupled reduced matrix elements in length L and velocity V forms for even-parity transitions into the ground state in Mo^{32+}.

	MBPT		First order	
$av(J)$	L	V	L	V
$2p_{3/2}3p_{1/2}(2)$	0.016832	0.016846	0.017202	0.016422
$2p_{3/2}3p_{3/2}(2)$	-0.016269	-0.016281	-0.016568	-0.015830
$2p_{1/2}3d_{3/2}(2)$	-0.015550	-0.015560	-0.015765	-0.015074
$2s_{1/2}3d_{3/2}(2)$	0.010632	0.010634	0.010784	0.010309
$2s_{1/2}3d_{5/2}(2)$	-0.043257	-0.043255	-0.043530	-0.041617

TABLE X. M2 uncoupled reduced matrix elements for odd-parity transitions with J=2 into the ground state in Mo^{32+}.

$av(J)$	$Z_R^{(1)}$	$Z_{RF}^{(1)}$	$Z_{RF}^{(2)}$	$B_{NES}^{(2)}$	$B^{(2)}$	$P_{RF}^{(\mathrm{derv})}$
$2p_{3/2}3s_{1/2}(2)$	-0.153944	-0.152793	-0.002071	-0.000310	-0.000283	-0.303282
$2p_{3/2}3d_{5/2}(2)$	0.799284	0.796894	0.021865	0.001117	0.001083	1.589006
$2p_{3/2}3d_{3/2}(2)$	0.000000	0.000000	-0.001750	0.000038	0.000008	0.000000
$2p_{1/2}3d_{3/2}(2)$	-0.099421	-0.099668	-0.001187	-0.000248	-0.000258	-0.199831
$2p_{1/2}3d_{5/2}(2)$	-0.326342	-0.325136	-0.012417	-0.000644	-0.000669	-0.647860
$2s_{1/2}3p_{3/2}(2)$	0.283552	0.281548	0.005763	0.000058	0.000031	0.559088

TABLE XI. Line strengths in a.u. for magnetic-quadrupole (M2) lines as functions of Z in Ne-like ions.

LS designations	Z=20	Z=30	Z=40	Z=50	Z=60	Z=70	Z=80	Z=90	Z=100	jj designations
$2p3s\ ^3P_2$	1.96[-1]	5.99[-2]	2.93[-2]	1.81[-2]	1.31[-2]	1.06[-2]	9.40[-3]	8.92[-3]	8.96[-3]	$2p_{3/2}3s_{1/2}(2)$
$2p3d\ ^3P_2$	2.99[0]	1.06[0]	2.24[-1]	1.97[-2]	2.76[-3]	5.83[-4]	1.57[-4]	4.96[-5]	1.75[-5]	$2p_{3/2}3d_{3/2}(2)$
$2p3d\ ^3F_2$	3.28[-1]	3.26[-1]	5.02[-1]	4.22[-1]	2.91[-1]	2.07[-1]	1.53[-1]	1.16[-1]	9.02[-2]	$2p_{3/2}3d_{5/2}(2)$
$2p3d\ ^3D_2$	2.83[-1]	5.00[-2]	1.53[-2]	7.45[-3]	4.34[-3]	2.74[-3]	1.79[-3]	1.17[-3]	8.32[-4]	$2p_{1/2}3d_{3/2}(2)$
$2s3d\ ^3D_2$	1.05[-2]	1.07[-1]	9.39[-2]	6.50[-2]	4.39[-2]	2.97[-2]	2.02[-2]	1.37[-2]	8.52[-3]	$2p_{1/2}3d_{5/2}(2)$
$2s3d\ ^1D_2$	2.00[-1]	9.71[-2]	5.91[-2]	3.83[-2]	2.52[-2]	1.65[-2]	1.05[-2]	5.67[-3]	3.51[-3]	$2s_{1/2}3p_{3/2}(2)$

TABLE XII. Energies (a.u.) for the $2p3s$ (J) and $2p3d$ (1) levels in Ne-like given relative to the ground state. Comparison with theoretical results presented in Refs. [19,20] - (a) and experimental data (b) given in in Refs. [19,20].

	$2p_{1/2}3s_{1/2}(0)$	$2p_{3/2}3s_{1/2}(2)$	$2p_{3/2}3s_{1/2}(1)$	$2p_{1/2}3s_{1/2}(1)$	$2p_{3/2}3d_{3/2}(1)$	$2p_{3/2}3d_{5/2}(1)$	$2p_{1/2}3d_{3/2}(1)$
	$2p3s\ ^3P_0$	$2p3s\ ^3P_2$	$2p3s\ ^3P_1$	$2p3s\ ^1P_1$	$2p3d\ ^3P_1$	$2p3d\ ^3D_1$	$2p3d\ ^1P_1$
Z=11	1.1609	1.1551	1.1663	1.1652	1.4729	1.4723	1.4793
(a)	1.2123	1.2062	1.2096	1.2233	1.5017	1.5045	1.5117
(b)	1.2133	1.2071	1.2106	1.2246	1.5065	1.5115	1.5178
Z=12	1.9133	1.9040	1.9168	1.9239	2.3985	2.3968	2.4108
(a)	1.9479	1.9380	1.9435	1.9647	2.4120	2.4255	2.4353
(b)	1.9495	1.9394	1.9450	1.9662	2.4168	2.4340	2.4429
Z=13	2.7971	2.7821	2.7966	2.8127	3.4524	3.4567	3.4826
(a)	2.8233	2.8079	2.8101	2.8448	3.4566	3.4878	3.5011
(b)	2.8252	2.8096	2.8180	2.8464	3.4610	3.4944	3.5122
Z=14	3.8183	3.7957	3.8127	3.8380	4.6345	4.6489	4.6985
(a)	3.8392	3.8163	3.8278	3.8642	4.6353	4.6858	4.7111
(b)	3.8413	3.8183	3.8300	3.8661	4.6394	4.6903	4.7245
Z=15	4.9784	4.9459	4.9659	5.0015	5.9496	5.9799	6.0536
(a)	4.9958	4.9630	4.9786	5.0235	5.9490	6.0196	6.0644
(b)	4.9986	4.9657	4.9814	5.0262	5.9536	6.0236	6.0789
Z=16	6.2823	6.2343	6.2566	6.3035	7.4059	7.4555	7.5528
(a)	6.2933	6.2479	6.2679	6.3232	7.3988	7.4903	7.5596
(b)	6.2960	6.2503	6.2705	6.3257	7.4030	7.4933	7.5735
Z=17	7.7200	7.6582	7.6853	7.7475	8.9920	9.0638	9.1888
(a)	7.7322	7.6708	7.6955	7.7637	8.9855	9.0989	9.1960
(b)			7.6977	7.6556	8.9869	9.0992	9.2071
Z=18	9.3015	9.2197	9.2517	9.3318	10.7192	10.8143	10.9688
(a)	9.3128	9.2314	9.2611	9.3458	10.7097	10.8462	10.9737
(b)			9.2646	9.3501	10.7057	10.843	10.984
Z=19	11.0257	10.9195	10.9559	11.0573	12.5724	12.6934	12.8806
(a)	11.0355	10.9295	10.9642	11.0697	12.5717	12.7325	12.8929
(b)			10.9683	11.0730	12.5764	12.7345	12.9049
Z=20	12.8951	12.7573	12.7962	12.9241	14.5810	14.7287	14.9499
(a)	12.9007	12.7650	12.8048	12.9361	14.5718	14.7584	14.9540
(b)			12.8074	12.9395	14.5771	14.7612	14.9644
Z=21	14.8971	15.0736	14.7878	14.9290	16.7164	16.8964	17.1523
(a)	14.9089		14.7823	14.9454	16.7103	16.9240	17.1576
(b)			14.786	14.948	16.7144	16.9255	17.1652
Z=22	17.0515	16.8371	16.8904	17.0895	18.9964	19.2030	19.5008
(a)	17.0604	16.8470	16.8967	17.0982	18.9872	19.2296	19.5046
(b)			16.900	17.103	18.9919	19.2267	19.5082
Z=23	19.3482	19.0847	19.1414	19.3870	21.4117	21.6502	21.9921
(a)	19.3560	19.0931	19.1477	19.3950	21.4027	21.6754	21.9957
(b)			19.149	19.397	21.3973	21.6783	21.994
Z=24	21.7891	21.4680	21.5288	21.8290	23.9656	24.2376	24.6284
(a)	21.7961	21.4755	21.5349	21.8365	23.9570	24.2614	24.6319
(b)		21.479	21.540	21.839	23.9618	24.2592	24.633
Z=25	24.3751	23.9872	24.0525	24.4163	26.6582	26.9653	27.4107
(a)	24.3816	23.9941	24.0583	24.4232	26.6501	26.9976	27.4143
(b)			24.063	24.426	26.6501	26.9893	27.421
Z=26	27.1068	26.6422	26.7119	27.1494	29.4896	29.8331	30.3404
(a)	27.1129	26.6486	26.7175	27.1560	29.4820	29.8541	30.3440
(b)	27.113	26.652	26.722	27.160	29.492	29.8516	30.353

	$2p_{1/2}3s_{1/2}(0)$	$2p_{3/2}3s_{1/2}(2)$	$2p_{3/2}3s_{1/2}(1)$	$2p_{1/2}3s_{1/2}(1)$	$2p_{3/2}3d_{3/2}(1)$	$2p_{3/2}3d_{5/2}(1)$	$2p_{1/2}3d_{3/2}(1)$
	$2p3s\ ^3P_0$	$2p3s\ ^3P_2$	$2p3s\ ^3P_1$	$2p3s\ ^1P_1$	$2p3d\ ^3P_1$	$2p3d\ ^3D_1$	$2p3d\ ^1P_1$
Z=27	29.9851	29.4327	29.5069	30.0291	32.4600	32.8412	33.4185
(a)	29.9906	29.4387	29.5122	30.0363	32.4529	32.8608	33.4222
(b)			29.516	30.0353	32.455	32.8608	33.424
Z=28	33.0108	32.3584	32.4372	33.0562	35.5692	35.9895	36.6464
(a)	33.0161	32.3641	32.4423	33.0620	35.5628	36.0077	36.6502
(b)		32.368	32.446	33.067	35.569	36.006	36.652
Z=29	36.1845	35.4193	35.5025	36.2314	38.8176	39.2780	40.0253
(a)	36.1896	35.4247	35.5075	36.2370	38.8117	39.2948	40.0293
(b)	36.195	35.436	35.520	36.246	38.821	39.292	40.020
Z=30	39.5072	38.6148	38.7026	39.5556	42.2050	42.7066	43.5567
(a)	39.5120	38.6200	38.7073	39.5609	42.1999	42.7222	43.5609
(b)			38.713	39.565	42.206	42.729	43.556
Z=31	42.9797	41.9448	42.0371	43.0296	45.7316	46.2755	47.2420
(a)	42.9844	41.9497	42.0417	43.0347	45.7272	46.2898	47.2462
(b)			42.060	43.053	45.742	46.295	47.250
Z=32	46.6030	45.4088	45.5057	46.6545	49.3975	49.9846	51.0826
(a)	46.6075	45.4137	45.5101	46.6593	49.3939	49.9976	51.0869
(b)			45.518	46.675	49.409	50.014	51.091
Z=33	50.3781	49.0068	49.1082	50.4310	53.2028	53.8342	55.0799
(a)	50.3825	49.0114	49.1124	50.4357	53.1999	53.8458	55.0844
(b)			49.158	50.434			
Z=34	54.3059	52.7381	52.8441	54.3604	57.1475	57.8241	59.2356
(a)	54.3102	52.7426	52.8481	54.3649	57.1454	57.8345	59.2402
(b)			52.890	54.412	57.188	57.864	59.289
Z=35	58.3876	56.6025	56.7130	58.4436	61.2316	61.9545	63.5511
(a)	58.3919	56.6069	56.7170	58.4480	61.2304	61.9637	63.5558
(b)			56.740	58.490	61.274	61.983	63.556
Z=36	62.6243	60.5996	60.7146	62.6818	65.4554	66.2256	68.0282
(a)	62.6285	60.6039	60.7186	62.6860	65.4551	66.2337	68.0330
(b)	62.628	60.602	60.720	62.686	65.472	66.245	68.066
Z=37	67.0170	64.7290	64.8486	67.0760	69.8188	70.6376	72.6684
Z=38	71.5671	68.9903	69.1144	71.6276	74.3220	75.1906	77.4735
Z=39	76.2759	73.3831	73.5118	76.3377	78.9650	79.8848	82.4453
Z=40	81.1445	77.9069	78.0402	81.2078	83.7481	84.7205	87.5857
(a)	81.1479	77.9112	78.0450	81.2131	83.7521	84.7224	87.5894
(b)					83.894	84.713	87.574
Z=41	86.1744	82.5613	82.6993	86.2390	88.6711	89.6979	92.8966
Z=42	91.3671	87.3459	87.4885	91.4330	93.7344	94.8171	98.3800
(a)	91.3705	87.3503	87.4933	91.4384	93.7406	94.8167	98.3837
(b)			87.573	91.491	93.914	94.839	98.390
Z=43	96.7239	92.2600	92.4073	96.7910	98.9379	100.0786	104.0380
Z=44	102.2465	97.3033	97.4552	102.3147	104.2819	105.4825	109.8727
Z=45	107.9363	102.4750	102.6317	108.0055	109.7663	111.0291	115.8865
Z=46	113.7950	107.7748	107.9362	113.8652	115.3914	116.7188	122.0817
(a)	113.7987	107.7796	107.9413	113.8711	115.4021	116.7138	122.0853
Z=47	119.8243	113.2020	113.3681	119.8952	121.1574	122.5519	128.4606
(a)	119.8278	113.2067	113.3733	119.9012	121.1692	122.5459	128.4642
(b)		113.215	113.381	119.894	121.186	122.551	128.467

	$2p_{1/2}3s_{1/2}(0)$	$2p_{3/2}3s_{1/2}(2)$	$2p_{3/2}3s_{1/2}(1)$	$2p_{1/2}3s_{1/2}(1)$	$2p_{3/2}3d_{3/2}(1)$	$2p_{3/2}3d_{5/2}(1)$	$2p_{1/2}3d_{3/2}(1)$
	$2p3s\ ^3P_0$	$2p3s\ ^3P_2$	$2p3s\ ^3P_1$	$2p3s\ ^1P_1$	$2p3d\ ^3P_1$	$2p3d\ ^3D_1$	$2p3d\ ^1P_1$
Z=48	126.0255	118.7560	118.9269	126.0972	127.0644	128.5289	135.0259
(a)	126.0290	118.7611	118.9323	126.1035	127.0774	128.5219	135.0293
Z=49	132.3993	124.4362	124.6119	132.4722	133.1132	134.6503	141.7800
Z=50	138.9412	130.2419	130.4224	139.0194	139.3062	140.9167	148.7258
(a)	138.9368	130.2473	130.4281	139.0258	139.3226	140.9078	148.7291
Z=51	145.7168	136.1724	136.3579	145.7737	145.6099	147.3294	155.8661
(a)	145.7728	136.1780	136.3637	145.7815	145.6217	147.3197	155.8692
Z=52	152.6165	142.2271	142.4175	152.6665	152.0933	153.8906	163.2038
(a)	152.6224	142.2329	142.4234	152.6736	152.1118	153.8804	163.2067
Z=53	159.7085	148.4050	148.6004	159.7425	158.7078	160.6065	170.7418
(a)	159.7145	148.4111	148.6065	159.6736	158.7274	160.5970	170.7444
Z=54	166.9877	154.7057	154.9060	166.9707	165.4626	167.5019	178.4834
(a)	166.9939	154.7120	154.9124	166.9801	165.4835	167.4993	178.4917
(b)		154.720	154.919	166.972		167.494	178.505
Z=55	174.4549	161.1280	161.3334	172.2316	172.3588	174.6980	186.4318
Z=56	182.1124	167.6714	167.8818	182.2736	179.3966	181.4493	194.5904
(a)	182.1192	167.6783	167.8886	182.2894	179.4200	181.4331	194.5978
(b)		167.688	167.895				
Z=57	189.9624	174.3356	174.5511	190.0994	186.5772	188.7563	202.9626
(a)	189.9696	174.3421	174.5575	190.1113	186.6011	188.7392	202.9693
(b)		174.352	174.572	190.125		188.754	
Z=58	198.0077	181.1174	181.3381	198.1346	193.8982	196.1942	211.5520
Z=59	206.2507	188.0181	188.2441	206.3728	201.3623	203.7749	220.3623
Z=60	214.6947	195.0363	195.2675	214.8141	208.9688	211.5009	229.3971
(a)	214.7029	195.0447	195.2755	214.8249	208.9978	211.4833	229.4005
(b)		195.057	195.291	214.861		211.500	
Z=61	223.3421	202.1705	202.4069	223.4662	216.7179	219.3735	238.6602
Z=62	232.1965	209.4200	209.6618	232.3139	224.6097	227.3937	248.1553
Z=63	241.2607	216.7833	217.0305	241.3779	232.6444	235.5622	257.8856
(a)	241.2701	216.7936	217.0400	241.3873	232.6782	235.5470	257.8784
(b)		216.813	217.072				
Z=64	250.5383	224.2596	224.5123	250.6556	240.8222	243.8796	267.8537
Z=65	260.0324	231.8472	232.1054	260.1499	249.1432	252.3463	278.0602
Z=66	269.7469	239.5452	239.8089	269.8647	257.6076	260.9629	288.5006
Z=67	279.6862	247.3530	247.6222	279.9045	266.2156	269.7299	299.1568
Z=68	289.8522	255.2669	255.5419	289.9711	274.9673	278.6477	310.8072
(a)	289.8659	255.2821	255.5561	289.9847	275.0064	278.6326	311.0330
(b)		255.317	255.585				
Z=69	300.2513	263.2881	263.5688	300.3707	283.8629	287.7170	321.9431
Z=70	310.8860	271.4132	271.6996	311.0059	292.9026	296.9380	333.4211
(a)	310.9010	271.4317	271.7172	311.0219	292.9556	296.9252	333.5564
(b)							333.526
Z=71	321.7622	279.6422	279.9345	321.8826	302.0866	306.3114	345.2147
Z=72	332.8836	287.9724	288.2705	333.0045	311.4150	315.8375	357.3134
(a)	332.8999	287.9936	288.2908	333,0219	311.4720	315.8275	357.3916
(b)		288.013	288.308				
Z=73	344.2547	296.4019	296.7060	344.3761	320.8880	325.5170	369.7159

	$2p_{1/2}3s_{1/2}(0)$	$2p_{3/2}3s_{1/2}(2)$	$2p_{3/2}3s_{1/2}(1)$	$2p_{1/2}3s_{1/2}(1)$	$2p_{3/2}3d_{3/2}(1)$	$2p_{3/2}3d_{5/2}(1)$	$2p_{1/2}3d_{3/2}(1)$
	$2p3s\ ^3P_0$	$2p3s\ ^3P_2$	$2p3s\ ^3P_1$	$2p3s\ ^1P_1$	$2p3d\ ^3P_1$	$2p3d\ ^3D_1$	$2p3d\ ^1P_1$
Z=74	355.8815	304.9298	305.2399	356.0033	330.5058	335.3502	382.4252
(a)	355.9000	304.9550	305.2643	356.0229	330.5693	335.3445	382.4875
(b)		304.998	305.303				
Z=75	367.7679	313.5527	313.8690	367.8901	340.2686	345.3378	395.4469
Z=76	379.9202	322.2696	322.5921	380.0426	350.1766	355.4802	408.7875
Z=77	392.3446	331.0793	331.4080	392.4673	360.2300	365.7779	422.4542
Z=78	405.0461	339.9781	340.3132	405.1690	370.4289	376.2316	436.4551
(a)	405.0692	340.0147	340.3487	405.1932	370.5096	376.2387	436.5143
(b)		340.073	340.398				
Z=79	418.0313	348.9643	349.3058	418.1543	380.7736	386.8416	450.7984
(a)	418.0557	349.0045	349.3449	418.1797	380.8596	386.8530	450.8592
(b)		349.070	349.412		380.646	386.592	450.577
Z=80	431.3071	358.0361	358.3840	431.4301	391.2642	397.6086	465.4932
(a)	431.3328	358.0802	358.4271	431.4301	391.3560	397.6249	465.5557
(b)		358.124	358.448				
Z=81	444.8794	367.1895	367.5440	445.0023	401.9009	408.5331	480.5490
Z=82	458.7562	376.4233	376.7845	458.8789	412.6839	419.6156	495.9755
(a)	458.7846	376.4766	376.8366	458.9083	412.7888	419.6433	496.0428
(b)		376.504	376.837				
Z=83	472.9449	385.7343	386.1023	473.0673	423.6135	430.8568	511.7832
(a)	472.9748	385.7929	386.1597	473.0982	423.7258	430.8911	511.8525
(b)			386.155	473.114		430.783	
Z=84	487.4528	395.1190	395.4938	487.5747	434.6897	442.2571	527.9830
Z=85	502.2894	404.5759	404.9577	502.4108	445.9129	453.8172	544.5861
Z=86	517.4634	414.1020	414.4909	517.5841	457.2831	465.5377	561.6045
Z=87	532.9815	423.6904	424.0866	533.1014	468.8005	477.4190	579.0516
Z=88	548.8556	433.3404	433.7444	548.9746	480.4654	489.4618	596.9399
Z=89	565.0945	442.9936	443.4591	565.2138	492.2780	501.6670	615.2859
Z=90	581.7111	452.8123	453.2289	581.8277	504.2382	514.0343	634.0970
(a)	581.7544	452.9223	453.3390	581.8719	504.4237	514.1378	634.1993
(b)		453.029	453.434				
Z=91	598.7129	462.6204	463.0453	598.8280	516.3465	526.5651	653.3961
Z=92	616.1176	472.4793	472.9120	616.2311	528.6030	539.2600	673.1913
(a)	616.1665	472.6117	473.0437	616.2809	528.8182	539.3926	673.3128
Z=93	633.9309	482.3737	482.8147	634.0426	541.0077	552.1192	693.5414
Z=94	652.1738	492.3100	492.7589	652.2834	553.5609	565.1438	714.3852
Z=95	670.8520	502.2709	502.7279	670.9593	566.2630	578.3331	735.7983
Z=96	689.9874	512.2614	512.7268	690.0921	579.1136	591.6901	757.7839
Z=97	709.5910	522.2685	522.7425	709.6930	592.1135	605.2135	780.3623
Z=98	729.6849	532.2938	532.7766	729.7838	605.2624	618.9053	803.4903
Z=99	750.2838	542.3261	542.8194	750.3790	618.5604	632.7678	827.7278
Z=100	771.4074	552.3600	552.8595	771.5000	632.0079	646.7941	852.0929

TABLE XIII. Energies ($10^3 cm^{-1}$) for the $2p3s$ (1), $2p3d$ (1) $2s3p$ (1) levels in Ne-like given relative to the ground state. Comparison with theoretical results presented in Refs. [3] - (a), adjusted data from [11] - (b) and NIST data (c) from Refs. [44–46] - (c).

	$2p_{3/2}3s_{1/2}(1)$ $2p3s\ ^3P_1$	$2p_{1/2}3s_{1/2}(1)$ $2p3s\ ^1P_1$	$2p_{3/2}3d_{3/2}(1)$ $2p3d\ ^3P_1$	$2p_{3/2}3d_{5/2}(1)$ $2p3d\ ^3D_1$	$2p_{1/2}3d_{3/2}(1)$ $2p3d\ ^1P_1$	$2s_{1/2}3p_{1/2}(1)$ $2s3p\ ^3P_1$	$2s_{1/2}3p_{1/2}(1)$ $2s3p\ ^1P_1$
Z=19	2404.538	2426.807	2759.329	2785.881	2826.962	3216.325	3224.787
(a)	2405.975	2429.386	2756.673	2795.695	2838.129	3212.275	3221.985
(b)	2406.761	2430.108	2759.996	2794.932	2832.026	3227.084	3240.304
(c)	2407.260	2430.250	2760.200	2794.200	2832.300	3219.400	3237.600
Z=20	2808.436	2836.516	3200.166	3232.582	3281.124	3693.357	3708.734
(b)	2810.916	2839.962	3199.085	3239.735	3284.354	3699.818	3714.962
(c)	2810.900	2839.900	3199.300	3239.700	3284.300	3692.900	3708.900
Z=21	3245.554	3276.531	3668.818	3708.321	3764.484	4177.784	4220.836
(a)	3243.467	3279.635	3664.463	3715.457	3773.739	4190.862	4204.502
(b)	3244.858	3280.911	3668.381	3714.261	3767.124	4203.670	4220.921
(c)	3245.100	3280.800	3668.400	3714.700	3767.300	4198.000	4215.000
Z=22	3707.018	3750.714	4169.222	4214.574	4279.932	4732.605	4750.466
(a)	3707.292	3751.931	4163.953	4221.413	4288.514	4727.428	4743.551
(b)	3709.188	3753.713	4168.372	4219.858	4281.680	4733.534	4754.037
(c)	3709.200	3753.600	4168.200	4219.800	4281.600	4733.300	4754.000
Z=23	4201.044	4254.946	4699.325	4751.677	4826.703	5301.064	5322.005
(a)	4201.086	4255.838	4693.872	4758.109	4834.850	5314.720	5295.722
(b)	4203.079	4257.444	4698.412	4756.308	4827.905	5303.751	5326.476
(c)	4202.700	4257.100	4699.000	4757.800	4827.200	5299.000	5324.000
Z=24	4725.036	4790.916	5259.842	5319.545	5405.300	5901.250	5925.623
(a)	4724.808	4791.483	5254.242	5325.579	5413.002	5895.900	5918.239
(b)	4727.457	4793.345	5259.466	5324.100	5406.372	5906.245	5931.550
(c)	4727.500	4793.200	5259.000	5324.200	5406.300	5894.500	5921.000
Z=25	5278.903	5358.754	5850.804	5918.192	6015.963	6533.504	6561.755
(a)	5278.431	5359.002	5845.077	5923.849	6023.195	6528.171	6554.314
(b)	5281.121	5360.992	5850.163	5923.566	6018.434	6536.611	6565.513
(c)	5281.200	5360.800	5849.700	5923.500	6018.300	6530.800	6562.500
Z=26	5862.583	5958.606	6472.229	6547.616	6658.944	7198.036	7230.687
(a)	5861.875	5958.580	6466.377	6552.899	6665.680	7192.646	7223.180
(b)	5864.648	5960.608	6471.488	6554.489	6665.390	7096.963	7130.425
(c)	5863.700	5960.500	6472.500	6552.200	6660.000	7198.900	7234.300
Z=27	6476.017	6590.631	7124.137	7207.815	7334.512	7895.037	7932.683
(a)	6475.085	6590.341	7118.176	7212.701	7340.742	7889.538	7925.068
(b)	6478.936	6593.317	7124.368	7215.417	7341.727	7774.915	7813.084
(c)	6477.900	6592.400	7122.000	7210.800	7334.600	7894.500	7932.700
Z=28	7119.145	7254.994	7806.545	7898.784	8042.949	8624.696	8668.005
(a)	7118.027	7254.451	7800.472	7903.283	8048.646	8619.036	8660.225
(b)	7122.615	7258.103	7806.753	7906.121	8049.949	8482.653	8526.152
(c)	7121.000	7257.400	7805.200	7901.400	8041.800	8621.400	8666.300

TABLE XIV. Energies (a.u.) for the $2p3s$ (1) and $2p3d$ (1) levels in Ne-like given relative to the ground state. Comparison with theoretical results presented in Refs. [19,20] - (a) and experimental data (b) given in Refs. [21].

	$2p_{3/2}3s_{1/2}(1)$	$2p_{1/2}3s_{1/2}(1)$	$2p_{3/2}3d_{3/2}(1)$	$2p_{3/2}3d_{5/2}(1)$	$2p_{1/2}3d_{3/2}(1)$
	$2p3s\ ^3P_1$	$2p3s\ ^1P_1$	$2p3d\ ^3P_1$	$2p3d\ ^3D_1$	$2p3d\ ^1P_1$
Z=39	73.5118	76.3377	78.9650	79.8848	82.4453
(b)					82.432
Z=40	78.0402	81.2078	83.7481	84.7205	87.5857
(a)	78.0450	81.2131	83.7521	84.7224	87.5894
(b)				84.706	87.570
Z=41	82.6993	86.2390	88.6711	89.6979	92.8966
(b)				89.693	92.878
Z=42	87.4885	91.4330	93.7344	94.8171	98.3800
(a)	87.4933	91.4384	93.7406	94.8167	98.3837
(b)	87.506	91.441		94.821	98.356
Z=43	92.4073	96.7910	98.9379	100.0786	104.0380
(b)	92.426	96.817		100.075	104.012
Z=44	97.4552	102.3147	104.2819	105.4825	109.8727
(b)	97.474	102.355		105.488	109.844
Z=45	102.6317	108.0055	109.7663	111.0291	115.8865
(b)	102.650	108.057		111.033	115.855
Z=46	107.9362	113.8652	115.3914	116.7188	122.0817
(a)	107.9413	113.8711	115.4021	116.7138	122.0853
(b)	107.955	113.923		116.712	122.046
Z=47	113.3681	119.8952	121.1574	122.5519	128.4606
(a)	113.3733	119.9012	121.1692	122.5459	128.4642
(b)	113.381	119.954		122.528	128.420
Z=48	118.9269	126.0972	127.0644	128.5289	135.0259
(a)	118.9323	126.1035	127.0774	128.5219	135.0293
(b)	118.933	126.155	126.963	128.489	134.978
Z=49	124.6119	132.4722	133.1132	134.6503	141.7800
(b)	124.616	132.521	133.020	134.584	141.734
Z=50	130.4224	139.0194	139.3062	140.9167	148.7258
(a)	130.4281	139.0258	139.3226	140.9078	148.7291
(b)	130.416	139.057	139.227	140.828	148.671
Z=51	136.3579	145.7737	145.6099	147.3294	155.8661
(a)	136.3637	145.7815	145.6217	147.3197	155.8692
(b)	136.344	145.598	145.737	147.221	155.804
Z=52	142.4175	152.6665	152.0933	153.8906	163.2038
(a)	142.4234	152.6736	152.1118	153.8804	163.2067
(b)	142.390	152.605	152.070	153.764	163.134
Z=53	148.6004	159.7425	158.7078	160.6065	170.7418
(a)	148.6065	158.7507	158.7274	160.5970	170.7444
(b)	148.560	158.680	159.714	160.463	170.668
Z=54	154.9060	166.9707	165.4626	167.5019	178.4834
(a)	154.9124	166.9801	165.4835	167.4993	178.4917
(b)	154.856	166.929	165.426	167.365	178.400
Z=55	161.3334	174.2316	172.3588	174.6980	186.4318
(b)	161.269	174.158	172.334		186.338
Z=56	167.8818	182.2736	179.3966	181.4493	194.5904
(a)	167.8886	182.2894	179.4200	181.4331	194.5978
(b)	167.802	182.217	179.411	181.345	194.482

	$2p_{3/2}3s_{1/2}(1)$	$2p_{1/2}3s_{1/2}(1)$	$2p_{3/2}3d_{3/2}(1)$	$2p_{3/2}3d_{5/2}(1)$	$2p_{1/2}3d_{3/2}(1)$
	$2p3s\ ^3P_1$	$2p3s\ ^1P_1$	$2p3d\ ^3P_1$	$2p3d\ ^3D_1$	$2p3d\ ^1P_1$
Z=57	174.5511	190.0994	186.5772	188.7563	202.9626
(a)	174.5575	190.1113	186.6011	188.7392	202.9693
(b)	174.465		186.629	188.636	202.837
Z=58	181.3381	198.1346	193.8982	196.1942	211.5520
(b)	181.246			196.022	211.411
Z=59	188.2441	206.3728	201.3623	203.7749	220.3623
(b)	188.146			203.535	220.198
Z=60	195.2675	214.8141	208.9688	211.5009	229.3971
(a)	195.2755	214.8249	208.9978	211.4833	229.4005
(b)	195.174			211.432	229.215

TABLE XV. Energies (a.u.) for the $2s3p$ (1) levels in Ne-like given relative to the ground state. Comparison with experimental data given in Refs. [21]-(a), [33]-(b), [32]-(c), [30]-(d), [27]-(e), and), [29]-(e).

	$2s_{1/2}3p_{1/2}(1)$	$2s_{1/2}3p_{1/2}(1)$	$2s_{1/2}3p_{3/2}(1)$	$2s_{1/2}3p_{3/2}(1)$		$2s_{1/2}3p_{1/2}(1)$	$2s_{1/2}3p_{3/2}(1)$
Z=39	85.9738	85.957[a]	86.759	86.744[a]	Z=60	231.9030	237.2592
Z=40	91.1661	91.190[a]	92.043	92.030[a]	Z=61	240.9588	246.7296
Z=41	96.5224	96.512[a]	97.500	97.491[a]	Z=62	250.2282	256.4375
Z=42	102.0441	102.039[a]	103.139	103.122[a]	Z=63	259.7168	266.3887
Z=43	107.7333	107.730[a]	108.939	108.930[a]	Z=64	269.4290	276.5867
Z=44	113.5907	113.587[a]	114.926	114.917[a]	Z=65	279.3742	287.0378
Z=45	119.6188	119.620[a]	121.094	121.082[a]	Z=66	289.5646	297.7464
Z=46	125.8192	125.824[a]	127.445	127.428[a]	Z=67	300.0247	308.7151
Z=47	132.1937	132.198[a]	133.983	133.962[a]	Z=68	309.9935	319.9571
		132.23[e]		133.99[e]	Z=69	320.9804	331.4692
Z=48	138.7444	138.743[a]	140.710	140.684[a]	Z=70	332.1460	343.2645
Z=49	145.4731	145.468[a]	147.628	147.597[a]	Z=71	343.5218	355.3432
Z=50	152.3819	152.37 6[a]	154.741	154.704[a]	Z=72	355.1332	367.7158
Z=51	159.4730	159.457[a]	162.050	162.009[a]	Z=73	366.9937	380.3897
Z=52	166.7485	166.728[a]	169.560	169.513[a]	Z=74	379.1092	393.3688
Z=53	174.2115	174.185[a]	177.274	177.213[a]	Z=75	391.4915	406.6652
Z=54	181.8632	181.824[a]	185.194	185.134[a]	Z=76	404.1440	420.2834
		181.875[f]		185.209[f]	Z=77	417.0715	434.2296
Z=55	189.7074	189.650[a]	193.325	193.253[a]	Z=78	430.2839	448.5158
Z=56	197.7458	197.672[a]	201.669	201.599[a]	Z=84	515.8963	541.8660
Z=57	205.9817		210.231	210.163[a]	Z=85	531.2878	558.7893
				210.25[f]	Z=86	547.0191	576.1301
Z=58	214.4177		219.014	218.960[a]	Z=87	563.1098	593.9118
Z=59	223.0571		228.022	227.976[a]	Z=88	579.5593	612.1370
Z=70	332.1460		343.264	343.29[d]	Z=89	596.3846	630.7702
Z=79	443.7867	443.62[c]	463.150	463.05[c]	Z=90	613.5816	649.9861
Z=80	457.5848		478.139		Z=91	631.1831	669.6440
Z=81	471.6890		493.496		Z=92	649.1720	689.7912
Z=82	486.1033		509.229		Z=93	667.5909	710.4783
Z=83	500.8355	500.77[b]	525.348		Z=94	686.4203	731.6814

TABLE XVI. Energies (a.u.) for the $2l3l'$ (J) levels in Ne-like given relative to the ground state. Comparison with experimental data given in Refs. [27]-(a), [29]-(b), [30]-(c), [32]-(d), [33]-(e), and [31]-(f).

2l3l LSJ	2lj3l'j'(J)	Z=47	Z=54	Z=57	Z=60	Z=63	Z=70	Z=79	Z=83	Z=90
$2p3s\ ^3P_0$	$2p_{1/2}3s_{1/2}(0)$	119.8243	165.2662	186.3611	208.7323	232.3873	292.5985	380.4162	423.2362	503.8333
$2p3d\ ^3P_0$	$2p_{3/2}3d_{3/2}(0)$	121.0107	166.9877	189.9624	214.6947	241.2607	310.8860	418.0313	472.9449	581.7111
$2s3p\ ^3P_0$	$2s_{1/2}3p_{1/2}(0)$	132.1357	181.7921	205.9025	231.8109	259.5977	332.2730	443.8077	500.8610	613.6337
$2p3s\ ^3P_1$	$2p_{3/2}3s_{1/2}(1)$	113.3681	154.9060	174.5511	195.2675	217.0305	271.6996	349.3058	386.1023	453.2289
		113.38[a]	154.91[b]	174.57[b]	195.29[b]	217.07[b]		349.36[d]	386.15[e]	453.44[f]
$2p3s\ ^1P_1$	$2p_{1/2}3s_{1/2}(1)$	119.8952	165.4626	186.5772	208.9688	232.6444	292.9026	380.7736	423.6135	504.2382
								380.65[d]		
$2p3d\ ^3P_1$	$2p_{3/2}3d_{3/2}(1)$	121.1574	166.9707	188.7563	211.5009	235.5622	296.9380	386.8416	430.8568	514.0343
		121.19[a]	166.97[b]	188.75[b]	211.50[b]			386.59[d]	430.78[e]	
$2p3d\ ^3D_1$	$2p_{3/2}3d_{5/2}(1)$	122.5519	167.5019	190.0994	214.8141	241.3779	311.0059	418.1543	473.0673	581.8277
		122.55[a]	167.49[b]	190.12[b]	214.86[b]			418.01[d]	473.11[e]	
$2p3d\ ^1P_1$	$2p_{1/2}3d_{3/2}(1)$	128.4606	178.4834	202.9626	229.3971	257.8856	332.1460	443.7867	500.8355	613.5816
		128.47[a]	178.50[b]					443.62[d]	500.77[e]	
$2s3p\ ^3P_1$	$2s_{1/2}3p_{1/2}(1)$	132.1937	181.8632	205.9817	231.9030	259.7168	333.4211	450.7984	511.7832	634.0970
		132.23[a]	181.87[b]				333.53[c]	450.58[d]		
$2s3p\ ^1P_1$	$2s_{1/2}3p_{3/2}(1)$	133.9836	185.1947	210.2313	237.2592	266.3887	343.2645	463.1498	525.3476	649.9861
		133.99[a]	185.21[b]	210.25[b]			343.29[c]	463.05[d]		
$2p3s\ ^3P_2$	$2p_{3/2}3s_{1/2}(2)$	113.2020	154.7057	174.3356	195.0363	216.7833	271.4132	348.9643	385.7343	452.8123
		113.21[a]	154.72[b]	174.35[b]	195.06[b]	216.81[b]				453.03[f]
$2p3d\ ^3P_2$	$2p_{3/2}3d_{5/2}(2)$	121.4152	165.7617	186.8875	209.2895	232.9745	293.2522	381.1478	423.9995	504.6473
$2p3d\ ^3F_2$	$2p_{3/2}3d_{3/2}(2)$	121.7022	166.3760	187.7072	210.3606	234.3489	295.5713	385.2934	429.2313	512.2778
$2p3d\ ^1D_2$	$2p_{1/2}3d_{3/2}(2)$	127.9008	177.8523	202.3058	228.7212	257.2068	332.4364	449.8699	510.8412	633.1404
$2p3d\ ^3D_2$	$2p_{1/2}3d_{5/2}(2)$	128.2939	178.6188	203.2958	229.9808	258.7880	335.0078	454.3341	516.4245	641.1849
$2s3p\ ^3P_2$	$2s_{1/2}3p_{3/2}(2)$	133.8535	185.0428	210.0698	237.0881	266.2076	343.0587	462.9070	525.0838	649.7353
$2p3d\ ^3F_3$	$2p_{3/2}3d_{3/2}(3)$	121.3050	165.6076	186.7144	209.0968	232.7614	292.9874	380.8057	423.6184	504.1901
$2p3d\ ^3D_3$	$2p_{3/2}3d_{5/2}(3)$	121.9073	166.6273	187.9769	210.6482	234.6540	295.9166	385.6893	429.6495	512.7344
$2p3d\ ^1F_3$	$2p_{1/2}3d_{5/2}(3)$	128.3810	178.7211	203.4035	230.0934	258.9049	335.1320	454.4624	516.5527	641.3112
$2p3d\ ^3F_4$	$2p_{3/2}3d_{5/2}(4)$	121.5734	166.2220	187.5401	210.1792	234.1523	295.3359	385.0008	428.9106	511.9033
$2p3p\ ^3P_0$	$2p_{3/2}3p_{3/2}(0)$	119.8473	165.3416	186.4373	208.8124	292.7069	292.7069	380.5905	423.4599	504.1876
$2p3p\ ^1S_0$	$2p_{1/2}3p_{1/2}(0)$	121.0890	166.9820	189.9413	214.6568	310.7837	310.7837	417.8620	472.7452	581.4620
$2s3s\ ^1S_0$	$2s_{1/2}3s_{1/2}(0)$	132.3858	182.1220	206.2776	232.2392	332.9500	332.9500	444.8342	502.0943	615.3271
$2p3p\ ^3S_1$	$2p_{3/2}3p_{1/2}(1)$	115.9920	158.1122	178.0202	199.0086	276.4273	276.4273	355.0453	392.3346	460.3836
$2p3p\ ^3D_1$	$2p_{3/2}3p_{3/2}(1)$	117.7044	161.3371	182.1548	204.2464	287.1541	287.1541	374.0687	416.4745	496.3290
$2p3p\ ^1P_1$	$2p_{1/2}3p_{1/2}(1)$	122.6299	170.3720	193.6125	218.6176	315.7872	315.7872	423.9170	479.3027	588.9376
$2p3p\ ^3P_1$	$2p_{1/2}3p_{3/2}(1)$	124.3562	173.6320	197.7867	223.8938	326.1776	326.1776	437.5113	494.0844	605.9099
$2s3s\ ^3S_1$	$2s_{1/2}3s_{1/2}(1)$	129.3252	178.3842	202.2290	227.8691	327.7359	327.7359	443.3871	503.9024	625.4330
$2s3d\ ^3D_1$	$2s_{1/2}3d_{3/2}(1)$	137.2833	189.1259	214.4380	241.7444	348.7010	348.7010	469.4722	532.0699	657.3906
$2p3p\ ^3D_2$	$2p_{3/2}3p_{1/2}(2)$	116.0854	158.1997	178.1050	199.0905	276.4962	276.4962	355.0962	392.3749	460.4015
		116.08[a]	158.21[b]	178.12[b]				355.24[d]	393.52[e]	
$2p3p\ ^3P_2$	$2p_{3/2}3p_{3/2}(2)$	117.9568	161.6428	182.4832	204.5977	287.5844	287.5844	374.5754	417.0173	496.9387
		117.96[a]	161.65[b]					374.48[d]		
$2p3p\ ^1D_2$	$2p_{1/2}3p_{3/2}(2)$	124.4371	173.7383	197.9083	224.0370	326.7711	326.7711	443.2845	503.8348	625.3802
		124.45[a]	173.77[b]	197.93[b]						
$2s3d\ ^3D_2$	$2s_{1/2}3d_{3/2}(2)$	137.3732	189.2517	214.5782	241.8981	348.8891	348.8891	469.6742	532.2717	657.6142
$2s3d\ ^1D_2$	$2s_{1/2}3d_{5/2}(2)$	138.0336	190.2871	215.8360	243.4240	351.7236	351.7236	474.4025	538.1211	665.8846
			190.32[b]	215.86[b]			351.73[c]	474.42[d]		
$2p3p\ ^3D_3$	$2p_{3/2}3p_{3/2}(3)$	117.7051	161.3384	182.1551	204.2452	287.1447	287.1447	374.0479	416.4475	496.2901
$2s3d\ ^3D_3$	$2s_{1/2}3d_{5/2}(3)$	137.7376	189.9326	215.4570	243.0204	351.2358	351.2358	473.8353	537.5178	665.2597

TABLE XVII. Oscillator strengths for the $2p3s\ ^{1,3}P_1$, $2p3d\ ^{2S+1}L_1$, and $2s3p\ ^{1,3}P_1$ transitions to the ground state in Ne-like given relative to the ground state. Comparison the present MBPT and MCDF theoretical results from Ref. [17].

	$2p_{3/2}3s_{1/2}(1)$		$2p_{1/2}3s_{1/2}(1)$		$2p_{3/2}3d_{3/2}(1)$		$2p_{3/2}3d_{5/2}(1)$		$2p_{1/2}3d_{3/2}(1)$		$2s_{1/2}3p_{1/2}(1)$		$2s_{1/2}3p_{3/2}(1)$
	$2p3s\ ^3P_1$		$2p3s\ ^1P_1$		$2p3d\ ^3P_1$		$2p3d\ ^3D_1$		$2p3d\ ^1P_1$		$2s3p\ ^3P_1$		$2s3p\ ^1P_1$
Z	MBPT	MCDF	MBPT	MCDF	MBPT	MCDF	MBPT	MCDF	MBPT	MCDF	MBPT	MCDF	MBPT
28	0.1306	0.1213	0.0972	0.0926	0.0099	0.0097	0.8440	0.7684	2.1894	2.5486	0.0499		0.2869
30	0.1328	0.1245	0.0922	0.0881	0.0094	0.0095	1.0316	0.9791	2.0966	2.4087	0.0610		0.2897
32	0.1340	0.1266	0.0887	0.0850	0.0085	0.0088	1.2108	1.1829	1.9956	2.2623	0.0716		0.2925
34	0.1347	0.1279	0.0864	0.0829	0.0071	0.0076	1.3740	1.3687	1.8972	2.1234	0.0813		0.2954
36	0.1350	0.1287	0.0850	0.0819	0.0056	0.0060	1.5179	1.5314	1.8072	1.9990	0.0900		0.2982
38	0.1350	0.1291	0.0846	0.0816	0.0039	0.0044	1.6419	1.6701	1.7278	1.8913	0.0976		0.3009
40	0.1349	0.1294	0.0851	0.0824	0.0023	0.0027	1.7472	1.7864	1.6590	1.7998	0.1042		0.3033
42	0.1348	0.1296	0.0869	0.0844	0.0010	0.0013	1.8353	1.8824	1.6003	1.7227	0.1097		0.3054
44	0.1347	0.1299	0.0905	0.0908	0.0002	0.0000	1.9077	1.9932	1.5502	1.6297	0.1141		0.3071
47	0.1346	0.1301	0.1017	0.0993	0.0004	0.0002	1.9881	2.0461	1.4889	1.5799	0.1186		0.3087
49	0.1347	0.1304	0.1174	0.1150	0.0028	0.0021	2.0197	2.0801	1.4558	1.5381	0.1201		0.3090
51	0.1350	0.1308	0.0246	0.0332	0.1388	0.1251	2.0188	2.0823	1.4278	1.5030	0.1203		0.3088
53	0.1354	0.1314	0.0020	0.0017	0.3238	0.3025	1.8924	1.9726	1.4045	1.4739	0.1189		0.3079
55	0.1359	0.1321	0.0060	0.0053	1.6943	1.5377	0.5486	0.7641	1.3857	1.4501	0.1155		0.3064
57	0.1367	0.1330	0.0104	0.0145	2.2598	2.3122	0.0048	0.0096	1.3713	1.4315	0.1095		0.3043
59	0.1377	0.1342	0.0156	0.0146	2.2779	2.3383	0.0037	0.0019	1.3620	1.4184	0.1000		0.3016
61	0.1390	0.1355	0.0214	0.0203	2.2828	2.3431	0.0119	0.0094	1.3589	1.4120	0.0853		0.2983
63	0.1404	0.1371	0.0279	0.0268	2.2864	2.3459	0.0177	0.0152	1.3644	1.4142	0.0630		0.2944
65	0.1422	0.1390	0.0350	0.0338	2.2888	2.3474	0.0215	0.0192	1.3809	1.4277	0.0302		0.2900
69	0.1464	0.1435	0.0502	0.0491	2.2893	2.3457	0.0260	0.0238	1.2417	1.3346	0.1378		0.2795
74	0.1534	0.1507	0.0704	0.0696	2.2821	2.3357	0.0285	0.0265	0.4754		0.8649	0.8764	0.2636
78	0.1604	0.1580	0.0866	0.0860	2.2712	2.3227	0.0294	0.0275	0.3579		0.9500	0.9782	0.2489
83	0.1711	0.1691	0.1058	0.1056	2.2531	2.3021	0.0298	0.0280	0.3092		0.9558	0.9888	0.2283
92	0.1966	0.1957	0.1360	0.1365	2.2120	2.2573	0.0295	0.0279	0.2803		0.9101	0.9356	0.1906

TABLE XVIII. E1 transition probabilities (s^{-1}) for the odd-parity states with J=1 transitions to the ground state in Ne-like given relative to the ground state. Comparison the present calculations and theoretical results from Refs. [8] - (a), [9] - (b), [12] - (c), [11] - (d), and [5] - (e). Designations: a[b]=$a \times 10^b$

.

	$2p_{3/2}3s_{1/2}(1)$	$2p_{1/2}3s_{1/2}(1)$	$2p_{3/2}3d_{3/2}(1)$	$2p_{3/2}3d_{5/2}(1)$	$2p_{1/2}3d_{3/2}(1)$	$2s_{1/2}3p_{1/2}(1)$	$2s_{1/2}3p_{3/2}(1)$
	$2p3s\ ^3P_1$	$2p3s\ ^1P_1$	$2p3d\ ^3P_1$	$2p3d\ ^3D_1$	$2p3d\ ^1P_1$	$2s3p\ ^3P_1$	$2s3p\ ^1P_1$
Z=14	6.59[09]	3.89[10]	1.96[09]	8.26[10]	2.27[11]	5.48[08]	4.71[10]
(a)	3.70[09]	4.50[10]	6.04[08]	1.54[10]	3.48[11]		
(d)	4.10[09]	3.69[10]	6.92[08]	2.33[10]	2.30[11]	9.54[07]	3.85[10]
Z=18	7.35[10]	1.64[11]	8.03[09]	2.52[11]	2.45[12]	4.44[09]	2.67[11]
(a)	6.41[10]	1.83[11]	4.80[09]	1.28[11]	3.00[12]		
(d)	6.69[10]	1.62[11]	6.63[09]	1.87[11]	2.37[12]	8.48[09]	4.85[11]
Z=19	1.19[11]	2.53[11]	2.26[10]	4.40[11]	4.01[12]	6.08[10]	6.17[12]
(d)	1.19[11]	2.08[11]	1.04[10]	3.13[11]	3.53[12]	1.61[10]	6.37[12]
Z=20	1.76[11]	2.70[11]	1.67[10]	6.10[11]	5.15[12]	4.37[10]	9.59[11]
(d)	1.63[11]	2.62[11]	1.59[10]	5.14[11]	4.98[12]	2.92[10]	8.41[11]
Z=21	2.59[11]	3.57[11]	2.84[10]	9.83[11]	7.30[12]	6.50[10]	1.13[12]
(d)	2.37[11]	3.23[11]	2.32[10]	8.27[11]	6.79[12]	5.14[10]	1.10[12]
Z=22	3.47[11]	4.06[11]	3.25[10]	1.43[12]	9.22[12]	1.05[11]	1.48[12]
(a)	3.13[11]	4.25[11]	2.33[10]	9.75[11]	1.08[13]		
Z=26	9.76[11]	8.28[11]	9.19[10]	6.33[12]	2.24[13]	4.51[11]	3.34[12]
(a)	8.49[11]	8.40[11]	8.86[10]	5.00[12]	2.59[13]		
(b)	9.44[11]	8.01[11]	8.27[10]	5.68[12]	2.64[13]	3.66[11]	3.21[12]
(c)	9.09[11]	7.54[11]	7.77[10]	5.23[12]	2.44[13]		
Z=29	1.79[12]	1.33[12]	1.57[11]	1.56[13]	3.70[13]	1.10[12]	5.75[12]
(c)	1.62[12]	1.16[12]	1.34[11]	1.37[13]	4.02[13]		
(e)	1.6[12]	1.2[12]	1.7[11]	1.6[13]	4.2[13]	1.1[12]	6.1[12]
Z=32	2.98[12]	2.07[12]	2.22[11]	3.25[13]	5.60[13]	2.26[12]	9.34[12]
(a)	2.36[12]	2.06[12]	1.63[11]	2.88[13]	6.45[13]		
(c)	2.61[12]	1.71[12]	1.87[11]	2.99[13]	6.03[13]		
(e)	2.9[12]	1.9[12]	2.5[11]	3.4[13]	6.23[13]	2.3[12]	9.8[12]
Z=34	4.04[12]	2.74[12]	2.50[11]	4.94[13]	7.15[13]	3.41[12]	1.26[13]
(c)	3.45[12]	2.18[12]	2.09[11]	4.62[13]	7.66[13]		
(e)	3.8[12]	2.5[12]	2.8[11]	5.2[13]	7.8[13]	3.5[12]	1.3[13]
Z=36	5.34[12]	3.58[12]	2.56[11]	7.15[13]	8.98[13]	4.93[12]	1.66[13]
(a)	5.38[12]	3.91[12]	1.79[11]	6.55[13]	1.03[14]		
(e)	5.0[12]	3.3[12]	2.9[11]	7.5[13]	9.7[13]	5.1[12]	1.7[13]
Z=37	6.09[12]	4.09[12]	2.47[11]	8.47[13]	1.00[14]	5.85[12]	1.90[13]
(e)	5.8[12]	3.7[12]	2.8[11]	8.9[13]	1.1[14]	6.0[12]	2.0[13]
Z=38	6.92[12]	4.65[12]	2.30[11]	9.96[13]	1.11[14]	6.88[12]	2.16[13]
(c)	5.64[12]	3.43[12]	1.85[11]	9.62[13]	1.18[14]		
(e)	6.6[12]	4.3[12]	2.6[11]	1.0[14]	1.2[14]	7.1[12]	2.2[13]
Z=42	1.11[13]	7.79[12]	9.39[10]	1.77[14]	1.66[14]	1.23[13]	3.49[13]
(c)	8.54[12]	5.29[12]	6.95[10]	1.74[14]	1.73[14]		
(e)	1.1[13]	7.2[12]	1.1[11]	1.9[14]	1.8[14]	1.3[13]	3.6[13]
Z=47	1.85[13]	1.57[13]	6.35[10]	3.20[14]	2.63[14]	2.23[13]	5.96[13]
(c)	1.33[13]	9.35[12]	4.84[10]	3.22[14]	2.69[14]		
(e)	1.8[13]	1.5[13]	6.0[10]	3.3[14]	2.7[14]	2.2[13]	6.1[13]
Z=50	2.46[13]	2.65[13]	1.76[12]	4.31[14]	3.42[14]	3.01[13]	7.95[13]
(e)	2.4[13]	2.5[13]	2.1[12]	4.5[14]	3.6[14]	3.0[13]	8.1[13]
Z=60	5.65[13]	8.62[12]	1.09[15]	3.96[12]	7.67[14]	5.40[13]	1.82[14]
(e)	5.5[13]	2.4[12]	1.1[15]	9.9[13]	8.0[14]	4.9[13]	1.8[14]

	$2p_{3/2}3s_{1/2}(1)$	$2p_{1/2}3s_{1/2}(1)$	$2p_{3/2}3d_{3/2}(1)$	$2p_{3/2}3d_{5/2}(1)$	$2p_{1/2}3d_{3/2}(1)$	$2s_{1/2}3p_{1/2}(1)$	$2s_{1/2}3p_{3/2}(1)$
	$2p3s\ ^3P_1$	$2p3s\ ^1P_1$	$2p3d\ ^3P_1$	$2p3d\ ^3D_1$	$2p3d\ ^1P_1$	$2s3p\ ^3P_1$	$2s3p\ ^1P_1$
Z=67	9.46[13]	3.22[13]	1.78[15]	2.03[13]	1.34[15]	2.36[10]	2.92[14]
(e)	9.3[13]	1.7[13]	1.8[15]	3.6[13]	1.3[15]	4.7[13]	3.0[14]
Z=74	1.53[14]	8.24[13]	2.75[15]	3.87[13]	7.35[14]	1.36[15]	4.39[14]
(e)	1.5[14]	9.1[13]	2.9[15]	3.3[13]	6.5[14]	1.5[15]	4.4[14]
Z=82	2.56[14]	1.86[14]	4.26[15]	6.71[13]	8.03[14]	2.53[15]	6.49[14]
(e)	2.5[14]	2.0[14]	4.4[15]	5.6[13]	7.8[14]	2.7[15]	6.5[14]
Z=92	4.70[14]	4.07[14]	6.89[15]	1.20[14]	1.27[15]	4.42[15]	9.77[14]
(e)	4.7[14]	4.0[13]	7.2[15]	1.0[14]	1.2[15]	4.6[15]	9.5[14]

TABLE XIX. M1 transition probabilities (s^{-1}) for the even-parity states with J=1 transitions to the ground state in Ne-like given relative to the ground state. Comparison the present calculations and theoretical results from Refs. [8] - (a), [9] - (b), [12] - (c), and [5] - (d). Designations: a[b]=$a \times 10^b$

	$2p_{3/2}3p_{1/2}(1)$	$2p_{3/2}3p_{3/2}(1)$	$2p_{1/2}3p_{3/2}(1)$	$2p_{1/2}3p_{1/2}(1)$	$2s_{1/2}3s_{1/2}(1)$	$2s_{1/2}3d_{3/2}(1)$
	$2p3p\ ^3S_1$	$2p3p\ ^3D_1$	$2p3p\ ^1P_1$	$2p3p\ ^3P_1$	$2s3s\ ^3S_1$	$2s3d\ ^3D_1$
26	2.04[05]	4.41[03]	5.09[03]	2.04[05]	2.20[04]	2.72[03]
(a)	2.49[04]	2.24[04]	9.86[02]	8.23[04]		
(b)	4.95[04]	5.94[04]	2.20[03]	1.99[05]	2.33[01]	1.67-01]
(c)	5.04[04]	6.07[04]	2.19[03]	2.03[05]		
29	8.50[05]	1.49[02]	2.68[04]	6.77[05]	8.39[04]	1.09[04]
(c)	2.60[05]	1.77[05]	1.89[03]	7.17[05]		
(d)	2.4[04]	7.4[05]	7.6[03]	8.5[05]	7.7[05]	3.2[03]
32	2.87[06]	3.53[04]	9.62[04]	1.97[06]	2.79[05]	3.62[04]
(c)	1.06[06]	3.89[05]	1.39[03]	2.19[06]		
(d)	2.9[05]	1.8[06]	4.2[04]	2.6[06]	1.1[06]	1.0[03]
34	5.87[06]	2.01[05]	1.99[05]	3.79[06]	5.85[05]	7.47[04]
(c)	2.38[06]	5.93[05]	9.50[02]	4.32[06]		
(d)	1.1[06]	2.7[06]	1.0[05]	5.0[06]	1.3[06]	6.8[02]
36	1.13[07]	7.13[05]	3.87[05]	7.04[06]	1.18[06]	1.47[05]
(d)	2.8[06]	3.6[06]	3.3[05]	8.6[06]	1.4[06]	5.9[03]
38	2.09[07]	1.98[06]	7.16[05]	1.26[07]	2.27[06]	2.76[05]
(c)	9.69[06]	1.15[06]	2.25[02]	4.91[07]		
(d)	6.9[06]	4.5[06]	4.7[05]	1.6[07]	1.4[06]	2.7[04]
42	6.34[07]	1.00[07]	2.19[06]	3.74[07]	7.72[06]	8.81[05]
(c)	3.18[07]	1.90[06]	1.10[01]	4.51[07]		
(d)	3.0[07]	4.8[06]	1.6[06]	4.6[06]	8.5[05]	1.8[05]
47	2.17[08]	4.87[07]	7.59[06]	1.27[08]	3.07[07]	3.21[06]
(c)	1.14[08]	3.17[06]	8.35[02]	1.55[08]		
(d)	1.4[08]	1.8[05]	6.3[06]	1.3[08]	7.8[05]	9.7[05]
50	4.26[08]	1.09[08]	1.51[07]	2.50[08]	6.62[07]	6.51[06]
(d)	3.0[08]	3.2[06]	1.5[07]	2.6[08]	7.8[06]	2.4[06]
60	3.11[09]	9.94[08]	1.16[08]	1.80[09]	6.91[08]	5.22[07]
(d)	2.7[09]	4.7[08]	1.4[08]	1.6[09]	4.1[08]	2.4[07]
67	1.04[10]	3.53[09]	4.08[08]	5.09[09]	3.76[09]	1.85[08]
(d)	0.94[10]	2.6[09]	6.4[08]	6.4[09]	3.0[09]	0.99[08]
74	3.08[10]	1.08[10]	1.30[09]	1.49[07]	2.83[10]	5.88[08]
(d)	2.9[10]	1.0[10]	2.0[09]	1.7[07]	2.6[10]	3.6[08]
82	9.54[10]	3.33[10]	4.42[09]	1.01[10]	8.62[10]	1.95[09]
(d)	9.4[10]	3.8[10]	6.2[09]	1.3[10]	7.4[10]	1.4[09]
92	3.42[11]	1.17[11]	1.84[10]	6.29[10]	3.33[11]	6.86[09]
(d)	3.4[11]	1.3[11]	2.8[10]	6.2[10]	3.1[11]	5.2[09]

TABLE XX. E2 transition probabilities (s^{-1}) for the even-parity states with J=2 transitions to the ground state in Ne-like given relative to the ground state. Comparison the present calculations and theoretical results from Refs. [8] - (a), [9] - (b), [12] - (c), and [5] - (d). Designations: a[b]=$a \times 10^b$

	$2p_{3/2}3p_{1/2}(2)$	$2p_{3/2}3p_{3/2}(2)$	$2p_{1/2}3p_{3/2}(2)$	$2s_{1/2}3d_{3/2}(2)$	$2s_{1/2}3d_{5/2}(2)$
	$2p3p\ ^3D_2$	$2p3p\ ^3P_2$	$2p3p\ ^1D_2$	$2s3d\ ^3D_2$	$2s3d\ ^1D_2$
14	6.33[05]	1.65[06]	1.49[06]	5.41[04]	3.98[07]
(a)	4.48[05]	2.28[06]	2.26[06]		
18	1.29[07]	2.08[07]	2.50[07]	6.45[06]	6.57[08]
(a)	1.26[07]	2.48[07]	3.32[07]		
22	1.04[08]	1.26[08]	1.57[08]	2.01[07]	4.93[09]
(a)	1.02[08]	1.38[08]	1.89[08]		
26	4.62[08]	4.93[08]	5.90[08]	2.50[07]	1.05[10]
(a)	4.48[08]	5.28[08]	7.13[08]		
(b)	5.28[08]	5.82[08]	6.64[08]	4.17[07]	1.02[10]
(c)	5.14[08]	5.66[08]	6.68[08]		
29	1.14[09]	1.18[09]	1.38[09]	1.20[08]	2.28[10]
(c)	1.27[09]	1.33[09]	1.53[09]		
(d)	1.1[09]	1.1[09]	1.2[09]	9.8[07]	1.9[10]
32	2.50[09]	2.54[09]	2.92[09]	4.86[08]	4.58[10]
(a)	2.29[09]	2.55[09]	3.55[09]		
(c)	2.75[09]	2.64[09]	3.17[09]		
(d)	2.4[09]	2.5[09]	2.7[09]	4.0[08]	4.0[10]
34	3.99[09]	4.02[09]	4.58[09]	1.12[09]	7.00[10]
(c)	4.36[09]	4.47[09]	4.92[09]		
(d)	3.9[09]	4.0[09]	4.2[09]	0.95[0]	9 6.2[10]
36	6.14[09]	6.16[09]	6.98[09]	2.43[09]	1.04[11]
(a)	5.38[09]	5.95[09]	8.53[09]		
(d)	6.0[09]	6.1[09]	6.3[09]	2.1[09]	0.94[11]
38	9.17[09]	9.16[09]	1.04[10]	4.94[09]	1.51[11]
(c)	9.93[09]	1.01[10]	1.09[10]		
(d)	9.0[09]	9.2[09]	0.94[10]	4.3[09]	1.4[11]
42	1.90[10]	1.89[10]	2.13[10]	1.75[10]	2.96[11]
(c)	2.04[10]	2.06[10]	2.19[10]		
(d)	1.9[10]	1.9[10]	1.9[10]	1.6[10]	2.7[11]
47	4.20[10]	4.16[10]	4.72[10]	6.56[10]	6.19[11]
(c)	4.48[10]	4.54[10]	4.73[10]		
(d)	4.2[10]	4.2[10]	4.2[10]	6.1[10]	5.7[11]
50	6.45[10]	6.38[10]	7.27[10]	1.29[11]	9.23[11]
(d)	6.5[10]	6.5[10]	6.5[10]	1.2[11]	8.6[11]
60	2.22[11]	2.19[11]	2.56[11]	7.88[11]	2.95[12]
(d)	2.2[11]	2.2[11]	2.2[11]	7.6[11]	2.7[12]
74	8.75[11]	8.69[11]	1.06[12]	4.82[12]	1.16[13]
(d)	8.9[11]	8.9[11]	0.94[12]	4.8[12]	1.1[13]
82	1.67[12]	1.68[12]	2.10[12]	1.12[13]	2.36[13]
(d)	1.7[12]	1.7[12]	1.7[12]	1.1[13]	2.2[13]
92	3.37[12]	3.46[12]	3.96[12]	3.33[13]	5.37[12]
(d)	3.4[12]	3.6[12]	3.7[12]	2.7[13]	5.0[13]

TABLE XXI. M2 transition probabilities (s^{-1}) for the odd-parity states with J=2 transitions to the ground state in Ne-like given relative to the ground state. Comparison the present calculations and theoretical results from Refs. [13] - (a) and [5] - (b). Designations: a[b]=$a \times 10^b$

	$2p_{3/2}3s_{1/2}(2)$	$2p_{3/2}3d_{5/2}(2)$	$2p_{3/2}3d_{3/2}(2)$	$2p_{1/2}3d_{3/2}(2)$	$2p_{1/2}3d_{5/2}(2)$	$2s_{1/2}3p_{3/2}(2)$
	$2p3s\ ^3P_2$	$2p3d\ ^3P_2$	$2p3d\ ^3F_2$	$2p3d\ ^1D_2$	$2p3p\ ^3D_2$	$2s3p\ ^3P_2$
12	9.016[00]	6.460[01]	8.617[00]	4.816[00]	2.465[00]	6.059[01]
(a)		7.72[01]	0.473[00]	6.15[00]	3.30[00]	
14	1.016[02]	2.124[03]	1.744[02]	2.297[02]	1.078-02]	2.143[02]
(a)	1.00[02]					
18	2.909[03]	8.444[04]	7.840[03]	9.567[03]	5.205[00]	7.163[03]
(a)	2.89[03]	9.26[04]	2.45[03]	1.28[04]	2.45[01]	
26	1.833[05]	5.560[06]	1.098[06]	3.688[05]	3.121[05]	7.403[05]
(a)	1.69[05]	6.34[06]	0.791[06]	4.39[05]	2.63[05]	
29	5.604[05]	1.614[07]	4.422[06]	8.852[05]	1.574[06]	2.315[06]
(a)	5.13[05]					
(b)	4.1[06]	1.2[07]	3.0[06]	6.7[05]	1.1[06]	2.0[06]
32	1.493[06]	3.880[07]	1.607[07]	1.912[06]	5.675[06]	6.371[06]
(a)		4.57[07]	1.26[07]	2.21[06]	5.32[06]	
(b)	1.1[06]	3.0[07]	1.1[07]	1.5[06]	4.2[06]	5.8[06]
42	2.025[07]	1.547[08]	5.773[08]	1.776[07]	1.217[08]	9.617[07]
(a)	1.87[07]					
(b)	1.7[07]	1.3[09]	4.7[08]	1.5[07]	1.0[08]	9.1[07]
50	1.030[08]	1.585[08]	3.450[09]	8.094[07]	7.186[08]	5.181[08]
(a)		1.76[08]	3.60[09]	9.05[07]	8.03[08]	
(b)	0.90[08]	1.4[08]	3.0[09]	7.1[07]	6.4[08]	5.0[08]
60	5.605[08]	1.687[08]	1.824[10]	4.132[08]	4.294[09]	2.892[09]
(a)	5.45[08]					
(b)	5.1[08]	1.5[08]	1.6[10]	3.8[08]	4.0[09]	2.9[09]
67	1.570[09]	1.844[08]	4.842[10]	1.129[09]	1.249[10]	8.034[09]
(a)	1.55[09]	1.92[08]	5.03[10]	1.23[09]	1.26[10]	
(b)	1.4[09]	1.7[08]	4.4[10]	1.1[09]	1.2[10]	8.0[09]
74	4.002[09]	2.032[08]	1.153[11]	2.828[09]	3.266[10]	1.992[10]
(a)		2.13[08]	1.20[11]	3.04[09]	3.22[10]	
(b)	3.8[09]	1.8[08]	1.1[11]	2.7[09]	3.1[10]	
82	1.059[10]	2.258[08]	2.803[11]	7.418[09]	8.895[10]	5.030[10]
(a)	1.07[10]	2.41[08]	2.90[11]	7.69[09]	8.62[10]	
(b)	1.0[10]	2.3[08]	2.6[11]	7.2[09]	8.6[10]	5.2[10]
92	3.167[10]	2.520[08]	7.523[11]	2.197[10]	2.796[11]	1.289[11]
(a)	3.23[10]	2.79[08]	7.76[11]	2.34[10]	2.65[11]	
(b)	3.1[10]	2.8[08]	7.0[11]	2.3[10]	2.6[11]	1.4[11]

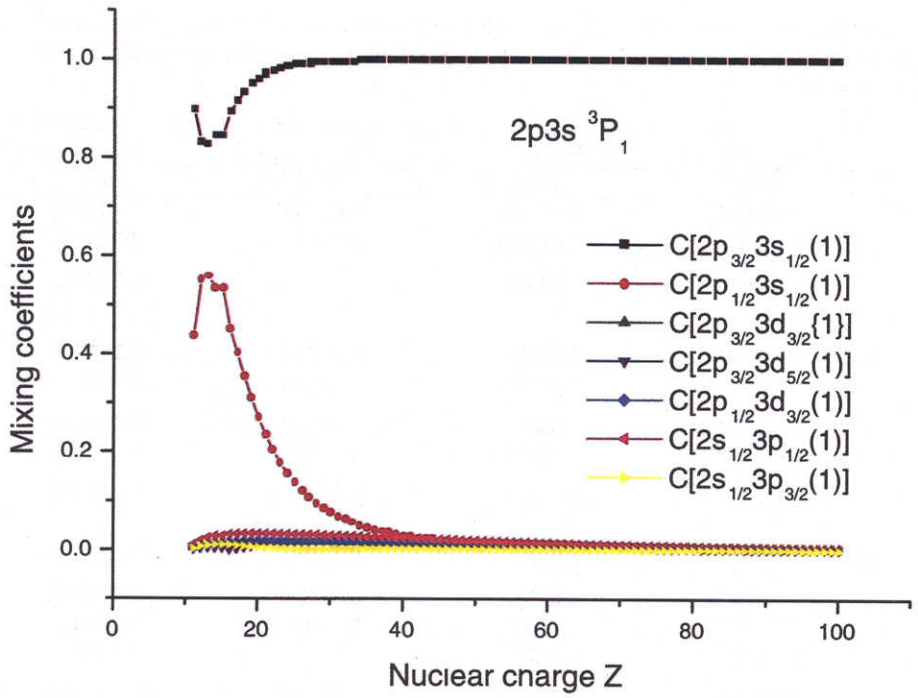

FIG. 1. Mixing coefficients for the $2p3s\ ^3P_1$ level as functions of Z

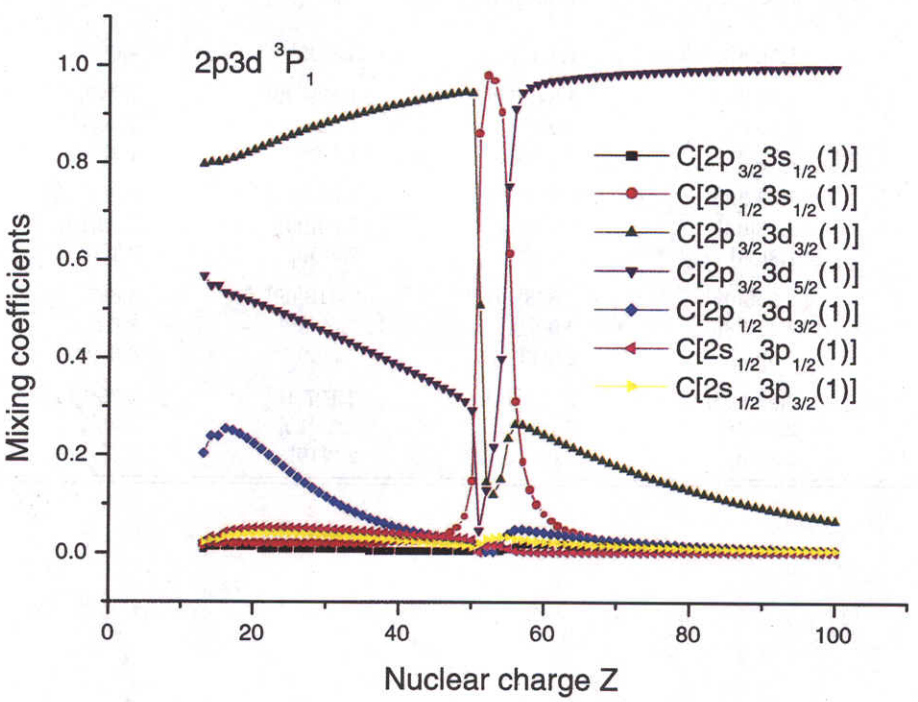

FIG. 2. Mixing coefficients for the $2p3d\ ^3P_1$ level as functions of Z

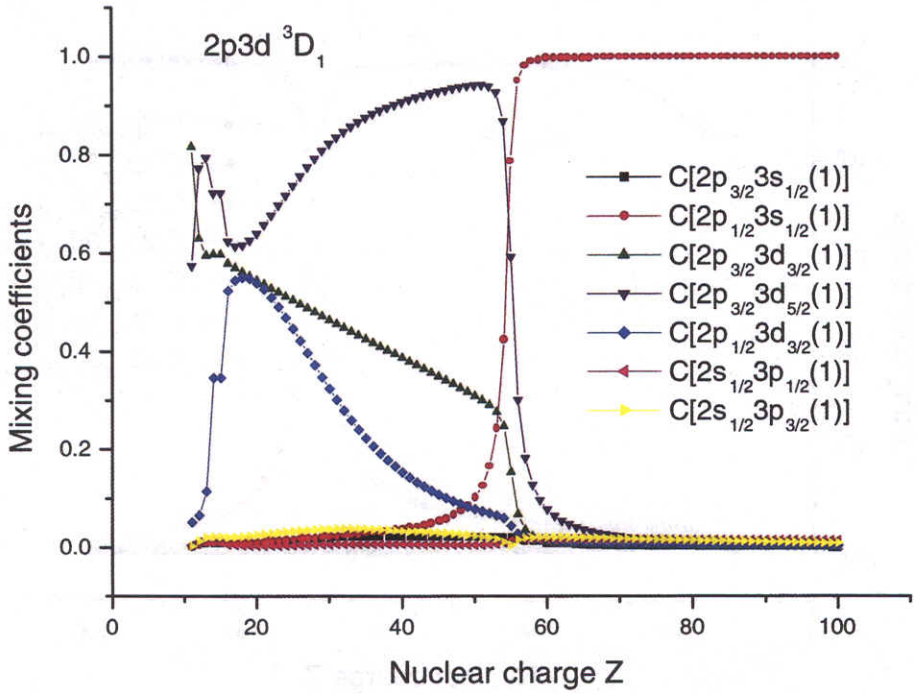

FIG. 3. Mixing coefficients for the $2p3d\ ^3D_1$ level as functions of Z

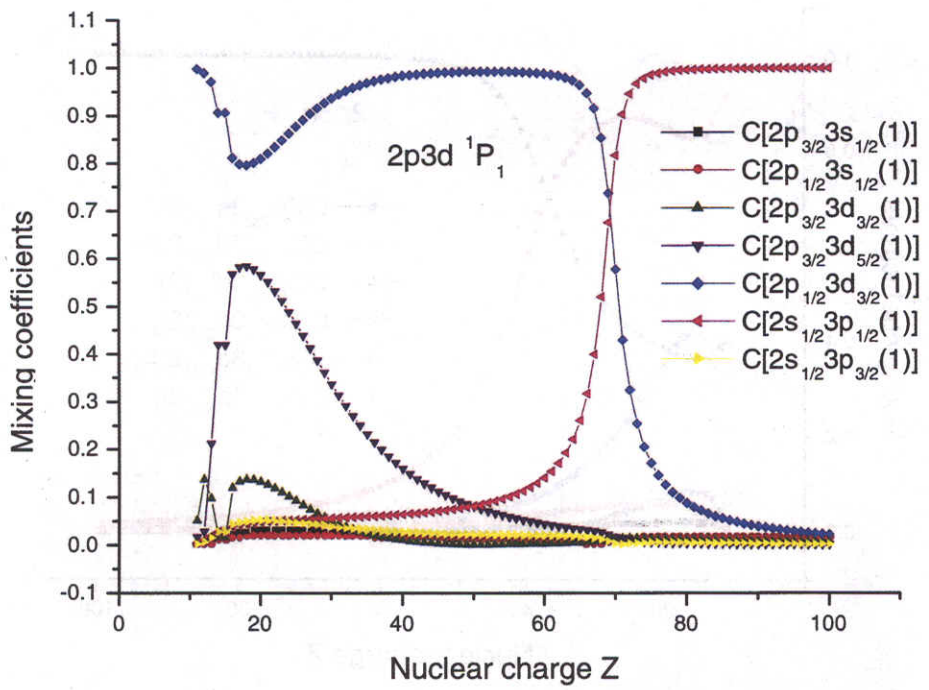

FIG. 4. Mixing coefficients for the $2p3d\ ^1P_1$ level as functions of Z

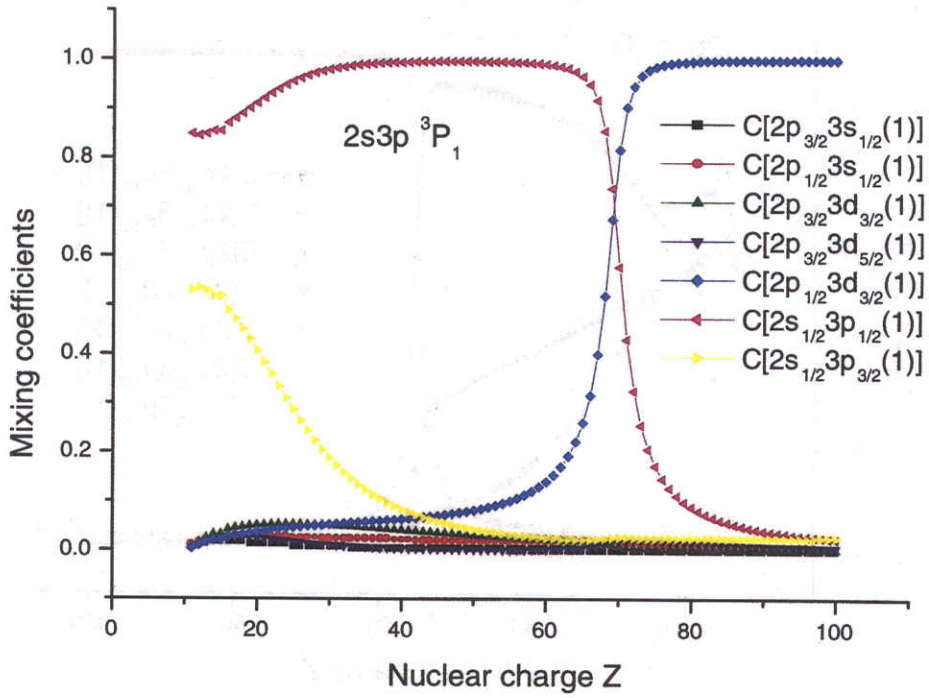

FIG. 5. Mixing coefficients for the $2s3p\ ^3P_1$ level as functions of Z

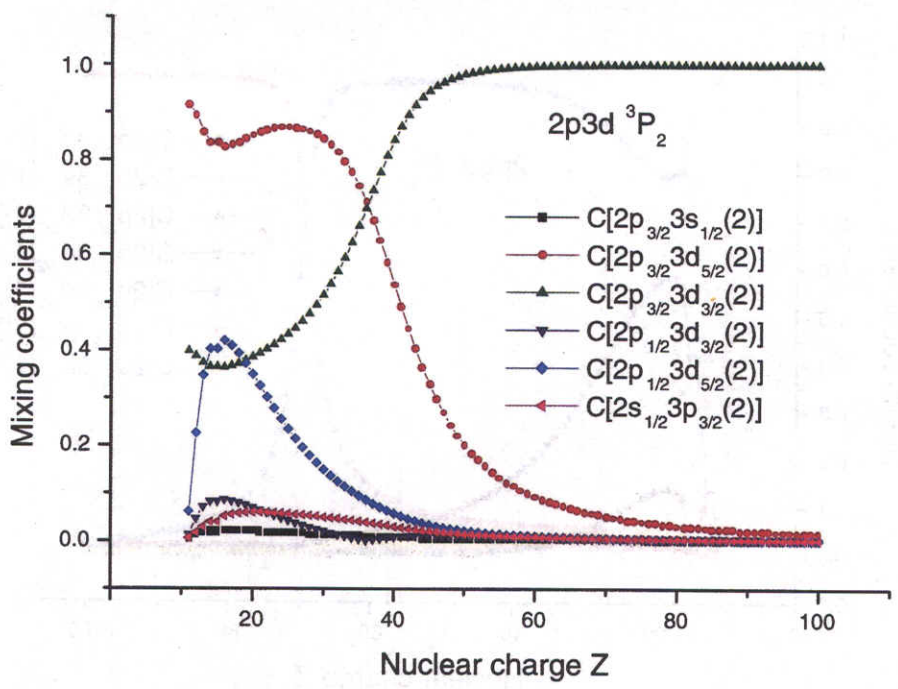

FIG. 6. Mixing coefficients for the $2p3d\ ^3P_2$ level as functions of Z

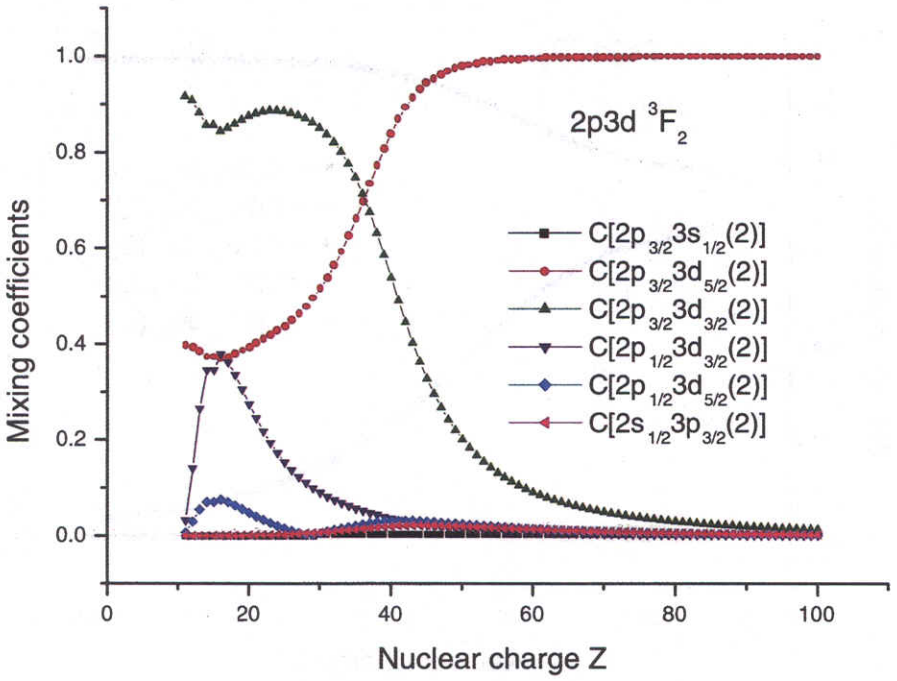

FIG. 7. Mixing coefficients for the $2p3d\ ^3F_2$ level as functions of Z

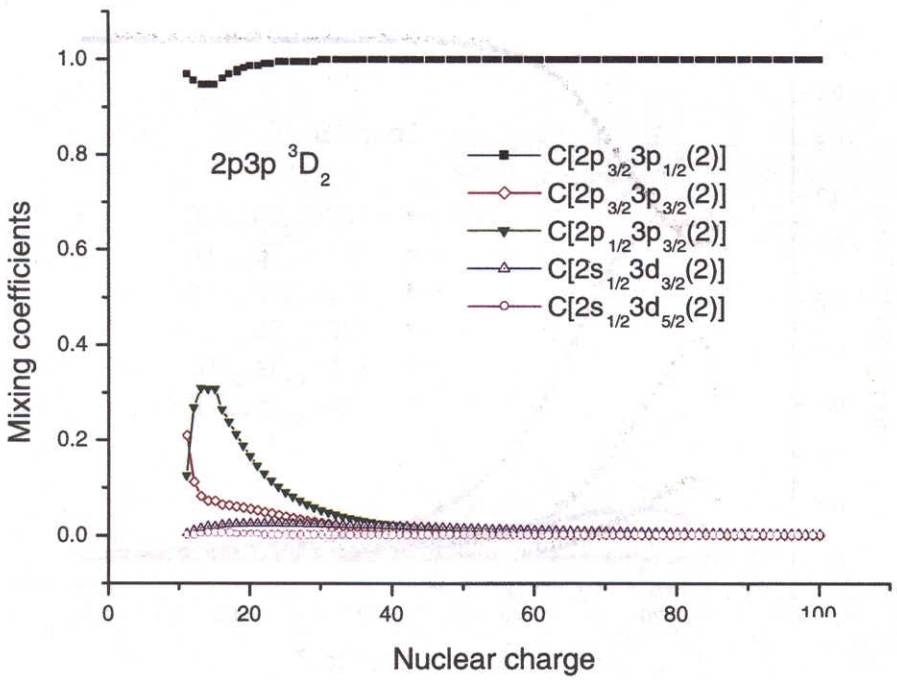

FIG. 8. Mixing coefficients for the $2p3p\ ^3D_2$ level as functions of Z

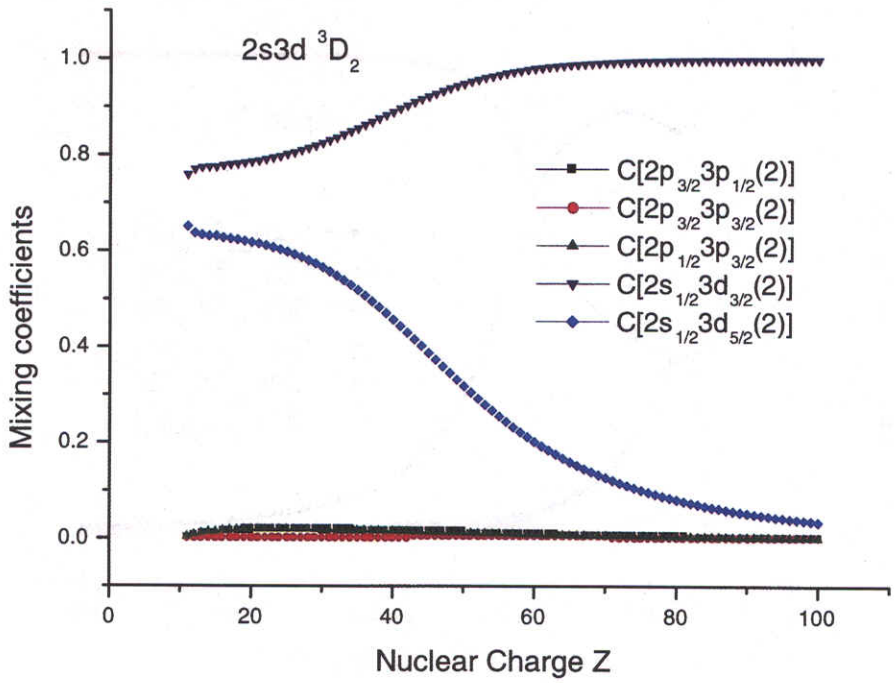

FIG. 9. Mixing coefficients for the $2s3d\ ^3D_2$ level as functions of Z

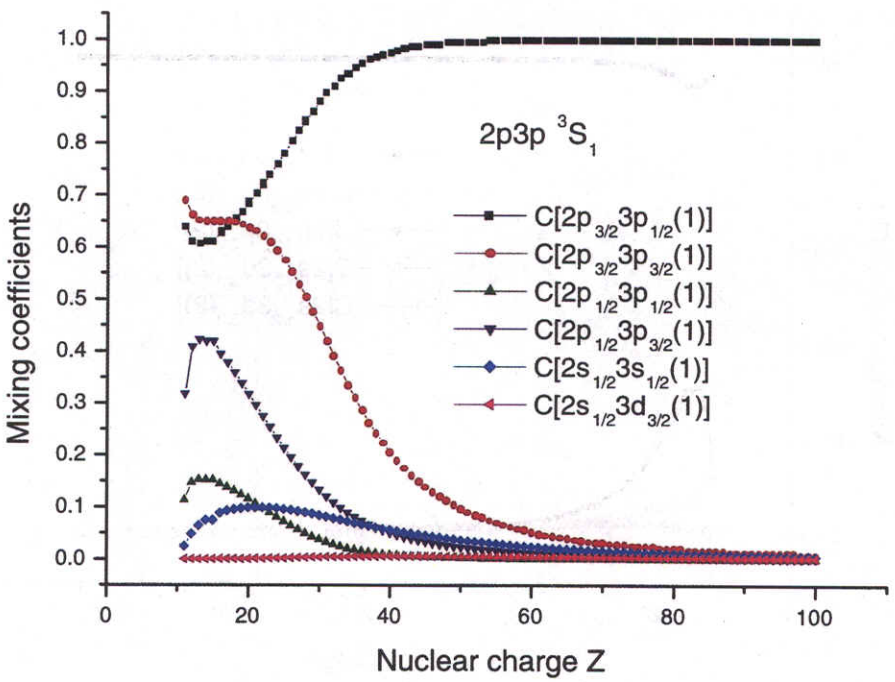

FIG. 10. Mixing coefficients for the $2p3p\ ^3S_1$ level as functions of Z

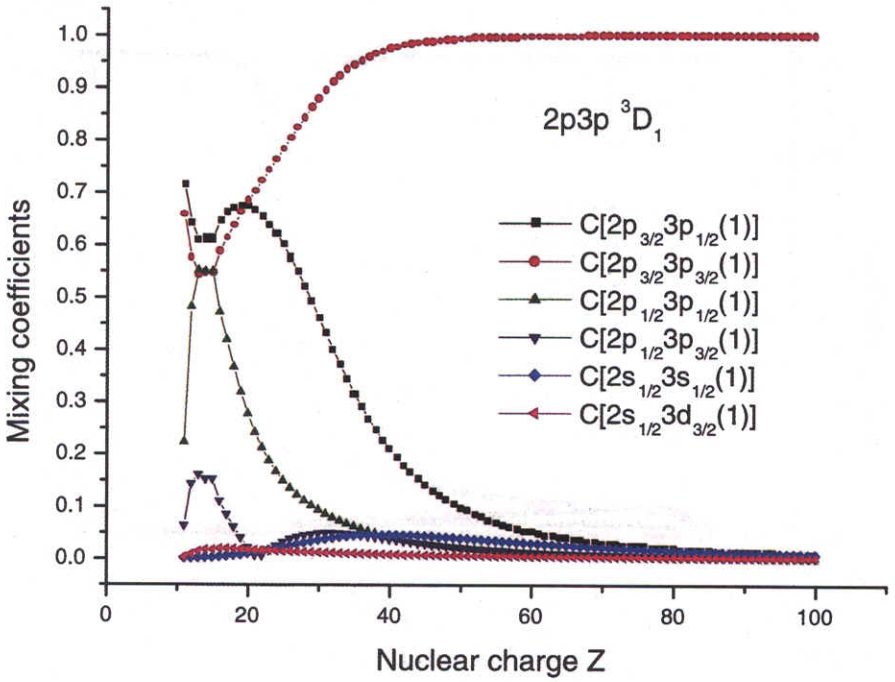

FIG. 11. Mixing coefficients for the $2p3p\ ^3D_1$ level as functions of Z

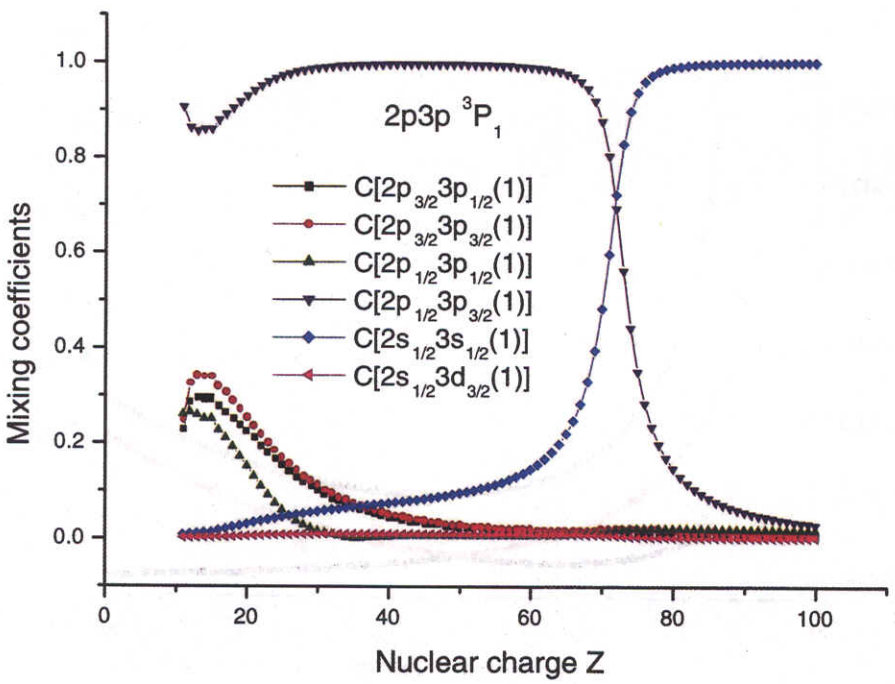

FIG. 12. Mixing coefficients for the $2p3p\ ^3P_1$ level as functions of Z

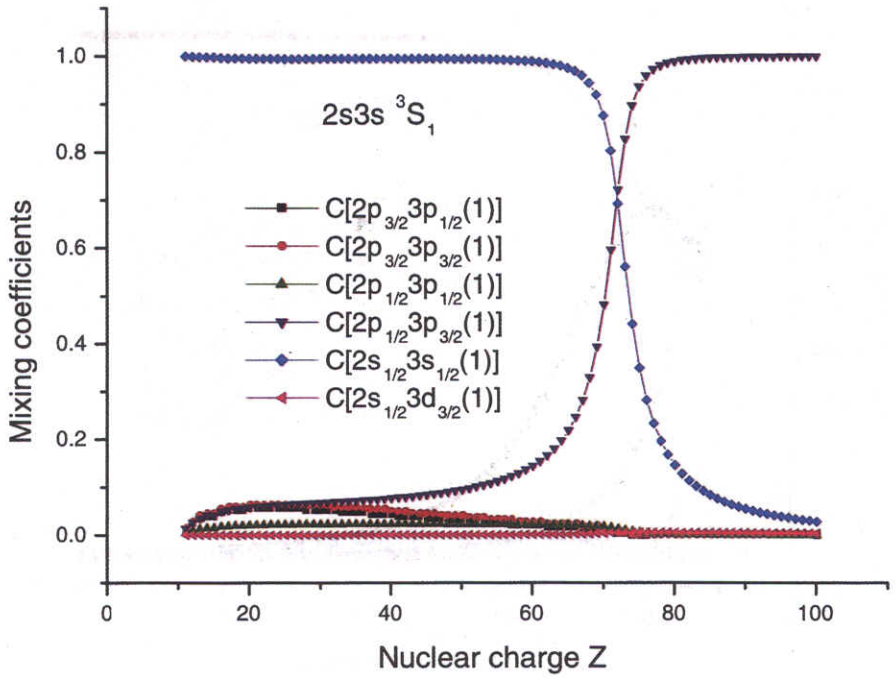

FIG. 13. Mixing coefficients for the $2s3s\ ^3S_1$ level as functions of Z

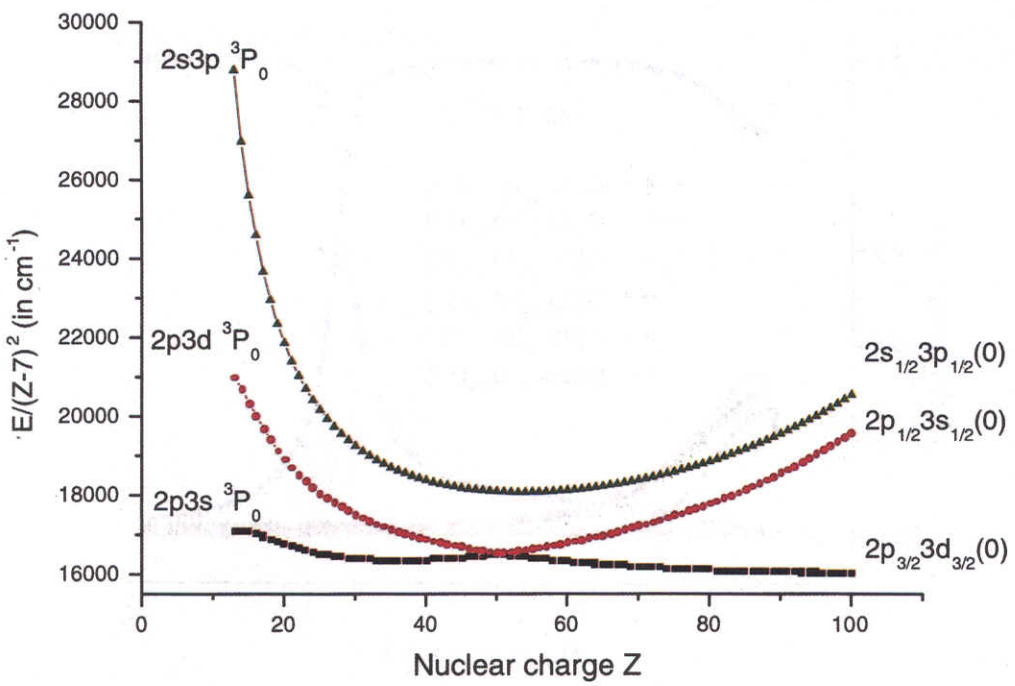

FIG. 14. Energies $(E/(Z-7)^2$ in $\mathrm{cm}^{-1})$ of odd parity states with J=0 as functions of Z

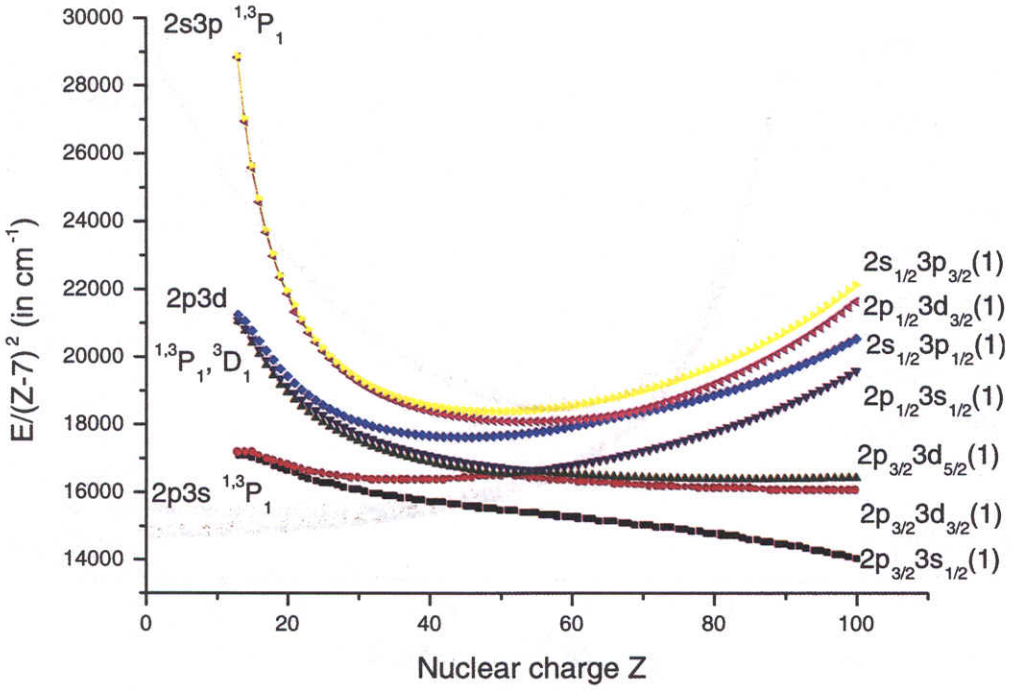

FIG. 15. Energies $(E/(Z-7)^2$ in cm$^{-1})$ of odd parity states with J=1 as functions of Z

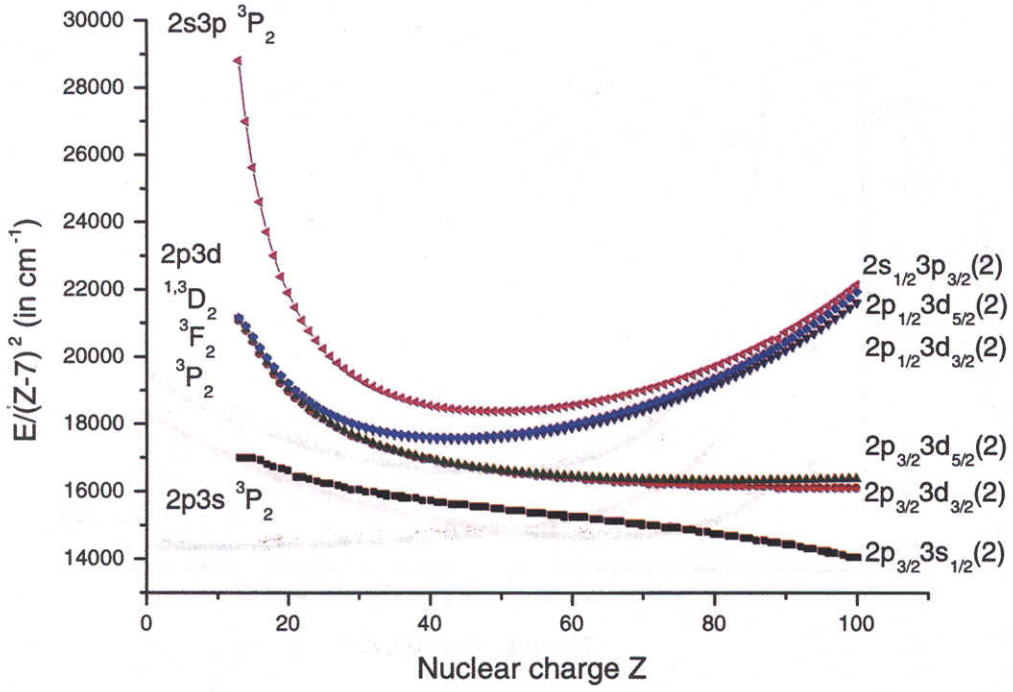

FIG. 16. Energies $(E/(Z-7)^2$ in cm^{-1}) of odd parity states with J=2 as functions of Z

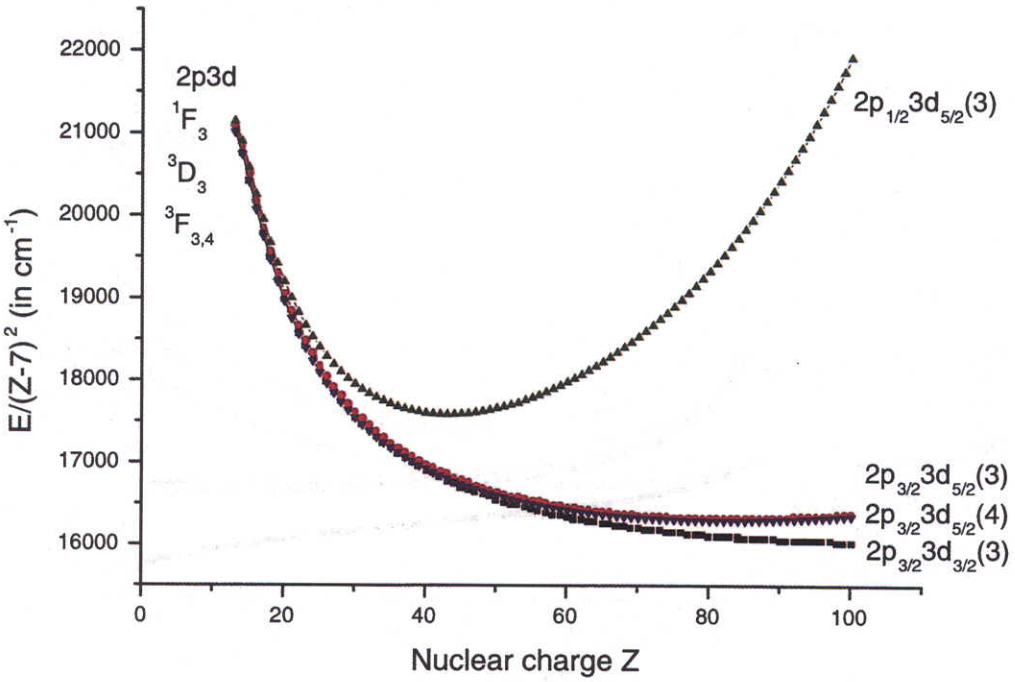

FIG. 17. Energies $(E/(Z-7)^2$ in $\mathrm{cm}^{-1})$ of odd parity states with J=3,4 as functions of Z

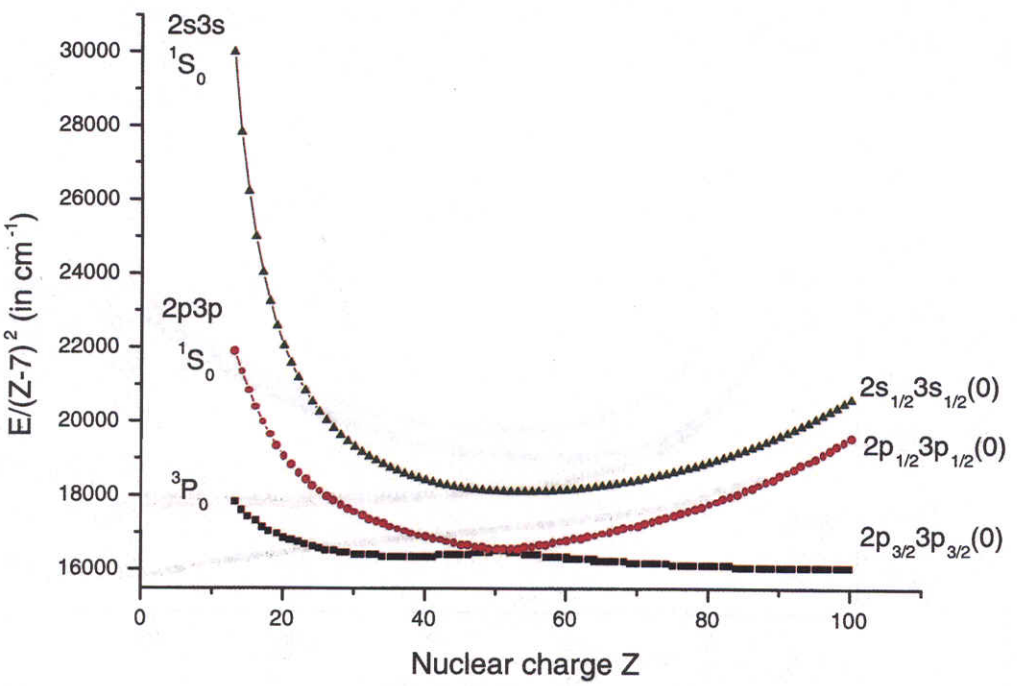

FIG. 18. Energies $(E/(Z-7)^2$ in $\mathrm{cm}^{-1})$ of even parity states with J=0 as functions of Z

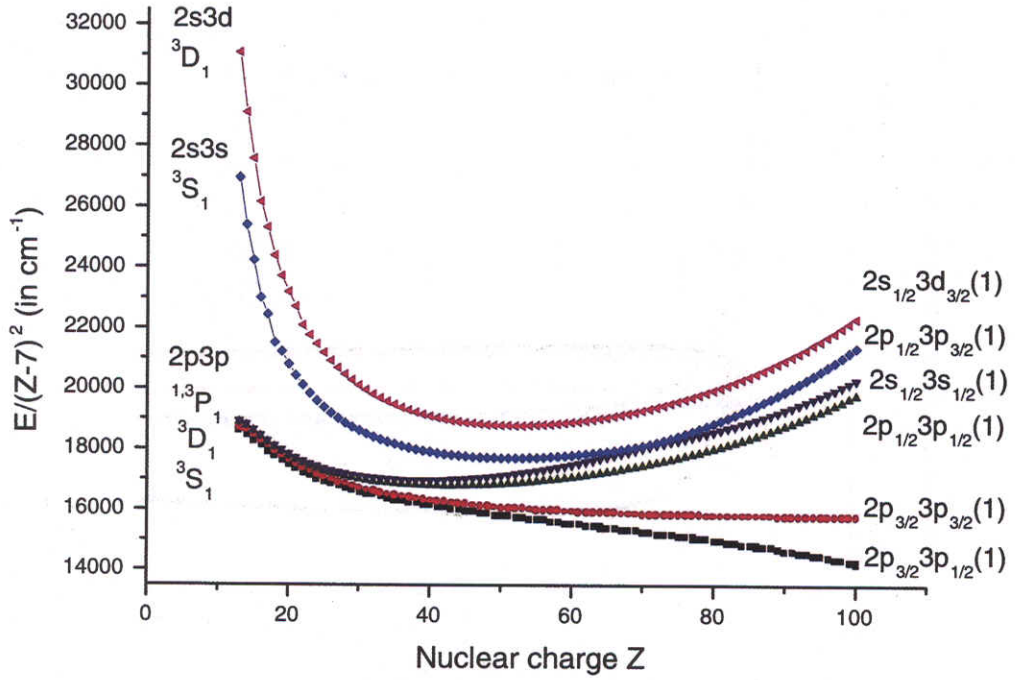

FIG. 19. Energies $(E/(Z-7)^2$ in $\mathrm{cm}^{-1})$ of even parity states with J=1 as functions of Z

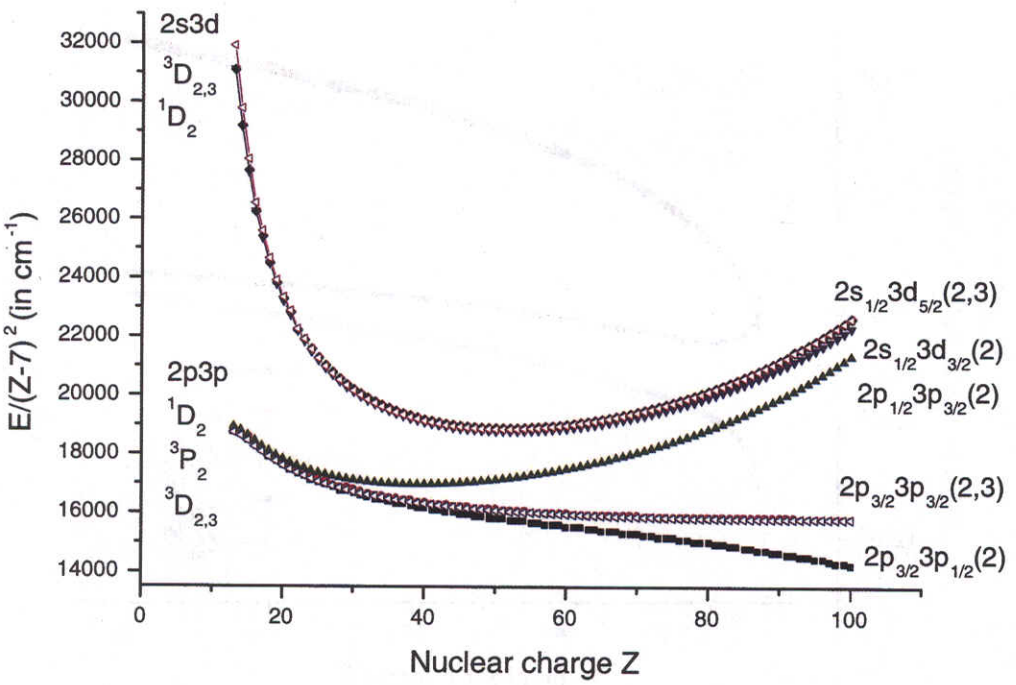

FIG. 20. Energies $(E/(Z-7)^2$ in $\mathrm{cm}^{-1})$ of even parity states with J=2,3 as functions of Z

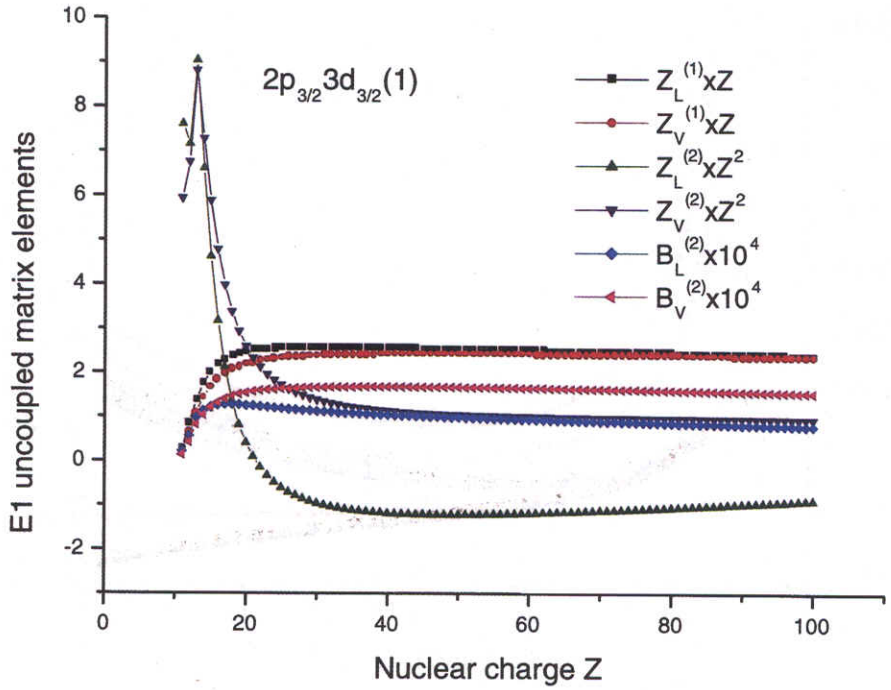

FIG. 21. Uncoupled matrix element for transition between $2p_{3/2}3d_{3/2}(1)$ and ground state calculated in length and velocity forms in Ne-like ions.

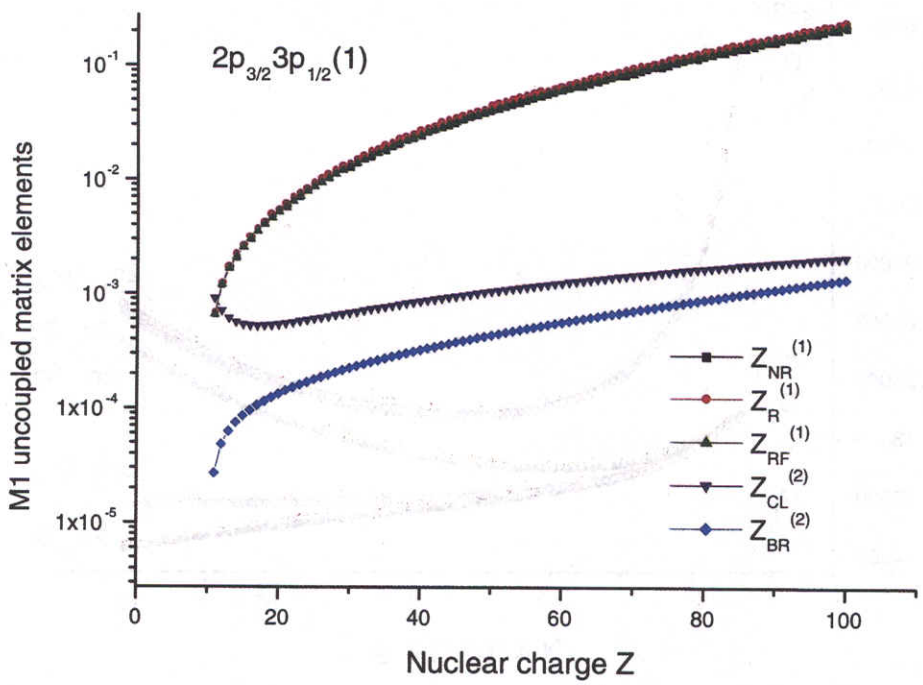

FIG. 22. $2p_{3/2}3p_{1/2}(1)$ matrix elements for magnetic-dipole transition for Ne-like ions as function of Z

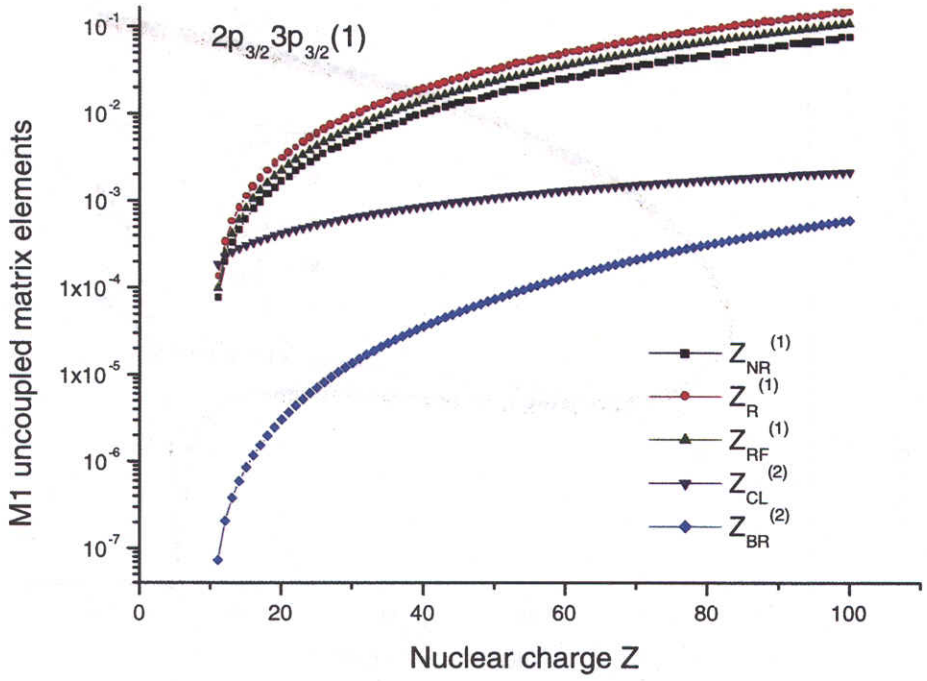

FIG. 23. $2p_{3/2}3p_{3/2}(1)$ matrix elements for magnetic-dipole transition for Ne-like ions as function of Z

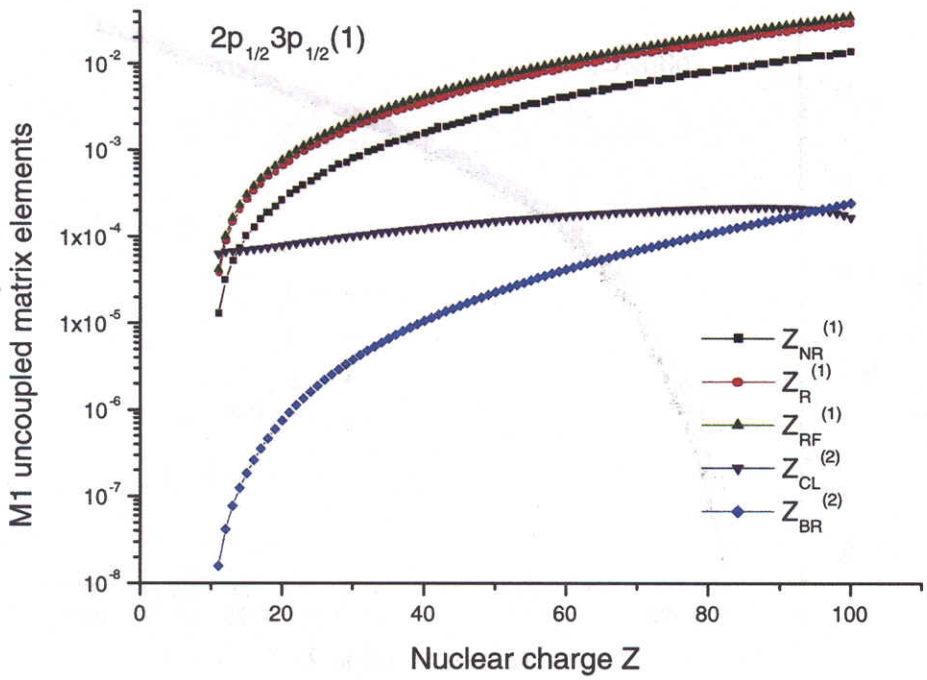

FIG. 24. $2p_{1/2}3p_{1/2}(1)$ matrix elements for magnetic-dipole transition for Ne-like ions as function of Z

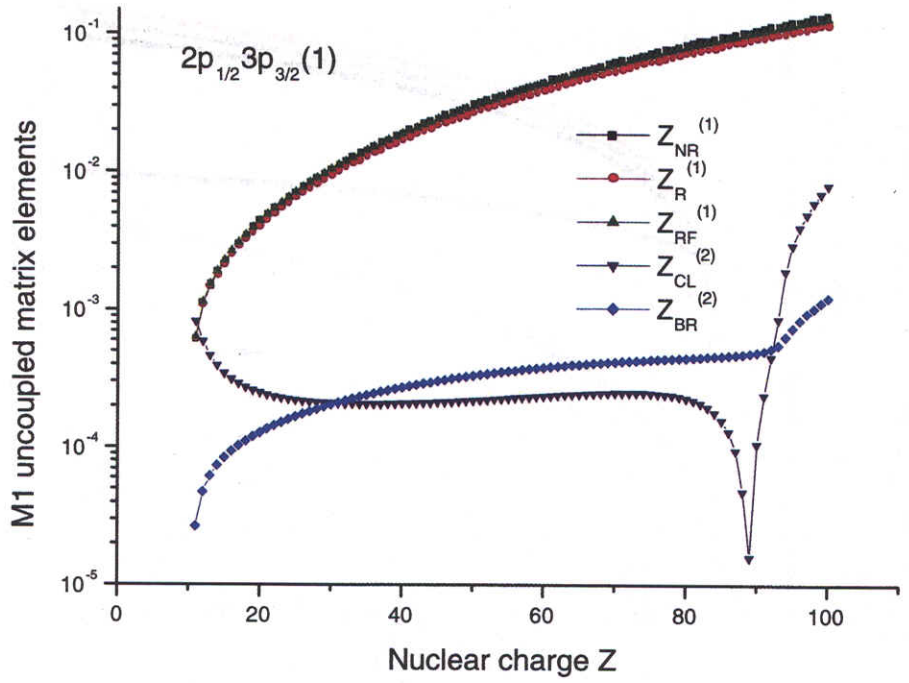

FIG. 25. $2p_{1/2}3p_{3/2}(1)$ matrix elements for magnetic-dipole transition for Ne-like ions as function of Z

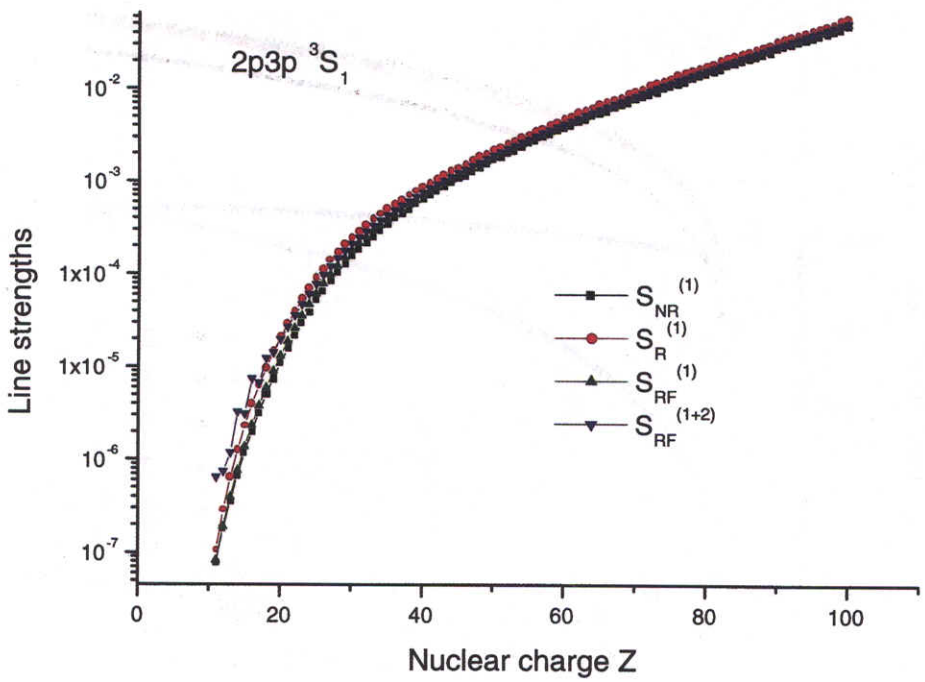

FIG. 26. Line strengths for $2p3p\ ^3S_1$ magnetic-dipole transition for Ne-like ions as function of Z

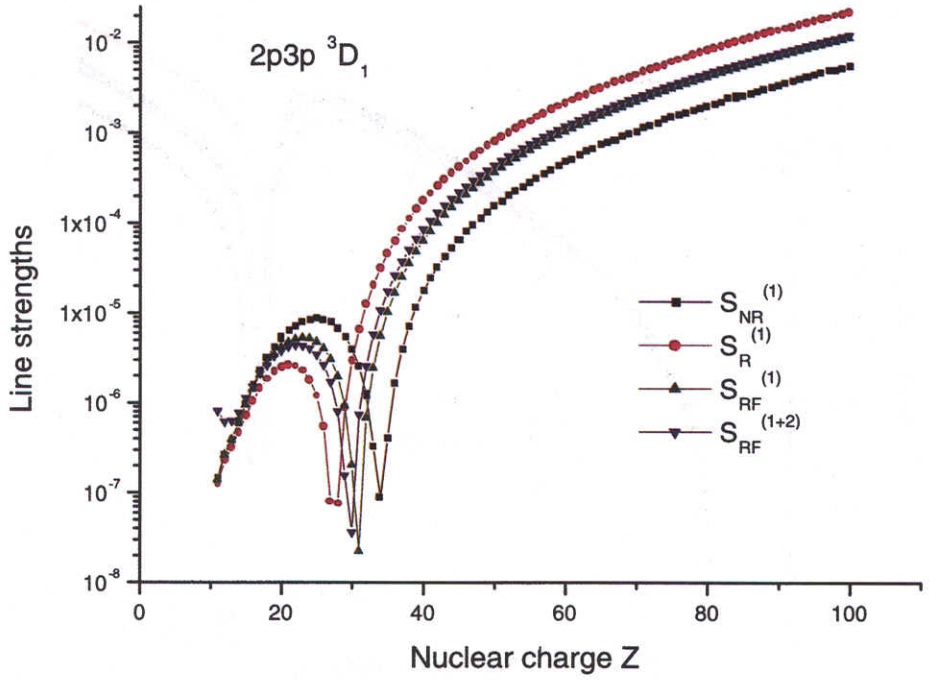

FIG. 27. Line strengths for $2p3p\ ^3D_1$ magnetic-dipole transition for Ne-like ions as function of Z

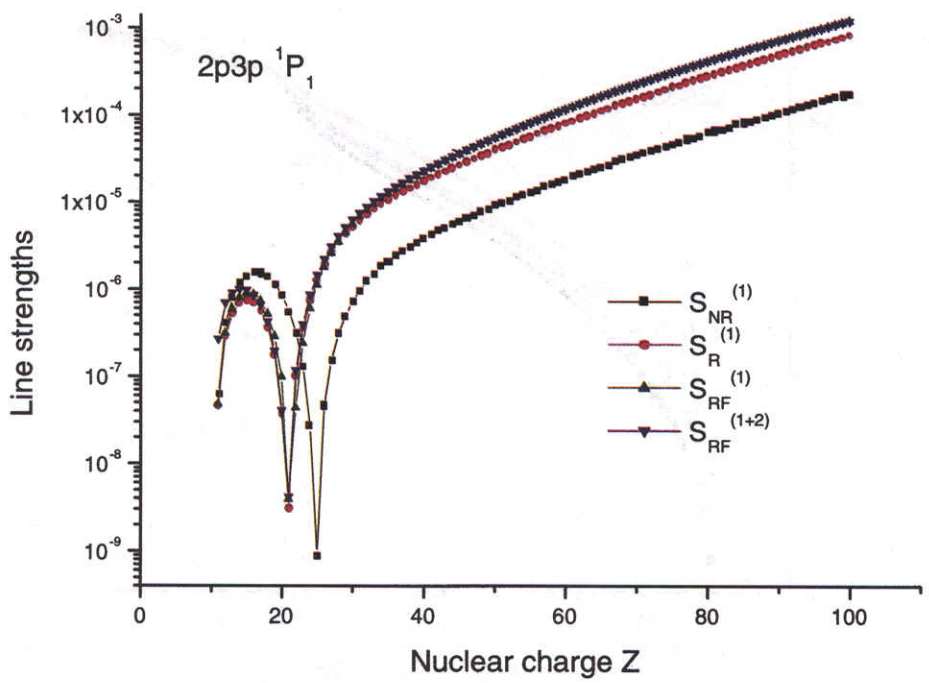

FIG. 28. Line strengths for $2p3p\ ^1P_1$ magnetic-dipole transition for Ne-like ions as function of Z

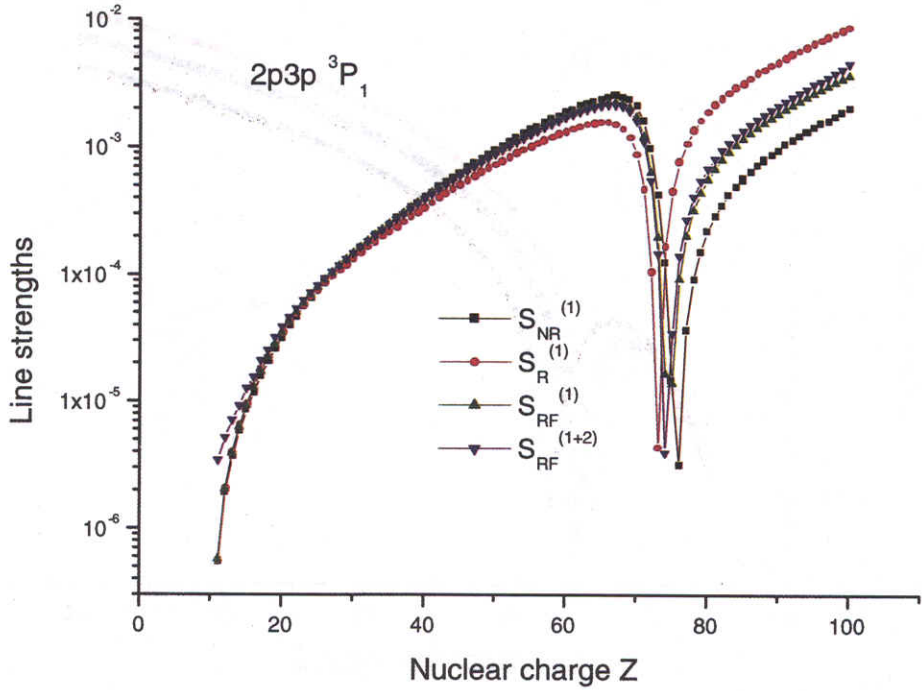

FIG. 29. Line strengths for $2p3p\ ^3P_1$ magnetic-dipole transition for Ne-like ions as function of Z

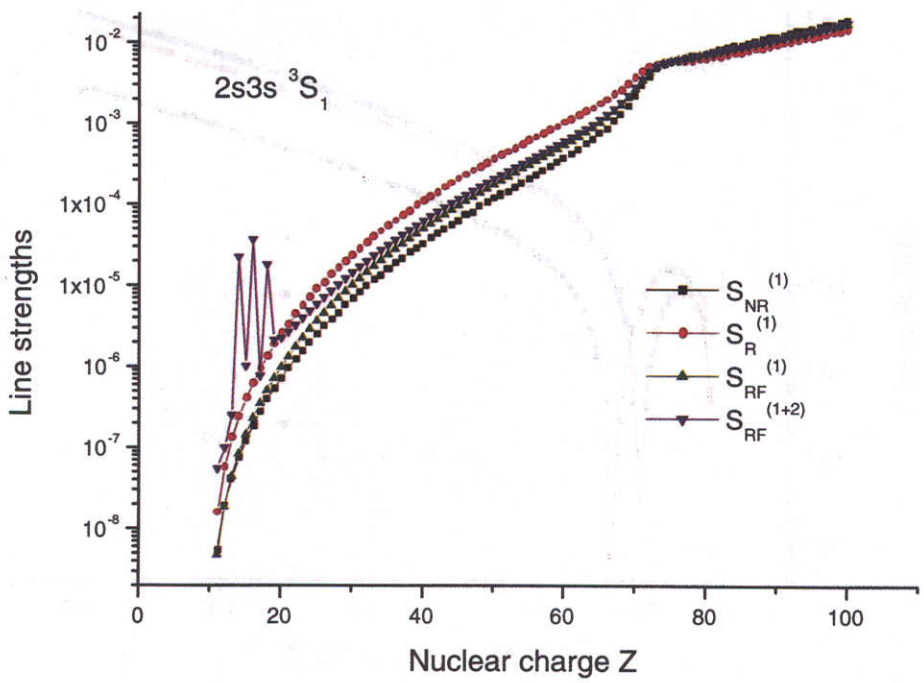

FIG. 30. Line strengths for $2s3s\ ^3S_1$ magnetic-dipole transition for Ne-like ions as function of Z

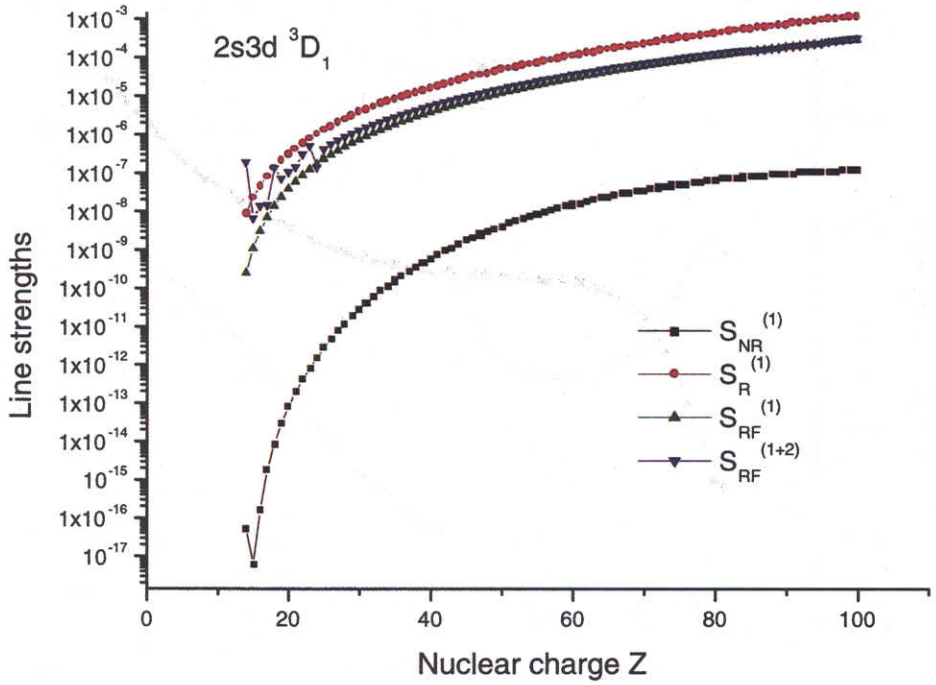

FIG. 31. Line strengths for $2s3d\ ^3D_1$ magnetic-dipole transition for Ne-like ions as function of Z

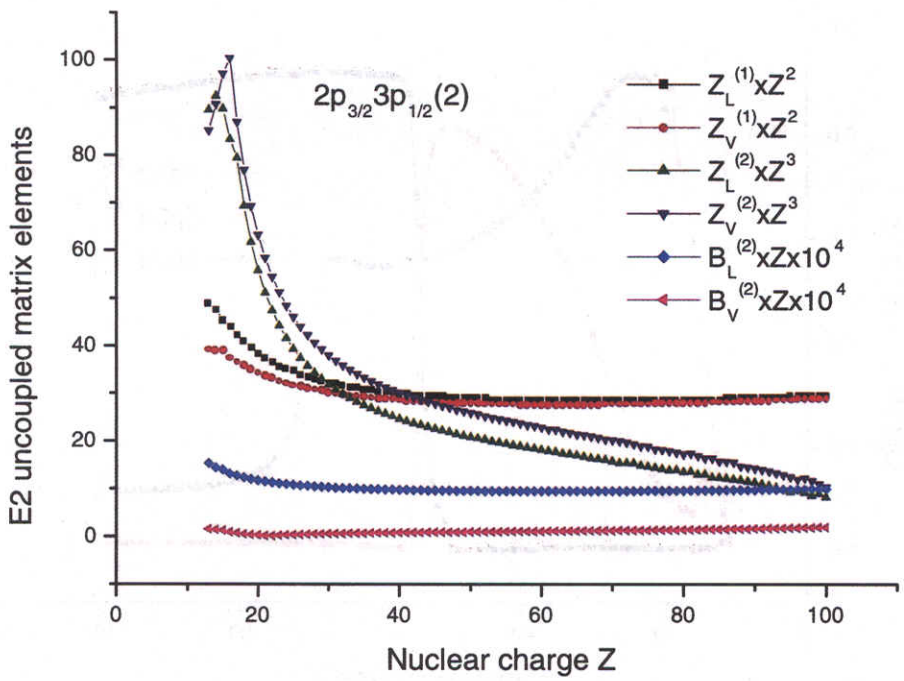

FIG. 32. E2 uncoupled matrix element for transition between $2p_{3/2}3p_{1/2}(1)$ and ground state calculated in length and velocity forms in Ne-like ions.

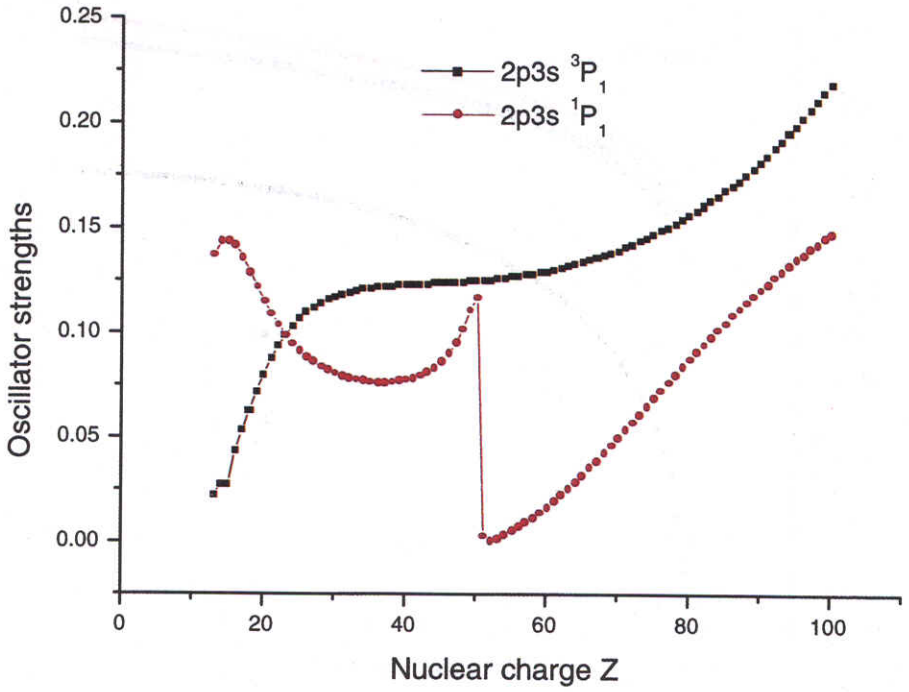

FIG. 33. Oscillator strengths of electric dipole $2p3s\ ^{1,3}P_1$ transitions for Ne-like ions as function of Z

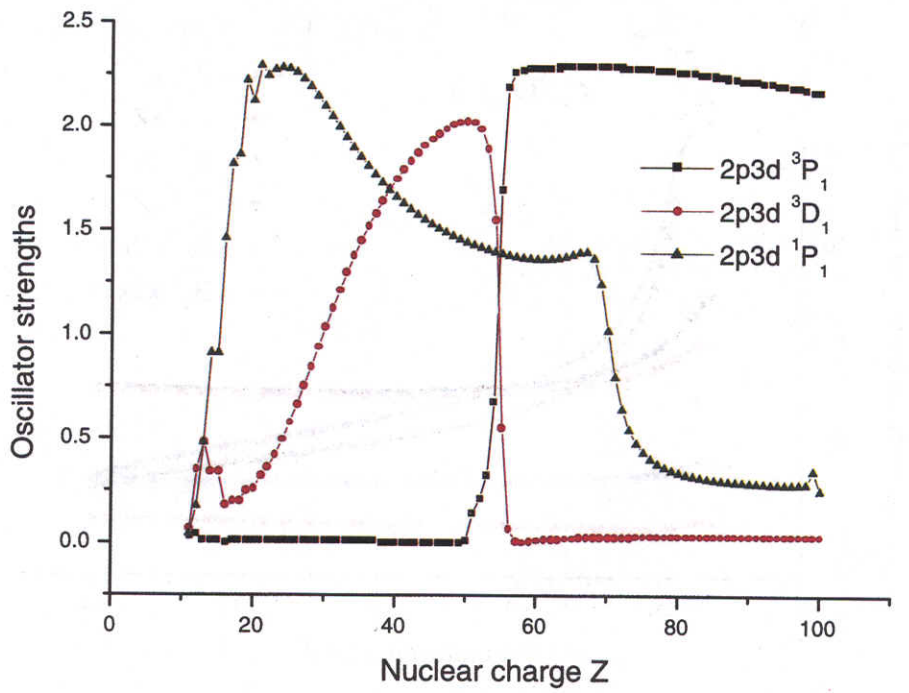

FIG. 34. Oscillator strengths of electric dipole $2p3d\ ^3D_1, ^{1,3}P_1$ transitions for Ne-like ions as function of Z

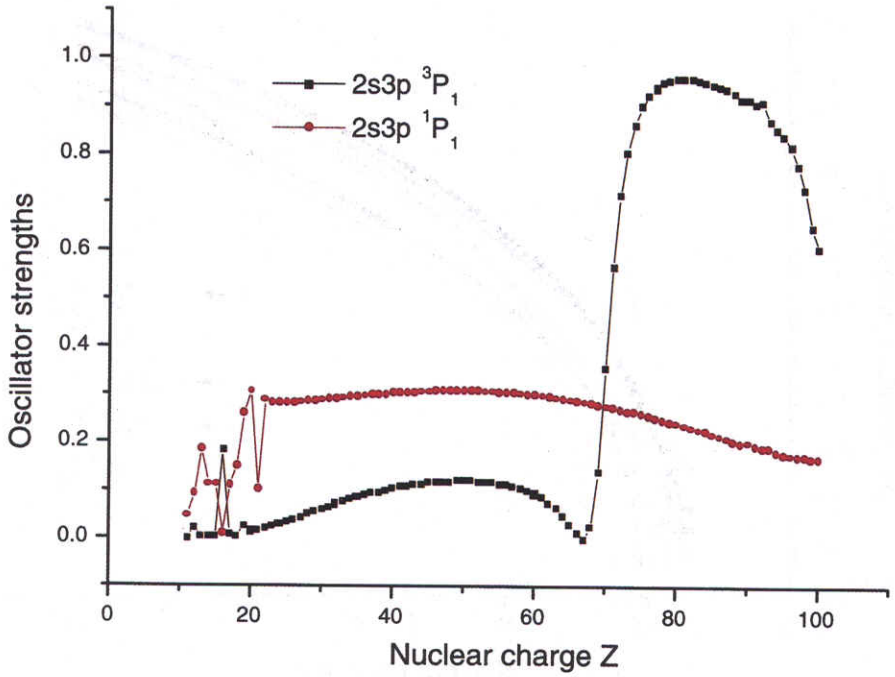

FIG. 35. Oscillator strengths of electric dipole $2s3p\ ^{1,3}P_1$ transitions for Ne-like ions as function of Z

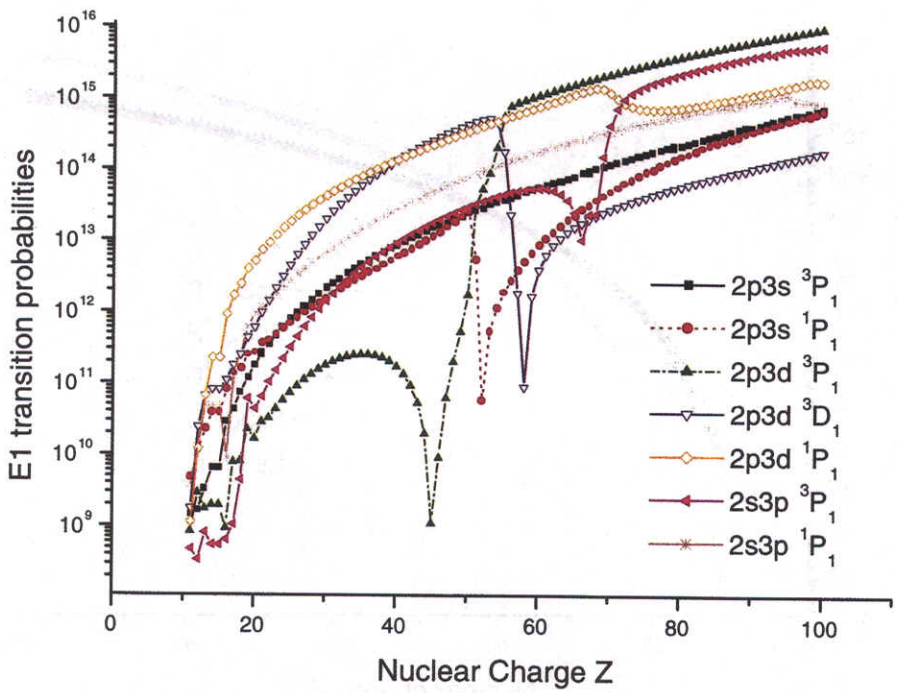

FIG. 36. E1 transition probabilities for Ne-like ions as function of Z

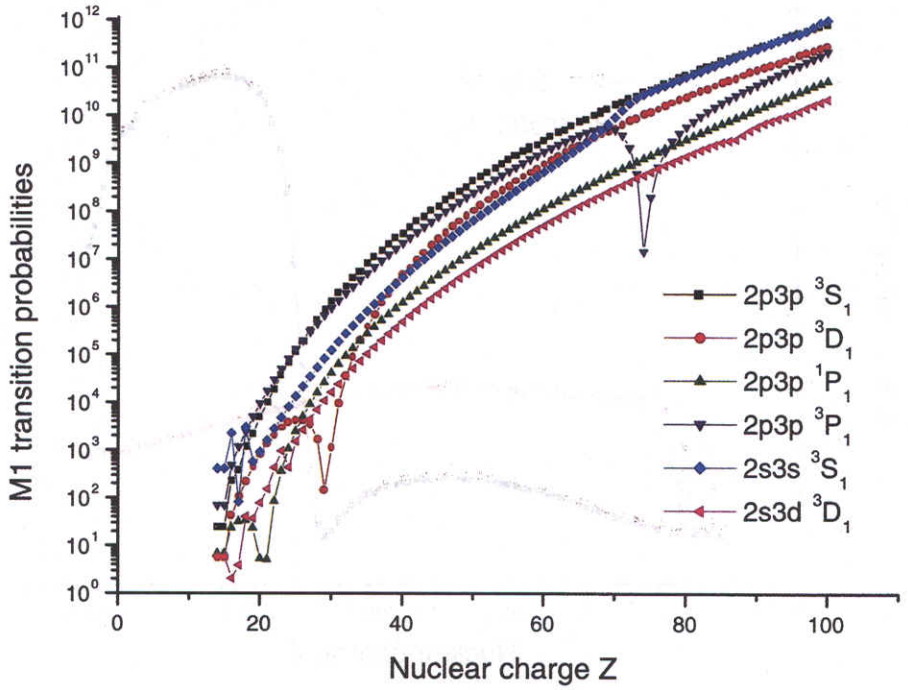

FIG. 37. M1 transition probabilities for Ne-like ions as function of Z

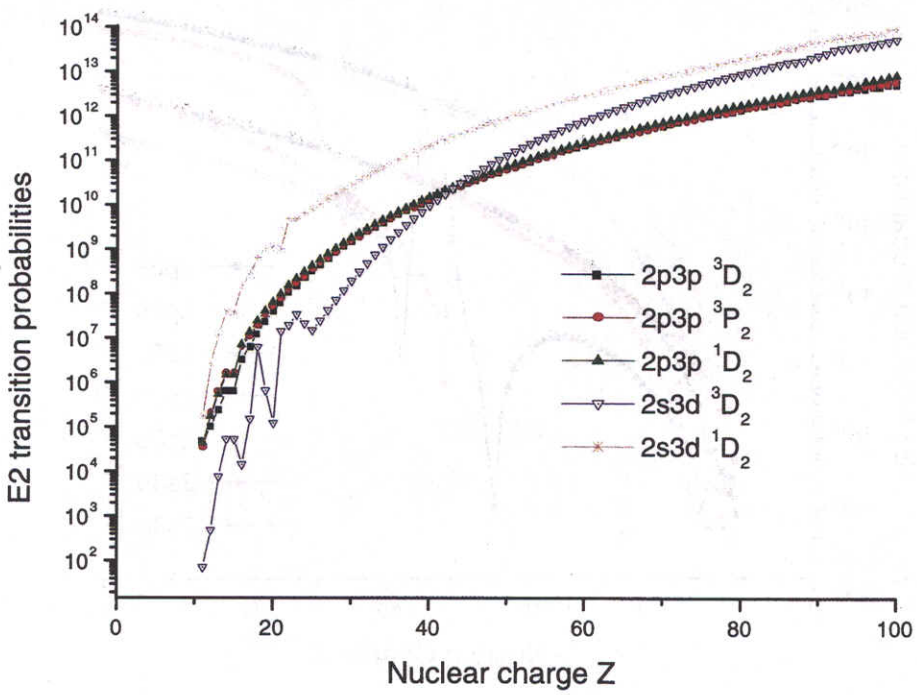

FIG. 38. E2 transition probabilities for Ne-like ions as function of Z

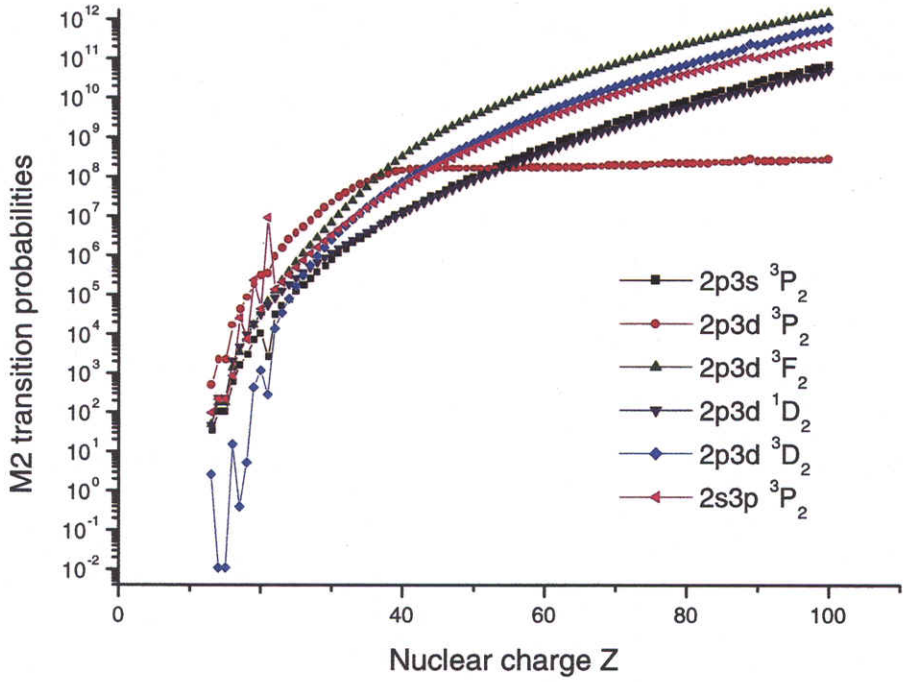

FIG. 39. M2 transition probabilities for Ne-like ions as function of Z

Recent Issues of NIFS-DATA Series

NIFS-DATA-42 H Tawara,
Bibliography on Electron Transfer Processes in Ion-ion / Atom / Molecule Collisions -Updated 1997 -,
May 1997

NIFS-DATA-43 M. Goto and T Fujimoto,
Collisional-radiative Model for Neutral Helium in Plasma: Excitation Cross Section and Singlet-triplet Wavefunction Mixing;
Oct 1997

NIFS-DATA-44 J. Dubau, T. Kato and U.I. Safronova,
Dielectronic Recombination Rate Coefficients to the Excited States of Cl From ClI;Jan. 1998

NIFS-DATA-45 Y. Yamamura, W. Takeuchi and T. Kawamura,
The Screening Length of Interatomic Potential in Atomic Collisions; Mar. 1998

NIFS-DATA-46 T. Kenmotsu, T. Kawamura, T. Ono and Y Yamamura,
Dynamical Simulation for Sputtering of B4C; Mar. 1998

NIFS-DATA-47 I. Murakami, K Moribayashi and T Kato,
Effect of Recombination Processes on FeXXIII Line Intensities; May 1998

NIFS-DATA-48 Zhijie Li, T Kenmotsu, T Kawamura, T Ono and Y. Yamamura,
Sputtering Yield Calculations Using an Interatomic Potential with the Shell Effect and a New Local Model, Oct 1998

NIFS-DATA-49 S. Sasaki, M. Goto, T. Kato and S. Takamura,
Line Intensity Ratios of Helium Atom in an Ionizing Plasma;Oct 1998

NIFS-DATA-50 I. Murakami, T. Kato and U. Safronova,
Spectral Line Intensities of NeVII for Non-equilibrium Ionization Plasma Including Dielectronic Recombination Processses,
Jan. 1999

NIFS-DATA-51 Hiro Tawara and Masa Kato,
Electron Impact Ionization Data for Atoms and Ions -up-dated in 1998-;Feb. 1999

NIFS-DATA-52 J.G. Wang, T. Kato and I. Murakami,
Validity of n^{-3} Scaling Law in Dielectronic Recombination Processes; Apr. 1999

NIFS-DATA-53 J.G. Wang, T Kato and I. Murakami,
Dielectronic Recombination Rate Coefficients to Excited States of He from He^{+}; Apr. 1999

NIFS-DATA-54 T Kato and E. Asano,
Comparison of Recombination Rate Coefficients Given by Empirical Formulas for Ions from Hydrogen through Nickel, June
1999

NIFS-DATA-55 H.P Summers, H. Anderson, T Kato and S. Murakami,
Hydrogen Beam Stopping and Beam Emission Data for LHD;Nov 1999

NIFS-DATA-56 S. Born, N Matsunami and H. Tawara,
A Simple Theoretical Approach to Determine Relative Ion Yield (RIY) in Glow Discharge Mass Spectrometry (GDMS);Jan.
2000

NIFS-DATA-57 T Ono, T. Kawamura, T. Kenmotsu, Y. Yamamura,
Simulation Study on Retention and Reflection from Tungsten Carbide under High Fluence of Helium Ions; Aug. 2000

NIFS-DATA-58 J.G. Wang, M. Kato and T. Kato,
Spectra of Neutral Carbon for Plasma Diagnostics; Oct 2000

NIFS-DATA-59 Yu. V. Ralchenko, R. K. Janev, T. Kato, D V. Fursa, I. Bray and F.J de Heer
Cross Section Database for Collision Processes of Helium Atom with Charged Particles.
I Electron Impact Processes; Oct. 2000

NIFS-DATA-60 U.I Safronova, C. Namba, W R. Johnson, M.S. Safronova,
Relativistic Many-Body Calculations of Energies for n = 3 States in Aluminiumlike Ions, Jan. 2001

NIFS-DATA-61 U.I. Safronova, C. Namba, I. Murakami, W.R. Johnson and M.S Safronova,
E1,E2, M1, and M2 Transitions in the Neon Isoelectronic Sequence; Jan. 2001